Abstracts of the AMP Europe 2023 Congress:

The Association for Molecular Pathology
June 18-20, 2023
Milan, Italy

Selected Genetics Abstracts

G01. Noncoding RNAs as Modulators for Drug Delivery and Epigenetic Changes in Immunotherapy Resistance of Cancer

F. Aliazami
Tehran Medical Sciences, Islamic Azad University, Islamic Republic of Iran.

Introduction: Cancer is considered a multifactorial disease arising from an alternative function of epigenetic modulations and genetic factors. A wide spectrum of strong evidence from research has shown that noncoding RNAs (ncRNAs) are related to the epigenetic modulation of cancer genes and their associated networks. A paramount consideration for molecular epigenetic mechanism is the expression of ncRNAs making a more significant contribution to the regulation of cancer pathogenesis and many other diseases. However, although cancer immunotherapy is a well-established method for treatment of a wide range of cancer types, the root of the problem lies in the different responses in patients and low-level responses or tumor cells evading the immune functions. With many tumors resentenced to immunotherapy in cancer, ncRNAs play an unprecedented role in enhancing the efficiency of immunotherapy towards tumors through epigenetic changes. **Methods:** We searched Scopus, PubMed, Science Direct databases, and Google Scholar. After a systematic review of the evidence, studies were considered to analyze. In this review, we will look back over current knowledge of the functions, expressions, critical mechanisms, and drug delivery of ncRNAs via epigenetic modulations. This review will bring great benefits to novel ncRNA-based immune classes in cancer immunotherapy. Finally, the ultimate purpose of this study is to arouse interested researchers to conduct studies on the theory because of a large knowledge gap in ncRNA-based cancer immunotherapy for responses to treatment. **Results:** However, not only have a few epigenetic drugs been approved by the FDA, but also a new hope has dawned on RNA-based therapeutics with epigenetic effects for cancer treatment. They potentially are a driving force in cancer immunotherapy without side effects. In addition, other molecular mediated RNA means, combined with nanoparticles, CRISPR/Cas9, polymer-based, lipid-based nanoparticles, can enhance RNA delivery to the tumors, tissues, and immune cells. They can promote immune responses by either silencing or upregulating the immune-relevant genes to improve the efficiency of new drug delivery to cross cell membranes. **Conclusions:** Now a more nuanced understanding of this research could pave the way for propelling new investigations. We hope that it will give scientists an appreciation of some of the issues involved. The bottom line is that future prospects of the research on personalized medicine would shed light on novel ncRNA-based cancer immunotherapy with epigenetic changes.

G02. Development of a Cell-Based Pan-Cancer Fusion FFPE RNA Reference Standard for Use in Targeted Oncology NGS and RT-PCR Applications

C. McGee, M. Fernández Muñoz, M. Fernández de Ara, B. Freeman, A. Van Brabant Smith, E. Chin
PerkinElmer (Horizon Discovery), Diagnostics Products R&D, Cambridge, UK.

Introduction: RNA-based biomarker profiling using next-generation sequencing RNA-seq, RT-qPCR and RT-ddPCR can overcome some of the limitations of traditional DNA-based methods (e.g., multiple intronic breakpoints, multiple fusion partners) for fusion biomarker detection in tumor samples. However, data interpretation can be challenging due to variabilities in sample quality, RNA extraction and quantification, and platform biases, which can result in low-confidence results or failure to detect biomarkers. To aid the development, validation, and routine monitoring of these RNA-based assays, Horizon has developed the Pan-Cancer 6-Fusion Panel, a multiplexed cell blend containing full-length mRNAs for six of the most prevalent kinase fusions spanning a range of cancer types; *TPM3-NTRK1*, *QKI-NTRK2*, *ETV6-NTRK3*, *EML4-ALK*, *CCDC6-RET,* and *SLC34A2-ROS1.* **Methods:** Cell lines, which were either engineered by Horizon to express the fusions of interest or derived from cells expressing fusions endogenously, were single-cell diluted to produce clonal cell populations for each fusion variant. After confirmation by Sanger sequencing and fusion expression profiling by RT-ddPCR, the cell lines were blended at defined ratios to ensure consistent expression levels of each fusion. The multiplexed cell blends were then fixed in 10% formalin before being embedded in formalin-fixed, paraffin-embedded

(FFPE) cores and finally embedded in paraffin blocks (Fig. 1). Three FFPE blocks were sectioned into 15 µm sections. RNA was extracted from sections using the Maxwell RSC RNA FFPE Platform (Promega) and assessed for average RNA yield by Qubit RNA (Thermo Fisher Scientific); RNA integrity (DV_{200}) TapeStation (Agilent); and fusion biomarker expression by RT-ddPCR using fusion specific probes on the QX200 (Bio-Rad). **Results:** All RNA yields (n = 90) were above the >100 ng minimum QC acceptance criteria, with average yields of 413 ng, 679 ng and 585 ng, respectively, from the three blocks tested (Fig. 2, A). DV_{200} values for all the sections tested (n = 90) were greater than the minimum acceptance criteria of 65%, with averages of 84%, 90%, and 87%, respectively, for three blocks (Fig. 2, B). Fusion expression for the six fusion biomarkers was consistent across the three blocks (n = 90) with average copies/ng RNA well above the minimum acceptance criteria for each fusion (Fig. 2, C). *TPM3-NTRK1*: 411 copies/ng (≥100); *QKI-NTRK2*: 605 copies/ng (≥100); *EML4-ALK*: 155 copies/ng (≥40); *SLC34A2-ROS1*: 175 copies/ng (≥40); *ETV6-NTRK3*: 40 copies/ng (≥4); *CCDC6-RET*: 42 copies/ng (≥4). **Conclusions:** The Pan-Cancer 6-Fusion Panel is a highly characterised, renewable cell line-derived FFPE RNA reference material that can be used to assess the performance of RNA-seq, RT-PCR, RT-qPCR, or RT-ddPCR assays aimed at detecting *TPM3-NTRK1, QKI-NTRK2, ETV6-NTRK3, EML4-ALK, CCDC6-RET,* and *SLC34A2-ROS1* fusions. This reference standard is commutable with biopsy samples and serves as an appropriate control for the end-to-end validation, optimization, and implementation of molecular diagnostic assays that use FFPE specimens.

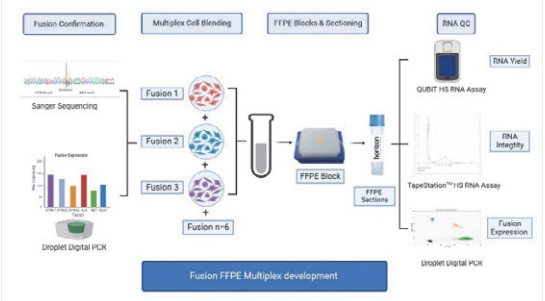

Figure 1. FFPE Process Development and Validation Pan-Cancer 6-Fusion Panel process development and validation.

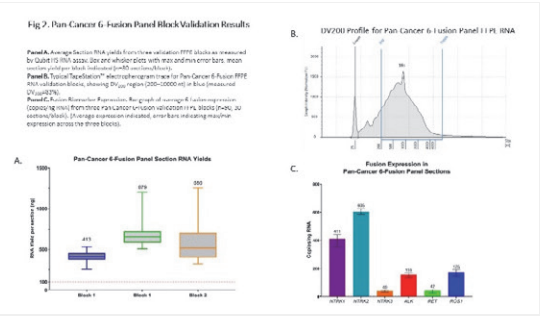

Figure 2. Pan-Cancer 6-Fusion Panel Block Validation Results: Results for average section RNA yields (ng), RNA integrity (DV200), and fusion biomarker expression results for three blocks for the Pan-Cancer 6-Fusion Panel.

G03. Establishment of Nepal's First Non-Invasive Prenatal Testing (NIPT) Service Laboratory (Selected for Oral Presentation, O-02-04)

S. Thapa, A.J. Kunwar, N. Thakur, S. Khanal, G. Joshi
Kathmandu Center for Genomics and Research Laboratory (KCGRL), Molecular Genetics, Lalitpur, Nepal.

Introduction: Non-invasive prenatal testing (NIPT) for fetal aneuploidies using cell-free DNA (cfDNA) has been widely adopted in clinical practice due to its improved accuracy. Several NIPT tests have been developed and validated. The core goal of cell-free-based prenatal testing is to provide minimally invasive, clinically accurate screening for fetal chromosomal aneuploidies in the early stages of pregnancy. **Methods:** The purpose of this study was to establish a validated NIPT workflow for cell-free fetal DNA (cffDNA) sequencing from maternal plasma for the detection of trisomy 13, 18, and 21 on a semiconductor sequencing instrument. A total of 91 standard samples from healthy pregnant women was provided by Yourgene Health; their cfDNA library was prepared and loaded on the Ion 540 chip for sequencing. The sequencing output data were analyzed by using the bioinformatics pipeline of Yourgene Health. **Results:** Eighty-one samples were successfully validated out of a total of 91 samples. However, 3% of samples did not meet quality, and 3% of sample libraries had low reads and failed validation. Moreover, building the validated workflow based on Ion Torrent Next-Generation Sequencing (NGS) would allow for fetal aneuploidy detection. **Conclusions:** This research aims to introduce and set up Nepal's first NGS laboratory for NIPT, utilizing the Ion Torrent technology to provide a complete in-house solution for pregnant women in Nepal.

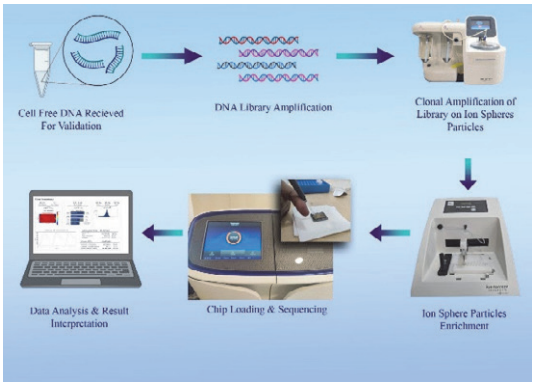

Workflow of NIPT
This is the outline of the workflow of NIPT. That includes sample collection, cffDNA, library preparation, analysis, and interpretation.

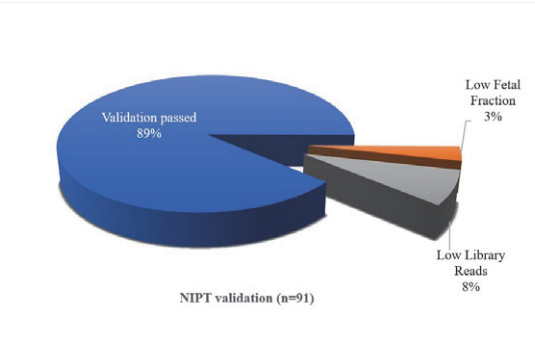

Results
This is the presentation of the results of the project.

G04. Withdrawn

G05. Combination of Next-Generation Sequencing Approaches for Characterization of Genetic Bases in a Large Brugada Syndrome Cohort

C. Di Resta[1,2], G. Peretto[2,3], S. Merella[4], A. Villatore[2], E. Rossetto[2], S. Bonfiglio[5], S. Benedetti[4], P. Carrera[1,4], S. Sala[3]
[1]IRCCS San Raffaele Hospital, Genomic Unit for the Diagnosis of Human Pathologies, Milan, Italy; [2]Vita-Salute San Raffaele University, Milan, Italy; [3]IRCCS San Raffaele Hospital, Department of Cardiac Electrophysiology and Arrhythmology, Milan, Italy; [4]IRCCS San Raffaele Hospital, Laboratory of Clinical Molecular Biology, Milan, Italy; [5]IRCCS San Raffaele, Center for Omics Science, Milan, Italy.

Introduction: Brugada syndrome (BS) is an inherited arrhythmogenic disease with a risk of sudden cardiac death in young asymptomatic adults. *SCN5A* is the only known causative gene, though 22 genes have been associated with BS susceptibility; nevertheless, 70% of patients remain genetically undiagnosed. To identify new candidate genes, we performed whole-exome sequencing (WES) of 200 patients, both sporadic and familial cases. **Methods:** WES was performed on the NovaSeq Illumina Platform (mean coverage: 180X, 97% target region >20X). Reads were analyzed exploiting the Dragen BioIT Platform, and coding and splice regions variants (MAF ≤0.01%) prioritized and classified according to ACMG guidelines with the support of eVai-EnGenome software. In addition, the burden test with Fisher exact test allowed us to extrapolate genes with higher mutation burden, suggesting a possible pathogenic role. A clinical database for the enrolled patients contains all the clinical information with a complete follow-up for more than 10 years. **Results:** WES analysis showed rare prioritized variants located in about 400 genes. Subsequent burden tests allowed us to focus on a smaller number of genes, confirming the role of *SCN5A* and highlighting possible associations of genes encoding proteins involved in muscle contraction, development, and differentiation, as also suggested by enrichment analysis with Panther tool. **Conclusions:** Preliminary data identified new candidate genes suggesting a role for structural proteins in disease pathogenesis. These results should be further investigated and confirmed in a larger cohort, also evaluating possible copy number variations. Genotype-phenotype correlations will be performed to better stratify patients, taking into account also the putative oligogenic inheritance of the disease and evaluating the possible role of multiple variants in the clinical phenotype.

G06. Withdrawn

G07. Carrier Frequency and Incidence Estimation of Aromatic L-Amino Acid Decarboxylase Deficiency by Genome Aggregation Database-Based Analysis: Focusing on East Asians

J.E. Park[1], E.H. Cho[2], T. Lee[3], K. Ha[3], C.-S. Ki[3]
[1]Hanyang University College of Medicine, Department of Laboratory Medicine, Hanyang University Guri Hospital, Guri, South Korea; [2]Sungkyunkwan University School of Medicine, Department of Laboratory Medicine, Kangbuk Samsung Hospital, Seoul, South Korea; [3]GC Genome, Yongin, South Korea.

Introduction: Aromatic L-amino acid decarboxylase (AADC) deficiency is an autosomal recessive neurotransmitter metabolism disorder and is clinically characterized by infancy hypotonia, ophthalmic crisis, and developmental delay. With the emergence of gene therapy for AADC deficiency, accurate prediction of AADC deficiency is required. This study aimed to analyze the carrier frequency and expected incidence of AADC deficiency using exome data from the Genome Aggregation Database (gnomAD). **Methods:** We analyzed 125,748 exomes from gnomAD, including 9,197 East Asian exomes, for the *DDC* gene. All identified variants were classified according to 2015 American College of Medical Genetics and Genomics and the Association for Molecular

Pathology guidelines. **Results:** The worldwide carrier frequency of AADC deficiency was 0.17%; the highest frequency was observed in East Asians at 0.78%, and the lowest was in Latinos at 0.07%. The estimated incidence of AADC deficiency was 1 in 1,374,129 worldwide and 1 in 65,266 in East Asians. **Conclusions:** The results demonstrated that East Asians have a higher carrier frequency of AADC deficiency than other ethnic groups. The variant spectrum of *DDC* genes in East Asian populations differed greatly from those of other ethnic groups. Our data will serve as a reference for further investigation of AADC deficiency.

G08. The Genomic Landscape of Colorectal Cancer in the Saudi Arabian Population

E.A. Alsolme
King Fahad Medical City, Research Center, Riyadh, Saudi Arabia.

Introduction: Colorectal cancer (CRC) is a malignant tumor of the large intestine (colon and rectum). CRC is the third most common cancer worldwide and the second highest cause of cancer-related deaths in most Western countries. CRC has a wide geographical distribution with high incident rates in North America, Northern and Western Europe, and Australia. On a global scale, CRC accounts for 9.4% of all cancers in men and 10.1% in women. In Saudi Arabia (SA), CRC cases were last reported as 10.1% in men and 9.3% in women. At present, CRC screening involves detection of early-stage CRCs and pre-cancerous lesions in asymptomatic people, before they become too advanced and unsuitable for treatment. In SA, despite its increasing incidence rates of CRC, there are no national screening policies in place for CRC. Protocols that aid rapid detection and diagnosis of CRC in SA are therefore urgently required. Comprehensive genomic panel can detect specific mutations that can provide treatment opportunities for CRC patients. We analyzed the mutation frequencies of common actionable genes and their association with clinicopathological characteristics and oncologic outcomes using targeted next-generation sequencing in 107 CRC Saudi Arabian patients. **Methods:** A total of 107 CRC samples were collected from KFMC. DNA and RNA were extracted from each formalin-fixed, paraffin-embedded clinical research sample using Invitrogen extraction kit for all samples. Oncomine Comprehensive Assay v3 sequencing was run using Ion AmpliSeq Kit for Chef DL8. The data were entered and analyzed using SPSS statistical package version 23. All survival analyses were completed in statistical software R V4.0.5 (supplementary methods). Two patients were omitted from the survival analysis because they were lost to follow-up and their survival outcomes were unknown. **Results:** In total, 98% (105) of patients had genetic alterations. Frequent mutations were observed in *BRCA2* (79%), *CHEK1* (78%), *ATM* (76%), *PMS2* (76%), *ATR* (74%), and *MYCL* (73%). A Cox proportional hazards model showed a positive association between poor differentiation of tumors and survival ($p < 0.05$). Although no univariate associations between specific mutations or overall mutation rate and overall survival proved significant, our preliminary analysis of the molecular markers for CRC in a predominantly SA population can provide insights into the molecular pathways that play a significant role in the underlying disease progression. **Conclusions:** In conclusion, we present a mutational landscape of actionable genes in CRC for the SA population in patients without a familial history of CRC. Additionally, we address the clinical relevance of low variant allele frequency variants. A comprehensive analysis of population-specific molecular markers for CRC can provide insights into the disease progression, with an aim of optimizing individualized therapeutic options and treatment regimens in the management of CRC in the SA population.

G09. Upregulation of IL-33 Expression in Heart Promotes Cardiac Fibrosis and Left Ventricle Dilatation in Diet-Induced Obesity Mice through PPARα and PPARγ Signaling

E. Vianello[1], M. Kalousová[2], E. Dozio[1], L. Tacchini[1], G. Tedeschi[3], P. Roccabianca[4], T. Zima[2], M. M. Corsi Romanelli[1,5]
[1]University of Milan, Department of Biomedical Sciences for Health, Milan, Italy; [2]Charles University and General University Hospital in Prague, Institute of Medical Biochemistry and Laboratory Diagnostic, First Faculty of Medicine, Prague, Czech Republic; [3]University of Milan, CRC "Innovation for Well-Being and Environment" (I-WE), Milan, Italy; [4]University of Milan, Department of Veterinary Medicine and Animal Science, Milan, Italy; [5]UOC SMEL-1 Clinical Pathology, IRCCS Policlinico San Donato, Milan, Italy.

Introduction: IL-33 is a cardiac alarmin expressed by endothelial cells and cardiac fibroblasts, and it is released in extracellular space to counteract detrimental stress volume overload in those tissues. Interestingly, IL-33 can also be considered a master regulator of obesity, since it controls cholesterol metabolism in fat and cardiac tissues. Due to the dual role of IL-33 in cardiac protection and lipid intake, the aim of this study is to analyze 1) the genomic expression of IL-33 in whole normal and fatty heart from diet-induced obesity (DIO) mice; and 2) the whole proteome of DIO mouse model to highlight the potential network sustained by IL-33 in the promotion of cardiac remodeling through fat metabolism in obese model. **Methods:** Fourteen 6-week-old male C57BL/6N

mice (Charles River Laboratories, Calco, Italy) were divided into two groups and fed for 20 weeks as follows: 1) normal chow diet (10% fat, control lean group) and 2) high-fat diet (60% fat group). At the age of 26 weeks, the mice were sacrificed through exposure to atmosphere saturation of carbon dioxide for 15 min. Kidneys were collected, immediately snap-frozen in liquid nitrogen, and stored at −80° until genomic and proteomic investigations. The Italian Ministry of Health approved all animal procedures (Number 5AD83.N.G1Q). The bioinformatic analyses on whole heart proteome were carried out using Cluego and Panther software, and the enriched networks were analyzed by String software and Ingenuity Pathway Analysis (IPA). **Results:** Genomic results showed that IL-33 is downregulated in fatty rather than control lean group. Cardiac proteome evaluation of DIO mice was carried out using IPA and demonstrated that the proteins differentially expressed in high-fat diet than normal group are related to fatty acid metabolism and lipid transport through PPARα and PPARγ mediators. In particular, functional network analysis suggested the presence of fibrosis and left ventricular dilatation and upregulated processes in metabolism (fatty acid metabolism and lipid transport, PPARα and PPARγ). Interestingly, the IPA network highlights the involvement of IL-33 as an upstream regulator of them as inhibitors of ACAT1, ApoE, EPHX2, IGHM, ITIH1, MYLK, MARKS, and UCP1 proteins, which are collectively involved in energy and cholesterol metabolism, inflammation, and cardiac matrix remodeling. **Conclusions:** Proteome network analysis demonstrated that IL-33 drove heart remodeling through deregulation of cardiac lipid metabolism through the upregulation of PPARα and PPARγ.

G10. Host and Microbial Regulation of Tryptophan Metabolism: From Preclinical Models to Human Diseases

G. Renga, F. D'Onofrio, M. Pariano, C. Stincardini, M. M. Bellet, C. Costantini, V. Oikonomou, L. Romani
University of Perugia, Department of Medicine and Surgery, PG, Italy.

Introduction: The intricate role of host and microbial metabolism on the coordination of immune system activity has recently gained more attention. In this context, tryptophan (Trp) metabolism is associated with several physiological functions. Trp, an essential amino acid supplied by the diet, is uptaken and metabolized by commensal microbes and host cells in the intestinal tract, where it is converted into different metabolites. Microbes recycle free Trp to build proteins and generate microbial metabolites such as indoles, while host cells metabolize Trp into kynurenine (Kyn) and serotonin (5-HT). Among the Trp metabolites, 5-HT is emerging as a key player in intestinal immune homeostasis and host-microbiota cross-talk. A serotonergic dysfunction has been reported in several genetic diseases, such as cystic fibrosis (CF) and celiac disease (CD), in which anxiety and depression are common complaints. CF and CD are two important inherited disorders characterized by an altered Trp metabolism. Whereas much is known about Kyn and indole pathways, the role of 5-HT in CF and CD is yet to be elucidated. Based on these premises, we have evaluated the contribution of 5-HT in CF and CD, and the effect of exogenous Trp metabolite administration in pulmonary and intestinal pathologies. **Methods:** To define the potential role of 5-HT in pulmonary and intestinal pathologies, we resorted to murine models of CF and CD. Specifically, *Cftr*^{F508del} mice were infected intranasally with *Aspergillus fumigatus*, one of the most common fungal pathogen colonising CF subjects, and evaluated for the expression of 5-HT-related genes and production. 5-HT levels were also observed in the sputa of CF patients. In the CD model, wild-type mice inbred for 3 generations on a gluten-free diet were challenged with gliadin for 4 weeks and evaluated for gene expression and 5-HT production. Additionally, we tested the effects of 5-HT exogenous administration in *Cftr*^{F508del} mice. **Results:** In both CF and CD, we found a defective activation of the serotonergic pathway that leads to reduced levels of 5-HT in the lung and gut. In *Cftr*^{F508del} mice, we observed an increased expression of *Aanat* and *Asmt* genes encoding for 5-HT-degrading enzymes in association with a significant increase of 5-OH-IAA, indicating active 5-HT catabolism. The reduction of 5-HT levels was also observed in the sputa of CF patients. 5-HT repletion by exogenous administration of 5-HTP improved pulmonary pathology and balanced Trp metabolic pathway. While contrasting results are reported in terms of 5-HT levels in human CD, we found a decisive decreased expression and production of 5-HT in our murine model of CD. **Conclusions:** Our results highlight the relevant, somewhat untold, contribution of the Tph1/5-HT pathway in the mucosal immune and microbial homeostasis in human inflammatory diseases such as CF and CD.

G11. A Genetic Deficiency in HMGA1, a *Trans*-Acting Regulatory Element of the *MAPT* Gene Promoter, Increases the Risk of Tauopathy

M. Mirabelli[1], E. Chiefari[1], B. Arcidiacono[1], A. Salatino[1], F. S. Brunetti[1], K.Y. Chin[2], S. Credendino[3], M. Fedele[3], M. Morelli[4], M. Greco[1], D. P. Foti[5], U. Aguglia[4], A. Brunetti[1]
[1]University "Magna Graecia" of Catanzaro, Department of Health Sciences, Catanzaro, Italy; [2]Universiti Kebangsaan Malaysia, Department of Pharmacology, Bangi Selangor, Malaysia; [3]CNR, Institute of Experimental Endocrinology and Oncology, Naples, Italy; [4]University "Magna Graecia" of Catanzaro, Department of Medical and Surgical Sciences, Catanzaro, Italy; [5]University "Magna Graecia" of Catanzaro, Department of Experimental and Clinical Medicine, Catanzaro, Italy.

Introduction: Tauopathies are a group of neurodegenerative disorders caused by the abnormal accumulation of aggregates of the Tau protein in neuronal cells. Tau is encoded by the microtubule-associated protein Tau gene (*MAPT*), and mutations in the regulatory region of this gene have been shown to produce a dysfunctional Tau protein that is more prone to forming aggregates, causing neurodegeneration. However, it is unclear whether abnormalities in the *trans*-acting factors interacting with the *MAPT* gene promoter, which could affect Tau protein expression, are also involved in the development of tauopathies. The high-mobility group A1 (HMGA1) has important *trans*-acting effects on genes related to both insulin resistance and type 2 diabetes, two conditions that are often associated with neurodegeneration. The role of HMGA1 on *Tau* gene transcription and the risk for neurodegeneration is not yet understood. The aim of this study was to investigate the role of HMGA1 and its genetic variant, *rs146052672* in the development of tauopathy. **Methods:** To determine if HMGA1 may affect Tau expression, experiments have been conducted both *in vitro,* in differentiated human SHSY-5Y neuroblastoma cells, and in primary embryonic mouse neurons, and *in vivo,* in *hmga1*-knockout mice. In addition, a case-control clinical study was conducted to examine the potential association of a genetic deficiency in HMGA1 (as caused by the *HMGA1 rs146052672* variant) with tauopathy. **Results:** Tau protein and mRNA levels were found to be inversely related to the HMGA1 levels in both cultured human neuronal cells and primary mouse embryonic neurons. This inverse relationship was confirmed in the cerebral cortex of *hmga1*-knockout mice, in which Tau was overexpressed, compared to wild-type mice. The role of HMGA1 in the regulation of Tau expression was substantiated by electrophoretic mobility shift assay, and luciferase assay, showing that HMGA1 can bind the *MAPT* promoter and repress *Tau* gene transcription. Furthermore, the HMGA1 *rs146052672* variant was considerably more common in patients with tauopathy than in control individuals. The association of this HMGA1 variant with tauopathy was strong (OR = 4.86, 95% CI, 1.88 to 12.61, $p = 0.001$), even when adjusting for potential confounding factors, such as insulin resistance. **Conclusions:** This study provides the first translational evidence that tauopathies may rise from abnormalities in *trans*-acting regulatory elements of the *MAPT* gene promoter. A genetic deficit in HMGA1 may cause derepression of the *Tau* gene, leading to an increase in Tau protein expression in neuronal cells, thereby conferring higher risk for human neurodegenerative disorders.

G12. Circulating miRNA Signatures in the Early Onset of Type 2 Diabetes

M. Greco[1], M. Mirabelli[1], A. Salatino[1], F. Accattato[1], E. Chiefari[1], S.A. Pullano[1], A.S. Fiorillo[1], D.P. Foti[2], A. Brunetti[1]
[1]University "Magna Graecia" of Catanzaro, Department of Health Sciences, Catanzaro, Italy; [2]University "Magna Graecia" of Catanzaro, Department of Experimental and Clinical Medicine, Catanzaro, Italy.

Introduction: There is growing evidence that circulating miRNAs may be used as biomarkers for type 2 diabetes (T2D) and its complications. T2D often develops from impaired fasting glucose (IFG), which represents an early feature of a pre-diabetic, insulin-resistant state that can eventually lead to T2D over time. Several miRNAs have been found to be dysregulated in the serum of T2D patients, and some of them may be linked to the onset of the disease. The aim of this study was to investigate the expression of circulating miRNAs in the early onset of T2D by comparing serum miRNA profiles of healthy controls with those of age- and sex-matched patients with IFG and new-onset T2D. **Methods:** The study population (aged 45 to 60 yr) was divided into three groups (n = 10 each): 1) healthy controls; 2) patients with IFG; and 3) patients with new-onset T2D (<5 yr since diagnosis) without complications (American Diabetes Association criteria). Patients with inflammatory states, liver and kidney failure, poor glycemic control, or severe obesity were excluded from the study. Circulating miRNAs were extracted from patients' sera using a commercial column-based system (miRNeasy). After quantification, equal amounts (100 ng) of the extracted RNA were pooled together for each patient group and reverse transcribed using the miScript II RT Kit. MiRNA profiling was performed by a high-throughput real-time PCR assay on a 384-well array containing spotted forward primers for 372 miRNAs. Data analysis was done with the GeneGlobe software. **Results:** A first exploratory analysis of 372 miRNAs found that 33 were differentially expressed between healthy controls and patients with IFG and new-onset T2D. Two miRNAs were found to be downregulated and 31 upregulated.

A second analysis of these same miRNAs using more stringent conditions found that 8 miRNAs (*miR-1260a, miR-3200-5p, miR-4651, miR-3135b, miR-1281, miR-4301, miR-195-5p, let-7a-5p)* had a significant (>2-fold) change in expression in new-onset T2D patients versus IFG patients, suggesting that they may be useful early markers of progression from pre-diabetes to T2D. Regarding the other miRNAs, it was found that *miR-146a-5p* was downregulated and *miR-1225-3p* upregulated only in new-onset T2D patients, whereas no change in their expression could be detected in IFG patients versus controls. *MiR-146a-5p* has a well-known role in glucose metabolism, insulin resistance, and T2D complications, while no association between *miR-1225-3p* and T2D has been reported so far. **Conclusions:** This study has highlighted differences in serum miRNA profiles in patients with IFG and new-onset T2D compared to healthy controls. Variations in *miR-1260a, miR-3200-5p, miR-4651, miR-3135b, miR-1281, miR-4301, miR-195-5p,* and *let-7a-5p* emerge as circulating miRNA signatures in the early onset of T2D. More research is needed to determine the functional role of these miRNAs in the development and treatment of T2D.

G13. Evaluation of Hi-C Sequencing as a Novel Diagnostic Technology for Detecting Genomic and Chromosomal Structural Variants in Constitutional Disorders (Selected for Oral Presentation, O-03-01)

Y. Liu[1], H. Fang[1], S. Eacker[2], Y. Wu[1], W. Neufeld-Kaiser[1]
[1]University of Washington, Department of Laboratory Medicine and Pathology, Seattle, WA; [2]Phase Genomics, Seattle, WA.

Introduction: Precise characterization of genomic structural variants (GSVs), such as chromosomal rearrangements (CRs) and copy number variants (CNVs), is essential for the diagnosis, prognosis, and management of genetic conditions. Methods such as karyotyping, fluorescence *in situ* hybridization (FISH), and chromosomal microarray analysis (CMA) all have limitations preventing a comprehensive understanding of GSVs and are often ordered reflexively in the clinical setting. In contrast, proximity ligation sequencing (Hi-C) is a novel method that detects a wide range of GSVs with a single assay. Hi-C captures chromatin contacts within the nucleus by proximity ligation followed by next-generation sequencing. Our study was to determine analytic validity and clinical utility of Hi-C and comparing it with the performance of optical genome mapping (OGM). **Methods:** We performed Hi-C on 114 clinical samples previously characterized by karyotyping, FISH, and/or CMA, including 33 normal samples as controls. The 81 abnormal samples represented various sample types (blood, amniotic fluid, chorionic villi, FFPE tissues) and various GSVs (translocations, inversions, insertions, deletions, duplications, and regions of homozygosity). We also performed OGM and Hi-C in parallel on 16 samples representing various GSVs. **Results:** We established Hi-C data of normal control cohorts for different sample types. All CRs and CNVs detected by conventional methods were detected by Hi-C with 100% concordance, including 18 unique CRs (reciprocal and Robertsonian translocations, insertions, and inversions) and 55 unique CNVs (>500kb) including aneuploidy with a sequencing depth of ≥30 million reads per sample. Of 86 smaller CNVs detected by CMA, 79 were detected by Hi-C, giving a sensitivity of 91% and a specificity of 100%. The 7 CNVs ≤1kb were missed by Hi-C. The sensitivity of detecting smaller CNVs by Hi-C increases with increasing sequencing depth. At deeper sequencing (i.e., >125M reads), Hi-C also detected long regions of homozygosity (including copy neutral loss of heterozygosity) and low-level mosaicisms (>7%). Our study showed that Hi-C had additional advantages over current test methods. Hi-C detected several novel findings (insertions and inversions) and provided sequence information near breakpoints. Unlike CMA, Hi-C was able to distinguish tandem duplications from insertional translocations. Hi-C and OGM showed complete concordance in 12 of 16 samples analyzed in parallel. OGM analysis failed in 2 samples of cultured amniocytes and failed to detect a Robertsonian translocation in 2 samples. **Conclusions:** Our study proves that Hi-C is a promising new diagnostic test method that allows for a comprehensive characterization of GSVs with a single assay. Unlike OGM and other long-read sequencing methods, Hi-C analysis does not require ultra-long DNA molecules and tolerates a variety of sample types, including FFPE samples. The requirements of sequence depth and sample types, cost comparison, and turnaround-time will be discussed.

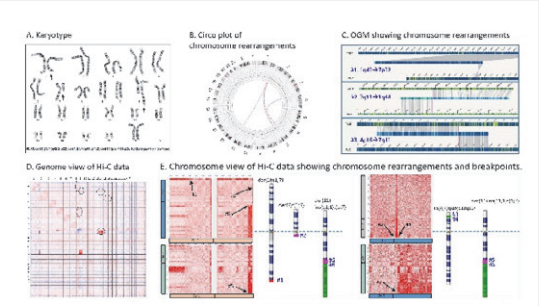

Figure 1. Examples of chromosome rearrangements detected by karyotyping, OGM, and Hi-C. Complex chromosomal rearrangements (CCRs) were characterized by karyotype analysis (A), OGM with track view showing the rearrangements around the translocation break points (C), and Hi-C with genome view (D) and chromosome view (E) of contact heatmap showing translocations and insertions between chromosome 1, chromosome 4, chromosome 7, and

chromosome 11. Detailed data interpretation will be presented.

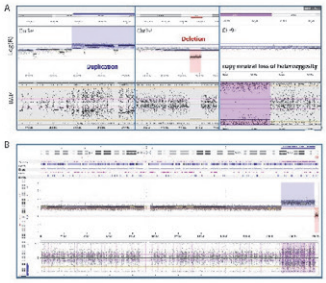

Figure 2. Detection of duplication, deletion, and copy neutral loss of heterozygosity by Hi-C.
Examples of duplication, deletion and copy neutral loss of heterozygosity (cnLOH) of chromosomal segments detected by Hi-C were shown. The plots of log(R) ratio (upper panel) and B allele frequency (lower panel) were shown for (A) regions of duplication on chr 3 (blue), deletion on chr 7 (pink) and cnLOH on chr 9 (purple) and (B) regions of duplication (blue) and deletion (pink) on chromosome 2.

G14. Molecular Epidemiology of Beta Thalassemia and Screening Variants of Beta Globin Gene (*HBB*) by Sanger Sequencing in Pakistan

K. Tariq, S. Ghani, Z. Ansar, A. Nasir
Aga Khan University Hospital, Molecular Pathology, Karachi, Pakistan.

Introduction: Hemoglobin disorders are one of the most common single-gene disorders and present a significant health burden. Beta globin (*HBB*) is a structural gene found on chromosome 11(11p 15.15) and forms the Beta chain of the adult hemoglobin. In Pakistan, many studies have shown that 6 mutations (*HBB*:c.27_28insG, *HBB*:c.92+5G >C, *HBB*:c.126_129delCTTT, NG_000007.3:g.71609_72227del619, *HBB*:c.47G >A, and *HBB*:c.92+1G >T) account for more than 90% of all thalassemia genotypes. For our project we have used Sanger screening methods to screen the novel variants in B-Globin genes. **Methods:** DNA from the *HBB* gene samples was amplified in 2 fragments per sample using 2 different PCR reactions to conduct a gap PCR. This required designing of forward and reverse primers accordingly. PCR I had 1 forward primer and 2 reverse primers, out of which 1 reverse primer was situated in the region deleted in 619bp deletion mutation. PCR II only had 1 forward and 1 reverse primer. In individuals not affected by 619bp deletion in *HBB* gene, PCR I would yield a 1,457 bp fragment and PCR II would yield a 1,212 bp fragment. However, in a patient suffering from 619bp deletion, fragment I from PCR I would yield a longer, 1,671 bp product and fragment II would yield a truncated product of 593 bps. This was followed by cycle sequencing (modification of Sanger sequencing). Samples were sequenced on a 3500/Genetic Analyzer (Applied Biosystems) and sequences were analyzed using Mutation surveyor. **Results:** Molecular analysis was carried out for 165 patients with beta-thalassemia minor and major. The most common mutations were IVS1-5G>C (15%), c.27dupG (12%), 126_129del (6%), c.364 G>C(HbD) (6%), c.92+1G>C(4%), c.619bp (4%) ,C.17-_18delCT (3%). Other mutations identified during this study included: c.138 C>T (-88), C.92 A>T (HbS), C.25-26 del AA(CD 8), C.315+1 G>A (IVSII-I), C.316-238 C>T. A unique mutation was observed in a thalassemia patient with compound homozygous c.51del C codon 16 (-C) with c.33 c>a codon 10 (C>A), and in another case we observed a patient with 3 heterozygous mutations: c.92+5 G>C, c.33CTA (codon 10), and c.51del C (codon 16). **Conclusions:** The PCR and the sequencing results are indicative of a compound heterozygous mutation consisting of *HBB*: g.71609_72227del619 (Fig. 1) and *HBB*: c.92+5G>C (Fig. 2). According to the Hbvar Database of Beta haemoglobin variants, both mutations lead to severe Beta thalassemia, with the patient being unable to produce functioning proteins; hence, molecular diagnosis shows the patient is suffering with Beta thalassemia major. In the results, the most common mutations were IVS1-5G>C (15%), c.27dupG (12%), 126_129del (6%), c.364 G>C(HbD) (6%), c.92+1G>C (4%), c.619bp (4%), and C.17-_18delCT (3%). Two unique mutations included a compound homozygous c.51del C codon 16 (-C) with c.33 c>a codon 10 (C>A), and in another case we observed a patient with 3 heterozygous mutations: c.92+5 G>C, c.33CTA (codon 10), and c.51del C (codon 16).

G15. Clinical Significance of Balance Translocation in Patients with Recurrent Miscarriage

A. Zehra, S. Hussain, U. Shakil, Z. Ansar Ahmed, T. Moatter
Aga Khan University, Karachi, Pakistan.

Introduction: Recurrent pregnancy loss (RPL) is an obstetric complication that affects couples in their reproductive age. It can be associated with many factors, including advanced maternal and paternal age, infectious diseases, environmental toxins, and genetic abnormalities. Chromosomal abnormalities, mainly balanced rearrangements, could commonly be present in couples with RPL. Determining the presence of such a rearrangement is useful because it provides an explanation for the miscarriages; information about the risk for a live-born child with potentially serious anomalies, as well as the risk for future miscarriages; availability of prenatal diagnosis in a future pregnancy; and information for members of the extended family who may be at risk and may wish to undergo

chromosome testing. Appropriate evaluation of RPL should include parental karyotyping. **Methods:** Metaphase chromosome preparations from the peripheral blood cultures were made according to the standard cytogenetic protocols. Peripheral blood was put for 72-h culturing where peripheral blood lymphocytes were induced with phytohemagglutinin. Cytogenetic analysis was performed by GTG-banding at approximately 550-band level. A cytogenetic study was performed on 993 specimens received in cytogenetic laboratory, Aga Khan University Hospital During 2017 to 2022. For Nomenclature ISCN was followed. **Results:** Metaphase chromosome preparations from the peripheral blood cultures were made according to the standard cytogenetic protocols. Peripheral blood was put for 72-h culturing where peripheral blood lymphocytes were induced with phytohemagglutinin. Cytogenetic analysis was performed by GTG-banding at approximately 550-band level. A cytogenetic study was performed on 993 specimens received in cytogenetic laboratory, Aga Khan University Hospital, during 2017 to 2022. For nomenclature, ISCN was followed. **Conclusions:** The couples struggling with RPL, genetic testing is recommended as part of the diagnostic workup. Parental karyotyping should be advised to all the couples undergoing evaluation for RPL. The carriers of a balanced translocation should be informed regarding the risk of congenital anomalies in their offspring. Hence, genetic counseling is indicated in all cases of RPL associated with parental chromosomal abnormalities.

G16. The Clinical Significance of Prenatal Screening in the Diagnosis of Chromosomal Abnormalities

U. Shakil, S. Hussain, A. Zehra, Z. Ansar Ahmed
Aga Khan University, Karachi, Pakistan.

Introduction: In the age of modern medicine, the prenatal diagnosis of genetic diseases has become a routine part of obstetric care. Congenital anomalies in the fetal developmental stage can be identified by many approaches, such as maternal age, positive serum screening, a history of a previous affected child, a parental chromosome rearrangement, or an ultrasound-identified anomaly. Invasive diagnostic testing can be performed in the first trimester by chorionic villus sampling or in the second trimester by amniocentesis. Both procedures are safe, with an equivalent 0.5% risk of procedure-induced pregnancy loss. This study aims to evaluate the number and type of chromosomal abnormalities that have been reported in the chorionic villus biopsy and amniotic fluid samples received in the past 2 years at the molecular pathology section, Clinical Laboratories, Aga Khan University Hospital. **Methods:** All samples of amniotic fluid and chorionic villus biopsies were received from Feto-Maternal unit of The Aga Khan University Hospital Karachi and Gynecology and Obstetrics unit of The South City Hospital Karachi. Amniotic fluid and chorionic villus biopsy specimens collected in sterile containers and transported at 2° to 8°C on the same day were accepted and processed for chromosomal analysis. **Results:** Our study revealed 12.5% numerical and 1.7% structural chromosomal abnormalities in amniotic fluid samples, and 15.7% numerical chromosomal abnormalities in chorionic villi samples (CVS). The abnormal numerical karyotypes reported in amniotic fluid samples included Down syndrome (4.4%), Patau syndrome (1.8%), Edward syndrome (1.8%), Turner syndrome (2.7%), and ploidy (1.8%), whereas in CVS specimens the numerical abnormalities found were Down syndrome (2.6%), Edward syndrome (5.2%), ploidy, and others (7.8%). The structural chromosomal abnormalities were only reported in amniotic fluid samples which included variant Turner syndrome (0.8%) and balanced translocations (0.8%). **Conclusions:** Karyotyping is an established tool for an initial examination of chromosomal morphology; more advanced technologies such as microarray or next-generation sequencing (targeted) might provide an answer for samples that showed normal karyotypes. Furthermore, couples with advanced maternal and paternal ages and those with consanguineous marriages are commonly at risk of having an abnormal pregnancy. Such couples should be provided genetic counseling and access to cytogenetic analysis for making a pre-informed decision regarding their pregnancies.

G17. Validation of epiHERA, a Minimally Invasive PCR Screening Tool for Hypermethylated *CDO1/CELF4* Genes Associated with Endometrial Cancer (Selected for Oral Presentation, O-03-02)

B. Vinod[1], A. Ahmed[1], C. Boey[1], T.S. Lau[2], K.W. Choy[2], J. Lee[2], C.P. Chang[1]
[1]INEX Innovate, R&D, Singapore, Singapore; [2]The Chinese University of Hong Kong, Department of OBGYN, Hong Kong, Hong Kong.

Introduction: Endometrial cancer is the second most common of diagnosed gynaecologic cancers, with abnormal uterine bleeding as a critical risk factor. During their lifetime, 30% of women experience abnormal uterine bleeding. Although abnormal uterine bleeding is a common risk factor for other endometrial pathologies such as polyps and adenomyosis, there is a current lack of a test for endometrial cancer screening. The current gold standard of endometrial cancer diagnosis is the extraction of biopsy samples through dilation and curettage or pipelle biopsy. In endometrial cancer, hypermethylation of *CDO1/CELF4* were detected using a

methylomics database. Thus, to overcome the invasive and painful procedure arising from current diagnostic methods which limit their uptake as screening tools, we introduce an outpatient molecular screening method combining endometrial swab, hypermethylated *CDO1/CELF4* and real-time PCR. Our preliminary data using endometrial cell lines and endometrial cancer cell lines showed a sensitivity, specificity, negative predictive value, and positive predictive value of 100%. Here, we show our current retrospective and prospective clinical data. **Methods:** For the retrospective study, 50 endometrial cancer positive formalin-fixed, paraffin-embedded (FFPE) samples were acquired from biobanks with varying histology types. For the ongoing prospective study, a total of 689 female patients over 18 years old with high endometrial risk factors, such as abnormal uterine bleeding, who visited the Obstetrics and Gynaecology clinic in The Chinese University of Hong Kong from January 2023 will be selected. To date, Thinprep exfoliated cells were acquired from 86 patients and used in this study. Concurrently, results were compared against the histology report attained from dilation and curettage. Genomic DNA was extracted from FFPE samples using ReliaPrep FFPE gDNA Miniprep System (Promega) and endometrial swabs using DNeasy Blood & Tissue Kits (Qiagen). Bisulfite treatment was performed to convert methylated cytosine to thymidine before real-time PCR. Samples were deidentified and histology results were blinded. The results were analysed based on the presence of a sigmoidal curve, internal control, and △Ct of the test genes. The sensitivity and specificity of *CDO1* and/or *CELF4* methylation detection were statistically analysed for the detection of endometrial cancer. **Results:** Our results showed that detection of methylated *CDO1* and/or *CELF4* in retrospective FFPE samples showed a sensitivity of 85.7% (95%CI: 75.1%, 96.3%) and an accuracy of 85.7%. Finally, our current ongoing prospective study using Thinprep samples shows that the sensitivity and specificity for the detection of methylated *CDO1* and/or *CELF4* were 87.5% (95%CI: 75.9%, 94.8%) and 90.8% (95%CI: 82.7%, 95.9%), respectively. **Conclusions:** The replacement of biopsy sample acquisition through dilation and curettage with the minimally invasive endometrial swabs using Thinprep, and the high diagnostic accuracy, poise epiHERA as a promising molecular tool for the screening of endometrial cancer.

G18. Effects of Xmn1 Polymorphism on Blood Transfusion and Its Relation to B-Thalassemia Phenotype and Genotype

K. Tariq, S. Ghani, A. Yunus, S. Riaz, Z. Ansar, A. Nasir
Aga Khan University Hospital, Molecular Pathology, Karachi, Pakistan.

Introduction: Xmn1 polymorphism inducing fetal haemoglobin expression is a prominent mediator ameliorating β-thalassemia phenotype**.** Due to impaired globin chain synthesis, β-thalassemia syndromes are the most common form of chronic hemolytic anemia. Xmn1 polymorphism is characterized by C>T transition at 158 bp upstream of the gamma-globin gene, and responsible for increased HbF concentration and reduced thalassemic burden. In the current study, we attempted to screen a cohort of β-thalassemia patients for the presence of Xmn1 trait and to evaluate its overall impact on the severity of disease. **Methods:** *HBB* gene mutations and Xmn1 polymorphism were determined by amplification-refractory mutation system PCR method. The PCR products were digested with the Xmn1 Restriction Enzyme. Digestion products were electrophoresed on a 3% Agarose gel. Amplification with the primers produced a 650 bp fragment in the wild genotype; the heterozygous genotype gives 2 bands at 400 bp and 250 bp. **Results:** The study participants consisted of 71 patients and included males and females. Overall, Xmn1 polymorphism was observed. Homozygous (TT) and heterozygous (CT) genotypes of the polymorphism represented with frequencies of 5 (26%) and 12 (7%), respectively. HbF level was significantly higher in patients with at least one Xmn1 allele (67.9 ± 17.9%) than those without the polymorphism (19.5 ± 20.3%, P <0.0001). Also, patients with the TT genotype demonstrated significantly higher HbF compared to CT cases (respective percentages of 85 ± 6.8 and 54.7 ± 10.5, p <0.0001). **Conclusions:** Our results highlighted the role of Xmn1 polymorphism as the main phenotypic modifier. Hence, genetic screening at this level can make the diagnosis precise for thalassemia patients.

G19. Real-World Evidence of Germline Alterations in Women with Breast and Ovarian Cancer beyond *BRCA1* and *BRCA2* from a South Asian Population

S. V. Rangan, T.D. Gupta, N. Parveen, S. Jayaraman, V. Javle, N. Jaiswal, H. Joshi, S.R. Peddagangannagari, K.D. Rishi, H.M. Goswami, R. Malhotra, V.H. Veldore
4basecare Onco solutions Pvt Ltd, Bengaluru, India.

Introduction: *BRCA1/2* predominates the risk of hereditary breast-ovarian cancer in young women. However, analysis using broader gene panels may reveal non-*BRCA1/2* mutations that may predispose to cancer. Here, we provide the results of our germline profiling method using a larger

gene panel (Germline+ [213 genes], 4basecare) in breast and ovarian cancer patients from the South Asian population. **Methods:** The study includes 233 patients with a diagnosis of breast/ovarian cancer, where we identified clinically relevant alterations (Pathogenic/Likely Pathogenic/Variants of Uncertain Significance with support) and classified as per ACMG guidelines. Germline+ panel sequencing was performed using Illumina sequencing at ~100X depth to identify novel biomarkers in breast and ovarian cancer patients. **Results:** In all, 47% (n = 109) of these patients carried either *BRCA1* or *BRCA2* mutations. In the non-*BRCA* group, nearly 53% (n = 123) (Fig. 1) of the patients carried mutations in the DNA repair pathway (*ATM, RAD54L, BRIP1, FANCM, PALB2, CHEK2*) (Fig. 2). We also found pathogenic variants in relatively uncommon genes like *AXIN2, PPM1D,* and *RET.* Variants were also reported in receptor tyrosine kinase (*CBL, PDGFRA, MET*), cellular metabolism (*SDHA, SDHB*), chromatin remodeling (*MRE11, ARID1A, NSD1*) and Wnt/beta-catenin (*APC, CTNNA1*) pathway-based genes. **Conclusions:** Key findings from this study demonstrate nearly 53% of the individuals with the clinical phenotype of hereditary breast and ovarian cancers *are BRCA* negative. However, they possess genetic alterations other than *BRCA1/2* genes, which are associated with cancer risk predisposition. This study summarizes the findings of >200 cases of several intriguing familial presentation with non-syndromic genetic alterations in pathways such as DNA repair, receptor tyrosine kinase, cellular metabolism, chromatin remodeling, and Wnt/beta-catenin. Based on our observations, limited panel testing of the *BRCA1/2* significantly reduces the diagnostic yield. Hence, we emphasize screening for rare genetic alterations in families with high risk of developing HBOC or other cancers. Though there are no standard guidelines/recommendations for germline panel testing, implementation of broader gene panels would aid in risk assessment, selection of appropriate treatment option, and better stratification of cancer patients in precision oncology practice.

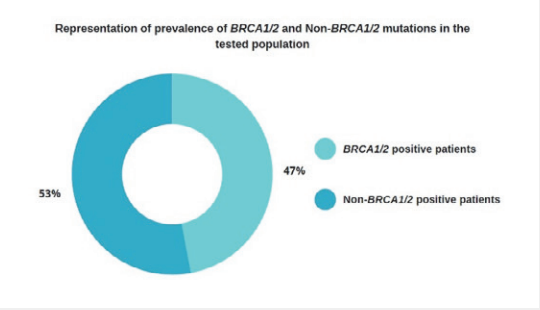

Figure 1: Distribution of BRCA and non-BRCA mutation in the cohort

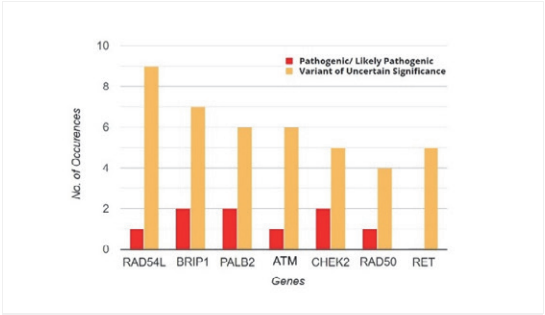

Figure 2: Recurrent non-BRCA genes and their classification

Selected Hematopathology Abstracts

H01. Comparison of Mutation Profiles Using Whole Bone Marrow Cells and CD138-Sorted Cells in Multiple Myeloma

Y.J. Hong, D. Chu, M. Kim, S.-H. Hwang, S. Jang, E.-J. Seo, C.-J. Park, Y.-U. Cho
Asan Medical Center, University of Ulsan College of Medicine, Department of Laboratory Medicine, Seoul, South Korea.

Introduction: Multiple myeloma (MM) is a neoplasm characterized by the accumulation of multiple genomic abnormalities in plasma cells (PCs). Emerging data suggest that MM risk stratification can be improved by integrating recurrent mutations and cytogenetic lesions with the current International Staging System. However, myeloma mutation analysis faces technical limitations with low PC recovery and PC enrichment issues. We investigated mutation detection yield using next-generation sequencing (NGS) of whole bone marrow (BM) cells and enriched PCs. **Methods:** BM samples were obtained from 32 patients with MM between January 2022 and December 2022. PCs were enriched using anti-CD138-positive beads from BM aspirates of 14 cases. The NGS panel included 652 genes for hematologic diseases. We analyzed mutation data from whole BM and the corresponding enriched PCs to evaluate the utility of BM pre-processing by CD138-sorting. The 23 myeloma-associated genes were selected from recent large clinical studies, whereas the clonal hematopoiesis (CH) driver mutations were identified from the bluebook of the 5th edition of the WHO classification of hematologic malignancies. **Results:** The median PC infiltration was 27.9% (3.2% to 92.0%), and the median PC purity was 90.4% (66.8% to 96.9%). The myeloma-associated gene mutations (Mut^{mm}) were detected in 21/32 (65.6%) of patients, with a higher frequency when using enriched PCs (12/14, 85.7%) than when whole BM alone was used (9/18, 50.0%). The median number of Mut^{mm} in enriched PCs was 3.5, whereas that of whole BM was 1.0 (P = 0.005). The median variant allele frequency (VAF) of Mut^{mm} was

significantly higher in enriched PCs (13.95%, range 0 to 89.3) than in whole BM samples (0.0%, range 0 to 31.7; P <0.001; Fig. 1). PC enrichment increased the mutation VAF by an average of 17.3% (2.0% to 61.9%). In 4 cases, the Mut^{mm} were detected in enriched PCs alone, including *NRAS, KRAS, IRF4, DIS3, FAM46C, CYLD, TP53*, and *HIST1H1E* mutations. Overall, CH driver mutations (Mut^{CH}) were detected in 14/32 (43.8%) of cases, including *DNMT3A, TET2, SF3B1, PTPN11, CUX1, PPM1D, STAG2, ETV6, WT1*, and *GNB1* mutations. The VAF of Mut^{CH} was marginally increased by PC enrichment (Fig. 2). **Conclusions:** Mutation detection yield is enhanced owing to PC enrichment. Therefore, CD138-sorted PCs should be used as a DNA source for mutation analysis in patients with MM. Furthermore, more accurate characterization of gene mutations can be expected through parallel analysis of mutation profiles derived from enriched PCs and whole BM cells.

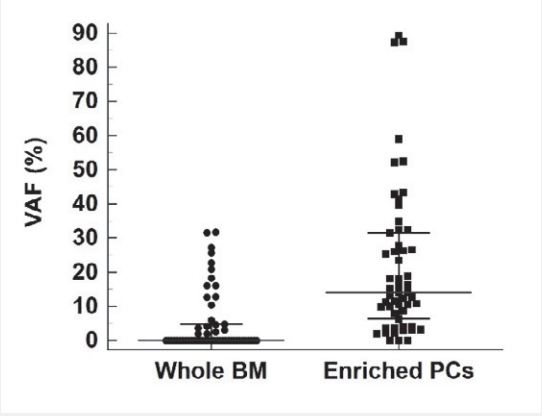

Figure 1. Myeloma-associated and clonal hematopoiesis gene mutation in patients.

Variant allele frequency of myeloma-associated mutations.

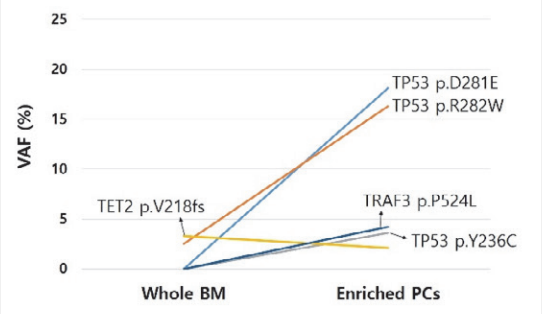

Figure 2. A representative case showing typical patterns of mutational change.
The size of TP53 and TRAF3 mutations significantly increased with PC enrichment, whereas the size of TET2 mutation did not change.

H02. Molecular-Pathological Correlation of a *CALR* and *MPL*-Double Mutated Post-Essential Thrombocythemia Myelofibrosis

M. Shi, J. Yuan, P.L. Ollila, D.S. Viswanatha, R. He
Mayo Clinic, Rochester, MN.

Introduction: Most *BCR-ABL1*-negative myeloproliferative neoplasms (MPNs) harbor a *JAK2*, *MPL*, or *CALR* mutation. *JAK2* V617F is found in >95% polycythemia vera and 50% to 60% essential thrombocythemia (ET) and primary myelofibrosis (PMF). *CALR* mutations occur in 20% to 30% of ET and PMF, whereas *MPL* mutations occur in 5% to 10% ET and PMF. They converge on the JAK-STAT pathway and have been reported as mutually exclusive. In the era of cost-effective, value-based medicine, professional MPN guidelines recommended reflexive testing for *JAK2*-V617F, *CALR,* and *MPL* sequentially until a mutation is detected. Here, we report a post-ET myelofibrosis (MF) patient harboring both *CALR* and *MPL* mutations, with the latter missed by the reflex test, highlighting the potential pitfall of the approach. **Methods:** DNA was extracted from the bone marrow (BM) aspirate using the Qiagen EZ1 DNA extraction kit (Germantown, US). *JAK2*-V617F analysis was performed by quantitative allele-specific real-time PCR. *CALR* exon 9 was done using fragment analysis and *MPL* exon 10 was analyzed by Sanger sequencing. Next-generation sequencing (NGS) was performed using a targeted, 42-gene panel with capture-based chemistry on an Illumina Novaseq sequencer (San Diego, US). **Results:** A 79-year-old patient had persistent thrombocytosis since 2005, and the BM was slightly hypercellular with mildly increased megakaryopoiesis without distinct clustering or MF. A diagnosis of ET was rendered. She remained asymptomatic with stable CBCs until 2018, when she developed mild anemia. A repeat BM revealed moderate hypercellularity with markedly increased megakaryopoiesis with clustering and grade 1 of 3 MF. *JAK2*-V617F was negative. In 2022, due to deteriorating anemia and thrombocytopenia, a third BM examination was performed which showed normocellularity with decreased erythropoiesis and granulopoiesis and moderately increased megakaryopoiesis with clustering and grade 3 of 3 MF. An MPN reflex test was negative for *JAK2*-V617F. The test proceeded to *CALR* and detected a pathogenic 52-bp deletion. *MPL* testing was not performed following the reflex algorithm. However, NGS revealed 2 pathogenic mutations: *CALR*: c.1099_1150del; p.Leu367Thrfs*46 (69%) and *MPL*:c.1543T>A; p.Trp515Arg (32%). Detailed information is listed in Table 1. **Conclusions:** *JAK2*, *CALR* and *MPL* mutations are not mutually exclusive in all MPN cases. Besides presenting in a clonal/subclonal combination pattern,

they may both present at clonal levels, indicating clonal heterogeneity and clonal evolution in MPNs. The widely adopted MPN reflex testing algorithm may have limitations in detecting the full spectrum of driver mutations in some cases. NGS with a broader breadth of target coverage offers a superior depiction of the mutational landscape of MPNs, which may be particularly helpful in disease progression. Further studies should be performed on collective patients to understand the pathogenesis and clinicopathologic features of *JAK2/CALR/MPL* double-mutated MPNs.

	2005	2018	2022
CBC			
WBC	7.2 x 10^9/L	6.9 x 10^9/L	5.4 x 10^9/L
Hemoglobin	12.2 g/dL	11.5 g/dL	7.6 g/dL
Platelet	982 x 10^9/L	911 x 10^9/L	113 x 10^9/L
Bone marrow biopsy			
Cellularity Erythropoiesis	Slightly hypercellular Normal	Moderately hypercellular Slightly increased	Normocellular Decreased
Granulopoiesis	Normal, no increased blasts	Normal, no increased blasts	Decreased, no increased blasts
Megakaropoiesis	Mildly increased with large hyperlobated forms	Markedly increased with large hyperchromatic and hyperlobated forms, forming clusters	Moderately increased, with large hyperchromatic and hyperlobated forms, forming clusters
Myelofibrosis	Negative, 0 of (3)	Mild, 1 of (3)	Marked, 3 of (3)
Cytogenetics			
FISH	Within normal limits for *BCR* and *ABL*	Within normal limits for *BCR* and *ABL*	Within normal limits for *BCR* and *ABL*; No monosomy 5/deletion 5q, monosomy 7/deletion 7q, trisomy 8, or deletion 20q.
Karyotype	46,XX[20]	46,XX[20]	46,XX[20]
Molecular studies			
JAK2V617F MPNR	Negative NA	Negative NA	See MPNR result *JAK2V617F*: negative; *CALR*: positive (52-bp deletion-type)
NGS	NA	NA	*CALR*: 52-bp deletion-type mutation; 69%; *MPL*: Missense p.Trp515Arg (W515R) mutation in the exon 10; 32%
Diagnosis	ET	ET with mild myelofibrosis	Post-ET myelofibrosis

MPNR: myeloid proliferative neoplasm reflex test for *JAK2V617F*, *CALR*, and *MPL*.

Table 1. Laboratory and pathologic features of the patient with ET progression to post-ET MF.

H03. Genetic Mutational Landscape of Diffuse Large B-Cell Lymphomas Using a Next-Generation Sequencing Lymphoid Panel: A Singapore General Hospital Study (Selected for Oral Presentation, Oth02)

F.P.S. Liaw[1], T. K.H. Lim[2,3], C.K. Ong[4], J.Q. Lim[4], G.S. Tan[3], L.S. Tay[3], A. S.T. Lim[1], S.L. Tien[1,5], N.F. Grigoropoulos[5]
[1]Singapore General Hospital, Department of Molecular Pathology/Cytogenetics Laboratory, Singapore, Singapore; [2]Singapore General Hospital, Department of Anatomical Pathology, Singapore, Singapore; [3]Singapore General Hospital, Department of Molecular Pathology/Translational Pathology Centre, Singapore, Singapore; [4]National Cancer Centre Singapore, Lymphoma Translational Research Laboratory, Singapore, Singapore; [5]Singapore General Hospital, Department of Haematology, Singapore, Singapore.

Introduction: Diffuse large B-cell lymphoma (DLBCL) is a genetically heterogeneous disease comprising many subtypes and significantly different treatment outcomes. Poor outcomes among some subtypes, especially the low-risk subgroups, highlight the need for better risk stratification. Cell-of-origin helps predict outcomes; however, germinal centre B-cell (GCB) and non-GCB, such as the activated B-cell subtypes, remain heterogeneous prognostically and in treatment response. Next-generation sequencing (NGS) analysis of DLBCL has facilitated the global identification of numerous and diverse genetic abnormalities in these neoplasms. In this study, we investigated the genetic mutational landscape of DLBCL using NGS on patients who did not achieve complete remission (CR) after initial treatment, relapsed after initial CR, and progressed after therapy. **Methods:** Seventy-seven deidentified formalin-fixed, paraffin-embedded tumour samples from adult Asian patients with *de novo* DLBCL were sequenced using a 29-gene lymphopanel (Ion Torrent). Fisher's Exact test and Kaplan-Meier (log-rank) were used to determine p-values, where the statistical significance was <0.05. In addition, comparisons of single-gene mutation recurrence between response groups were performed using odds ratios. **Results:** Patients with initial CR response (n = 56) achieved significantly longer overall survival (OS) compared to those who did not (p <0.05). CR failure includes partial remission (PR, n = 9), stable disease (SD, n = 2) and progressive disease (PD, n = 10). Patients who relapsed after initial CR (n = 4) also showed significantly worsened OS compared to those without evidence of remission (n = 42) at the last response. However, patients with disease progression (PR to SD or PD, n = 4) did not show significantly worsened OS after treatment. Patients who did not achieve initial CR showed an increased likelihood of mutations in *MYC, ID3, PRDM1, TNFAIP3, CD79B, BCL6, EP300, TNFRSF11A, CARD11, CREBBP*, and *MEF2B* in decreasing order with odd ratios (3.2 to 1.1) compared to those who did. In patients who relapsed after initial CR, the odds of mutations in *CARD11, FAS, B2M, MTOR, TRAF3, BCL6, TNFAIP3, TP53, MYD88*, and *PRDM1* are 13.7 to 1.1 in decreasing order of likelihood. Patients with disease progression, mainly those with PR after initial treatment (n = 4), showed an odds ratio of 3.0 likelihood of *CREBBP* and *KMT2D* mutations. There was no significant difference in GCB and non-GCB subtypes among the groups. **Conclusions:** NGS may offer more comprehensive mutational profiling of high-risk patients who may not achieve initial CR and those who may relapse after initial CR. We have identified mutations in a Singapore cohort of patients with primary DLBCL that may be associated with poor treatment outcomes, affecting disease progression, thus laying the foundation for more predictive molecular testing-based prognostic models with potentially more relevance to therapy choice.

H04. Assessment of Chimerism by Next-Generation Sequencing: A Comparison to STR-PCR Method

D. Brow, J. Kendrick, D. Viswanatha, M. Kharfan Dabaja, M. Elrefaei
Mayo Clinic, Jacksonville, FL.

Introduction: Chimerism analysis enables the assessment of engraftment and minimal measurable residual disease (MRD) for early detection of relapse in patients post-hematopoietic stem cell transplantation (HSCT). The objective of this study is to demonstrate the utility and sensitivity of novel multiplex next-generation sequencing (NGS)-based chimerism assay compared to the gold standard Short Tandem Repeat-PCR (STR-PCR) method. **Methods:** Five patients were evaluated for chimerism and MRD at various times post-HSCT. DNA was extracted from peripheral blood samples, and chimerism testing was performed by a multiplex NGS-based chimerism assay and compared to STR-PCR method. Limit of detection for complete chimerism by NGS and STR-PCR methods was 0.1% and 5%, respectively. **Results:** NGS-based chimerism assay identified 9 informative markers that were used to detect and quantify MRD less than 5%. In addition, NGS-based chimerism assay detected a wide range (0.1% to 92%) of recipient mixed chimerism (Table 1). In contrast, the STR-PCR method detected at least 95% donor DNA, yet was unable to quantify MRD below 5%. **Conclusions:** The multiplex NGS-based chimerism assay is more sensitive and may allow for better quantitative monitoring of engraftment and MRD post-HSCT compared to the STR-PCR method.

Recipient	Weeks Post-Transplant	NGS [a]	STR-PCR [b]
1	4	1.94	<5
	16	1.66	<5
2	9	16.8	20
	13	8.24	10
	22	2.62	<5
3	11	0.17	5
	15	3.41	5
	31	91.93	90
4	4	0.48	<5
	9	0.49	<5
	14	0.73	<5
5	4	0.53	<5
	7	4.81	<5

[a] limit of detection for complete chimerism by NGS = 0.1%
[b] limit of detection for complete chimerism by STR-PCR = 5%

Table 1

H05. Chimerism Analysis Post-Hematopoietic Stem Cell Transplantation by Next-Generation Sequencing: A Case Report

D. Brow, J. Kendrick, D. Viswanatha, M. Kharfan Dabaja, M. Elrefaei
Mayo Clinic, Jacksonville, FL.

Introduction: Chimerism analysis in hematopoietic stem cell transplant (HSCT) patients is usually performed using the gold standard Short Tandem Repeats-PCR (STR-PCR) method. However, the use of highly sensitive methods such as next-generation sequencing (NGS) for chimerism analysis in HSCT may be more clinically beneficial. The objective of this case report is to demonstrate the utility and sensitivity of NGS-based chimerism assay. **Methods:** Chimerism analysis in HSCT patients is usually performed using the gold standard STR-PCR method. However, the use of highly sensitive methods such as NGS for chimerism analysis in HSCT may be more clinically beneficial. The objective of this case report is to demonstrate the utility and sensitivity of NGS-based chimerism assay. **Results:** Complete chimerism was reported by both NGS and STR-PCR methods at 5 weeks post-HSCT. However, 4.8% recipient mixed chimerism was detected by NGS-based chimerism assay but not STR-PCR method at 7 weeks post-HSCT (Table 1). The patient was clinically asymptomatic with no reports of engraftment dysfunction. A bone marrow biopsy was performed on week 13 and demonstrated mixed chimerism and disease relapse. **Conclusions:** NGS-based chimerism assay demonstrated a higher sensitivity and earlier detection of patient DNA in peripheral blood cells that may predict clinical relapse earlier compared to the gold standard STR-PCR method.

Weeks Post-Transplant	NGS [a]	STR-PCR [b]
5	Complete chimerism	Complete chimerism
7	4.8% recipient	Complete chimerism

[a] limit of detection for complete chimerism by NGS = 0.1%
[b] limit of detection for complete chimerism by STR-PCR = 5%

Figure 1

H06. Quantitative *WT1* Gene Expression Assay Is a Validated Method for Follow-up: A Subset of Acute Myeloid Leukemia

H. Huang[1], A. Momeni Boroujeni[1], L. Dong[1], P. Salazar[1], K. Mullaney[1], P. Sukhadia[1], M. Zaidinski[1], J.O. Jeon[1], N. Chaves[1], S. DiNapoli[1], I. Rijo[1], U.D. Chunduri[1], K. Nafa[1], A. Maria[1]
[1]Memorial Sloan Kettering Cancer Center, Department of Pathology and Laboratory Medicine, New York, NY; [2]Alverno Laboratories, Central Lab, Hammond, IN.

Introduction: *WT1* expression has been proposed as a highly promising marker of disease in acute myeloid leukemia (AML) and myelodysplastic syndrome, which may be longitudinally monitored and even represent a target for treatment. Despite its potential value, expression assessment is not part of the routine evaluation in clinical laboratories. Here, we describe our clinical laboratory validation of a *WT1* assay for this purpose. **Methods:** Diagnostic samples of AML submitted for routine molecular testing were selected. Initial screening was performed using the MSK-Fusion Heme panel, a customized version of the FusionPlex Pan-Heme panel (Integrated DNA Technologies, Inc.), which concurrently targets *WT1* for

expression. The commercially available reverse-transcription PCR-based assay (Qiagen/Ipsogen WT1 ProfileQuant Kit) was utilized for further quantification and clinical validation. Accuracy, reproducibility, and sensitivity studies were performed. Levels of *WT1* expression were normalized to an internal control (ABL transcript) and expressed as copy number per 10,000 copies of ABL. Normalized levels of >250 at baseline were considered high based on published literature for this assay. **Results:** In total, 61 clinical samples were selected based on RNA availability, including 6 bone marrow samples without disease, and 55 with variable levels of AML involvement. Log2 normalized RNA expression of *WT1* by the MSK fusion assay ranged from -3.51 to 11.65. Quantitation by qPCR ranged from 4.23 to 31,908.75 *WT1* copies per 10K copies of ABL; 50 samples had copies above 250, which were all AML cases. Normalized *WT1* transcripts were significantly higher among AML cases (mean 6,140.07; range 4.23 to 31,908.75) compared to samples without disease (mean 41.65; range 14.35 to 120.64). However, there was high variability in expression among AML samples and overall poor correlation with corresponding blast counts (R^2 = 0.0693). *WT1* expression levels detected by MSK-Fusion panel correlated well with qPCR in diagnostic samples (R^2 = 0.8174). Based on preliminary data, a *WT1* level of 3.5 log2 normalized RNA expression may be established as defining criteria for amplification, consistently corresponding to a normalized *WT1* level of >250 by qPCR. Sensitivity studies are pending for the fusion assay. Highly concordant *WT1* levels by qPCR were obtained between the clinical laboratory and independent laboratory (R^2 = 0.99) with excellent intra- and inter-assay reproducibility. *WT1* transcripts were detectable down to the 10^{-5} dilution (0.001%). **Conclusions:** The *WT1* qPCR assay performs robustly for detection of *WT1* expression with excellent intra- and inter-assay reproducibility. *WT1* transcripts can be detected down to 10^{-5} dilutions, offering opportunities for initial baseline expression determination and disease monitoring. Previously established cutoffs of high expression correlate well with high expression by the MSK-Fusion assay, which could be used for cursory screening. Further studies are needed to establish distinct cutoffs.

H07. Novel *NUTM1* Fusions in Relapsed/Refractory Acute Myeloid Leukemia with Monocytic Differentiation (Selected for Oral Presentation, O-03-04)

L. Chang[1], J. Arias Stella[1], A. Salhotra[2], K. Gaal[3], J. Song[3], L. Soma[3], M. Telatar[1], H. Yew[1], T. Dyer[1], M. Gust[1], P. Tizro[3], A. Munteanu[3], A. Stein[2], G. Marcucci[2], M. Afkhami[1]
[1]City of Hope Comprehensive Cancer Center, Pathology, Molecular Pathology and Therapy Biomarkers Division, Duarte, CA; [2]City of Hope Comprehensive Cancer Center, Hematology and Transplant, Leukemia Division, Duarte, CA; [3]City of Hope Comprehensive Cancer Center, Pathology, Hematopathology, Duarte, CA.

Introduction: We are reporting two novel fusions in the *NUTM1* gene in acute myeloid leukemia (AML). *NUTM1* (NUT Midline Carcinoma Family Member 1) rearrangements are very uncommon in AML. They have been more commonly reported in *NUTM1* midline carcinomas, thoracic, and head and neck regions. However, rearrangements of *NUTM1* have been reported in hematologic malignancies primarily in pediatric B-cell precursor acute lymphoblastic leukemia. A novel *AVEN::NUTM1* fusion has been reported in one AML case in the literature. Here we report two AML patients with monocytic features that presented with relapsed/refractory (R/R) disease with no response either to transplant or navitoclax/venetoclax plus decitabine therapy. **Methods:** Bone marrow aspirates were tested with City of Hope's flow cytometry analysis and HopeSeq Heme Comprehensive panel. DNA sequencing of 523 genes and RNA sequencing of 233 genes were completed. Conventional cytogenetics was performed for confirmation of the results. **Results:** The first case is a 65-year-old male with persistent AML since 2020. Flow cytometry analysis (FCA) revealed CD34 negative immature "monocytic" population expressing CD4, CD11c, CD13, CD15, CD33, CD38, CD123, and HLA-DR. A *LARP1::NUTM1* fusion was detected by RNAseq, and DNA sequencing revealed *ASXL2*, *BCOR*, *DNMT3A*, and *IDH2* pathogenic/likely pathogenic (P/LP) alterations. Cytogenetic analysis through karyotyping detected t(5;15) in 2022 consistent with the *LARP1::NUTM1* fusion. (Fig. 1) The second case is a 67-year-old male with persistent AML since March 2022. FCA demonstrated blasts expressing CD4, CD9, CD11b, CD11c, CD13, CD14, CD15, CD16, CD33, CD38, CD45 (bright, monocytic gate), CD56, CD64, CD123, and HLA-DR. The population is negative for CD34 and MPO. RNA sequencing detected a novel *ARHGAP15::NUTM1* fusion. Additionally, *ASXL1*, *RUNX1*, and *TET2* P/LP mutations has been detected. Cytogenetic analysis reported t(2;15) consistent with the *ARHGAP15::NUTM1* fusion (Fig. 2). **Conclusions:** The first case has been transplanted; however, it relapsed 120 days post-transplant with a chimerism of 20%.

The second case has shown R/R AML since the initial diagnosis. Additionally, the novel *AVEN::NUTM1* fusion case reported in the literature, relapsed post-chemotherapy and was minimal residual disease positive 3 months after transplant with DNA sequencing detecting *IDH1* and *RUNX1* mutations. Although all three cases have mutations associated with poor prognosis including *BCOR* and *RUNX1* based on recent ELN and WHO recommendations, the short relapse post-transplant and persistent disease might be due to having additional *NUTM1* fusions. Both cases demonstrated AML with monocytic features, as well as the one reported *AVEN::NUTM1* novel fusion case in the literature. Further study is under progress for evaluation of acute myelomonocytic biorepository samples retrospectively to evaluate prevalence for *NUTM1* fusions. Both initial AMLs had normal karyotype; therefore, these fusions might represent clonal evolution or post-therapy development.

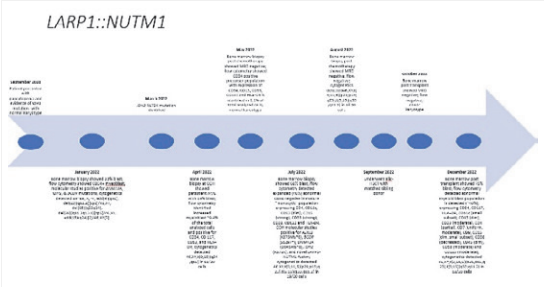

Figure 1. Case 1 timeline

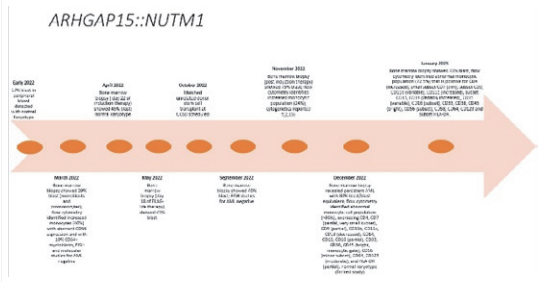

Figure 2. Case 2 timeline

H08. *STAT5B-RARa* Fusion Positive Variant Acute Promyelocytic Leukemia: Role of Next-Generation Sequencing in Detection of a Rare Malignancy

I. Dey[1], S. Vinarkar[2], M. Parihar[3], R. Demde[1], A. Mandloi[4], K. Saha[1], A. Nag[5], D.K. Mishra[2]

[1]Tata Medical Center, Department of Molecular Pathology, Kolkata, India; [2]Tata Medical Center, Department of Molecular Pathology & Laboratory Haematology, Kolkata, India; [3]Tata Medical Center, Department of Molecular Pathology, Cytogenetics & Laboratory Haematology, Kolkata, India; [4]Tata Medical Center, Department of Laboratory Haematology, Kolkata, India; [5]Tata Medical Center, Department of Clinical Hematology and Bone Marrow Transplant, Kolkata, India.

Introduction: Variant acute promyelocytic leukemia (APL) due to *STAT5B-RARa* fusion t(17;17) is a rare retinoic acid-unresponsive APL. The *RARa* fusion partner plays a critical role in the therapy and prognosis of APL and needs to be distinguished from the classic retinoic acid responsive *PML-RARa* APL and other RARa partners (i.e., *PLZF, NuMA,* etc.). **Methods:** We present a rare case of *STAT5B-RARa* translocation positive APL and highlight the role of next-generation sequencing (NGS) as an important diagnostic modality in its definitive diagnosis. **Results:** A 42-year-old male presented with complaints of severe weakness, decreased appetite, loss of weight, fever, visual disturbances and slurred speech for 3 months. Mild splenomegaly was noted upon examination. Complete blood count (CBC) showed leukocytosis with white blood cell count of 42,200/µl along with thrombocytopenia and anemia. Peripheral blood smear (PBS) examination revealed 76% blast/abnormal promyelocyte/atypical monocytoid cells with many of them showing salmon-pink cytoplasmic granules and strong cytochemical myeloperoxidase staining. No Auer rods were seen. Flow cytometric immunophenotyping on peripheral blood revealed 60% blasts/abnormal promyelocytes with high side scatter, dim CD45, showing expression of CD117, CD13, CD33, CD56, cMPO, and negativity of CD34, HLA DR. The PBS morphology and immunophenotyping were suggestive of possibility of APL. Fluorescence *in situ* hybridization (FISH) for PML-RARa using dual-color dual-fusion probe (MetaSystem, Germany) was negative. RT-PCR for PML-RARA (*BCR1, BCR2*, and *BCR3* fusion transcripts) was negative. FISH utilizing RARa break-apart probe (Kreatek, Leica, Amsterdam) revealed an atypical RARa rearrangement (1F1G signal pattern). Bone marrow aspirate revealed a cellular marrow with 30% MPO positive blasts/abnormal promyelocytes, with many of them showing prominent Auer rods and occasional faggot cells. NGS-based Oncomine Myeloid Research Assay (Thermo Fisher Scientific) was performed. RNA sequencing revealed *STAT5B-RARa* fusion positivity (6,094 read-counts). A missense variant in *GATA2*

gene NM_032638.5:c.1084C>G;p.(Arg362Gly) was detected on DNA sequencing. The patient received ATO, steroid, and azacytidine; however, within 7 days he developed respiratory distress followed by cardiac arrest which proved fatal. **Conclusions:** *STAT5B-RARa* t(17;17) is a rare variant of APML. It exhibits diagnostic, therapeutic, and prognostic difference with the common *PML-RARa* positive APL and, hence, the need for its prompt identification. Our case demonstrates the valuable role of NGS in reaching a definite diagnosis of such challenging and rare malignancy.

H09. Distinguishing between Primary Mediastinal Large B-Cell Lymphoma and Diffuse Large B-Cell Lymphoma Using the Lymph3Cx Gene Expression Profiling Assay

R. S. Robetorye[1,2], C.A. Ramsower[2], C.L. McKinney[2], L.M. Rimsza[1,2]

[1]Mayo Clinic, Department of Laboratory Medicine and Pathology, Phoenix, AZ; [2]Molecular Diagnostics Arizona-Laboratory (MDAZL), Department of Laboratory Medicine and Pathology, Scottsdale, AZ.

Introduction: Primary mediastinal large B-cell lymphoma (PMBL) is a distinct lymphoid neoplasm arising in the mediastinum that is morphologically similar to diffuse large B-cell lymphoma (DLBCL) but has distinct clinical, immunophenotypic, genotypic, and molecular features. Although the differentiation of PMBL from DLBCL can be important for guiding subsequent therapy, the interpretation of morphologic findings and the associated immunohistochemistry in small, and often crushed mediastinal biopsies can be difficult. Therefore, we developed and fully validated a clinical gene expression profiling assay in the Molecular Diagnostics Arizona Laboratory (MDAZL) that utilized the Lymph3Cx gene expression signature to distinguish between these lymphomas using formalin-fixed paraffin-embedded tissue specimens. This assay includes and builds upon the Lymph2Cx expression signature and can categorize DLBCL into germinal center B-cell (GCB)-type, activated B-cell (ABC)-type, and unclassifiable (UNC) categories as well as accurately and robustly differentiate PMBL from DLBCL. **Methods:** First, a hematopathologist identifies a large B-cell lymphoma based on histologic and immunophenotypic assessment of the specimen, and then requests Lymph3Cx testing from MDAZL to aid in further classification. Tumor content is assessed using a hematoxylin and eosin (H&E)-stained slide, and then additional unstained slides are used to isolate total RNA from the specimen. The RNA is hybridized overnight on a thermal cycler to fluorescently labeled probes in the Lymph3Cx assay panel. The probe/RNA complexes are then quantitated on a NanoString nCounter Digital Analyzer and subsequently subjected to an algorithmic analysis for further classification and subtyping. **Results:** So far, 62 clinical specimens have been subjected to Lymph3Cx testing in the MDAZL with the following results: PMBL: 36 (58%); DLBCL: 16 (26%); Unclear: 8 (13%); Failed QC: 2 (3%). Of the 16 cases with gene expression signatures consistent with DLBCL, subsequent cell-of-origin determination showed the following results: GCB: 9 (56%); ABC: 5 (31%); UNC: 2 (13%). Average in-laboratory turnaround time for these cases was 1.8 days, with an average of 3.3 days from sample receipt to final report. **Conclusions:** MDAZL has performed a full clinical validation of the performance characteristics of the Lymph3Cx assay and is the first molecular diagnostics laboratory to offer the Lymph3Cx assay as a clinical molecular diagnostic test for distinguishing PMBL from DLBCL and molecular cell-of-origin subtyping of DLBCL. With a relatively rapid turnaround time, the Lymph3Cx assay is suitable for use in routine hematopathology practice for distinguishing PMBL and DLBCL. Real-world case examples can also clearly illustrate the clinical utility of the Lymph3Cx assay, especially in cases of small biopsies with prominent crush artifact, cases with non-specific immunohistochemistry, or cases with atypical anatomic site presentations, such as mediastinal DLBCL or non-mediastinal PMBL.

H10. Diagnostic Challenges of Chromosomal 3q26.2 Aberrations/*MECOM* Rearrangement: An Extended Study from a Single Institute

Z. Tang[1], G. Tang[1], G.A. Toruner[1], S. Hu[1], S. Yang[1], J.D. Khoury[1,2], L.J. Medeiros[1]

[1]The University of Texas MD Anderson Cancer Center, Houston, TX; [2]Department of Pathology and Microbiology, University of Nebraska Medical Center, Omaha, NE.

Introduction: Rearrangements of *MECOM* locus at 3q26.2 are associated with rapid disease progression and a poor prognosis in myeloid malignancies. The 3q26.2 aberrations/*MECOM-R* are considered a defining genetic abnormality for acute myeloid leukemia (AML) under the 5th WHO (regardless of blast count) and the ICC (if >10% blasts) guidelines. We previously reported 129 *MECOM-R* cases with a wide spectrum of 3q26.2 aberrations. This study is currently extended to a cohort of 295 cases. Many newly identified 3q26.2 aberrations are subtle or cryptic for karyotyping. They presented huge diagnostic challenges. **Methods:** Karyotyping, interphase-, metaphase-, and/or map-back MECOM Breakapart fluorescence *in situ* hybridization (FISH) were performed on bone marrow cultures in all cases and optical genome mapping (OGM) in 2 cases. **Results:** This cohort included 295 patients (M/F = 173/122) with *MECOM-R*. Their median age was 65 years (range 17 to 92 years). Their

diagnoses following the WHO 2017 were 166 AML, 94 myelodysplastic syndrome (MDS), 27 chronic myelogenous leukemia, 4 chronic myelomonocytic leukemia (CMML), and 5 mixed phenotype acute leukemia. All the MDS and CMML cases can be re-categorized as AML by following the 5th WHO; and 70 MDS and all CMML cases can be re-categorized as AML by following the ICC guidelines, respectively. During a follow-up of 0 to 122 months (average 9 months), 218 (73.9%) patients died with disease, 56 (19%) had persistent disease or achieved partial remission, and 21 (7.1%) achieved complete remission. Less than 50% of cases presented classic inv(3)(q21q26.2) (n = 122) or t(3;3)(q21;q26.2) (n = 19), whereas the rest showed a wide spectrum of non-classic 3q26.2 aberrations, including pericentric inv(3)s (n = 17); non-classic paracentric inv(3) (n = 5); other translocations (n = 98) including t(1;3), t(2;3), t(3;4), t(3;6), t(3;8), t(3;10), t(3;12), t(3;13), t(3;17), t(3;21), and t(3;22); insertions (n = 8); and unknown mechanisms (n = 27). About 54.6% cases exhibited a complex karyotype, and 12.9% had an isolated 3q26.2 aberration; 37.3% cases had -7/7q- but their frequency was much higher in cases with pericentric inv(3)s (70.6%), non-classic paracentric inv(3)s (80%) and t(3;3) (47.4%) but much lower in cases with t(2;3) (23.8%), t(3;6) (14.3%), t(3;8) (27.3%), and t(3;12) (26.7%) than the average level. No statistical significances for frequencies of complex karyotype and -7/7q- and overall survivals were observed between cases with classic inv(3)/t(3;3) and those with non-classic 3q26.2 aberrations. **Conclusions:** The status of 3q26.2 aberrations/*MECOM-R* is vital for diagnosis, prognosis, and clinical management of patients with myeloid malignancies, but the *MECOM-R* associated 3q26.2 aberrations are complicated. Due to the complicated nature of 3q26.2 aberration/*MECOM-R*, some are cryptic/subtle for karyotyping, a highly sensitive and specific testing such as MECOM Breakapart FISH, OGM, and/or whole-genome sequencing are warranted for all cases with myeloid neoplasms at their initial workup.

H11. Distribution of Molecular Markers of Chronic Myeloproliferative Neoplasm among Pakistani Population

Z. Ansar Ahmed, S. Naz, A. Ujala, T. Moatter
Aga Khan University, Pathology and Lab Medicine Molecular Pathology Section, Karachi, Pakistan.

Introduction: Myeloproliferative neoplasms (MPNs) are clonal hematopoietic stem cell malignancies, characterized by excessive production of blood cells. The World Health Organization (WHO) provides diagnostic criteria for the following MPN subtypes: chronic myelogenous leukemia; *BCR-ABL1*–positive; polycythemia vera (PV); essential thrombocythemia (ET); primary myelofibrosis (PMF); chronic neutrophilic leukemia; chronic eosinophilic leukemia, not otherwise specified; mastocytosis; and MPN-unclassifiable (MPN-U). Common molecular events in MPNs are the V617F mutation in the *JAK2* gene, mutations of exon 10 of the *MPL* gene (mainly involving codon W515), and *JAK2* mutations on exon 12, which are included as one of the diagnostic criteria. Recently, novel frameshift mutations in exon 9 of the *Calreticulin* (*CALR*) gene were found using next-generation sequencing in patients with *JAK2* or *MPL* nonmutated PMF and ET. In this study, we investigated the mutation profiles of *BCRABL1, CALR, JAK2*, and *MPL* mutations in 4 different MPN subtypes in Pakistani patients with PMF, ET, PV, and MPN-U in a single tertiary health care center. **Methods:** This retrospective observational study was conducted at the Section of Molecular Pathology, Aga Khan University Hospital, Karachi, Pakistan, over a period of 6 months (from November 2021 to April 2022) that included patients with MPNs diagnosed as per the World Health Organization (WHO) criteria. Laboratory-integrated system was then used to retrieve the data including age, gender, and MPN mutations. **Results:** Out of the tested 916 patients, males comprised 73% of the total, whereas females were 27% included in the full analysis. The median age was 46 years (range, 16 to 87 years). A total of 56 patients were reported to have the *BCR-ABL1* transcript (b2a2, b3a2, and e1a2) . A total of 166 patients were reported with non-*BCR-ABL* MPN mutations in *JAK2* exon 14, 157 (65%); *CALR* fs46/*CALR* fs47, 7 (27%); *MPL*, 1 (4%); *CKIT*, 1 (4%), and no mutation detected in *JAK2* exon 12 during the study period. **Conclusions:** The prevalence and incidence of MPNs in Pakistan were derived using the number of patients visiting hospital. Thus, the prevalence reported here is not directly comparable with the entire country. Currently, there are no data in percentage of PV, ET, PMF, and *JAK2*(V617F) exon 14 mutation found significantly in Philadelphia -ve (non-*BCR-ABL*) myeloproliferative neoplasms.

H12. Additional Chromosomal Abnormalities in Philadelphia Positive Chronic Myeloid Leukemia in the Era of Tyrosine Kinase Inhibitor Therapy of Pakistani Patients

Z. Ansar Ahmed, S. Hussain, H. Hayat, T. Moatter, A. Zehra
Aga Khan University, Pathology and Lab Medicine Molecular Pathology Section, Karachi, Pakistan.

Introduction: Chronic myeloid leukemia (CML) is a myeloproliferative disorder characterized by the presence of the Philadelphia (Ph) chromosome resulting from the reciprocal translocation t(9;22)(q34;q11). It has been reported that in 5% to 10% of newly diagnosed CML cases, 1 or more

additional chromosomes are added to 9 and 22 and are involved in the translocation, and this is termed variant translocation. In certain cases chromosome changes are submicroscopic, so the translocation can be masked and revealed only by fluorescence *in situ* hybridization or by BCR-ABL PCR analysis. In the pre-imatinib era, some studies reported a strong association of variant translocations with the presence of der(9) deletions, which indicate that the poor prognosis may be due to the increased frequency of the latter change. To the best of our knowledge, in Pakistani patients, no systematic studies of early chronic phase patients in large prospective clinical trials with imatinib have been reported. **Methods:** Analysis was performed on pretreatment bone marrow samples using conventional G-banding techniques. Bone marrow samples were cultured using standard culture techniques followed by harvesting (incubation, centrifugation, and addition of hypotonic solution). After addition of fixative (3:1 methanol to glacial acetic acid) and trypsin treatment, Giemsa staining was performed. Slides were examined under microscope and at least 20 mitosis were analyzed whenever possible. In all cases, the diagnosis of CML was confirmed by morphology on peripheral blood and bone marrow aspirate and H&C on trephine where possible using standard methodologies. **Results:** A total of 1,021 patients were diagnosed with CML during the study period from January 2017 to June 2019. There were 627 males and 394 females (M:F = 1.6:1. A normal karyotype was identified in 180 (17.6%) patients and abnormal karyotype in 825 (80%) patients (Table 1). The most prevalent chromosomal abnormality was t (9;22) (q34; q11.2), which was present in 699 (68.5%) of 1,021 patients. CML with 3-way translocation including t(9;22) occurred in 44 (4.3%) and CML with additional translocation including with t (9;22) was present in 23 (2.2%) patients. Numerical cytogenetic abnormalities including trisomy 8 (80%), -Y:63% and monosomy 7 (21%) were identified in 49 (4.8%) patients (Table 1). Ten patients (1%) had CML with Double Ph t (9;22). **Conclusions:** In conclusion, we report the additional abnormalities in Philadelphia positive CML include 3- way and numerical cytogenetic abnormalities; however, for further strengthening our finding we need larger studies to understand the evolving mechanism and occurrence. Therefore, our data suggest that patients with variant translocations do not constitute a "warning" category in the imatinib era

H13. AML Relapse after Stem Cell Transplant from a Presumed Carrier of MyD88 Deficiency

C. Karakas[1], M. Buldo[2], K. P. Loh[3], O. Aljitawi[3], Z. Oltvai[2], V. L. Casler[4], A. N. Jajosky[2]

[1]University of Rochester Medical Center, Department of Pathology and Laboratory Medicine/Anatomic Pathology, Rochester, MN; [2]University of Rochester Medical Center, Molecular Pathology and Laboratory Medicine/Molecular Diagnostics Laboratory, Rochester, MN; [3]University of Rochester Medical Center, Department of Medicine/Hematology and Oncology, Rochester, MN; [4]University of Rochester Medical Center, Department of Pathology and Laboratory Medicine/Molecular Pathology, Rochester, MN; [5]University of Rochester Medical Center, Department of Pathology and Laboratory Medicine/Bioinformatics, Rochester, MN.

Introduction: A 64-year-old man with a history of myelodysplastic syndrome (MDS) developed acute myeloid leukemia with myelodysplasia-related changes (AML-MRC). Given the poor prognosis, he underwent an HLA-matched unrelated donor (MUD) hematopoietic stem cell transplantation (HSCT). His post-transplant course was complicated by infections, chronic graft-versus-host-disease (GvHD) requiring a cornea transplant, and AML relapse. Targeted next-generation sequencing (NGS) unexpectedly revealed his MUD was likely a carrier of MyD88 deficiency, a rare autosomal recessive immunodeficiency caused by inactivating *MYD88* variants and characterized by susceptibility to life-threatening bacterial infections in infancy and childhood. About 24 cases of MyD88 deficiency have been reported to date. **Methods:** NGS was performed on pre- and post-transplant bone marrows (BMs) using a 34-gene Illumina Myeloid panel. Post-transplant chimerism testing was performed by PCR of informative short tandem repeats (STRs). **Results:** NGS of his initial BM biopsy involved by MDS with excess blasts-2 (MDS-EB-2) identified an oncogenic *IDH2* p.R172K variant. Subsequent transformation of MDS-EB-2 to AML-MRC was accompanied by acquisition of an *SRSF2* p.P95L mutation. Although chimerism studies initially showed full donor BM engraftment, rising levels of recipient DNA (12%) were detected 20 months after transplant. This prompted re-evaluation of the BM (Fig. 1), confirming relapsed AML with: 1) re-emergence of the *IDH2* p.R172K mutation at a variant allele frequency (VAF) of 7%, and 2) acquisition of a new *NRAS* p.G12D mutation at a VAF of 3%, likely reflecting tumor evolution. Surprisingly, a likely pathogenic *MYD88* p.Q262Ter variant was also found at a VAF of 45%, seemingly aligned with the 88% donor DNA in the sample. To investigate a possible heterozygous germline *MYD88* variant in the stem cell donor, retrospective NGS of the donor's pre-transplant blood was performed and

confirmed *MYD88* p.Q262Ter was present at a VAF of 48%. **Conclusions:** This is the first reported case of HSCT from a presumed carrier of MyD88 deficiency. Since the impact of donor immune system defects on HSCT outcomes is largely unexplored, we do not know why this patient ultimately relapsed. Studies in Myd88-deficient mouse models suggest the donor's T-cells may exhibit impaired graft-versus-leukemia (GvL) activity that promoted AML evolution and relapse. This case also raises important ethical considerations: Should clinicians inform stem-cell donor registries about incidental germline findings (associated with inherited disease and/or hereditary predisposition to cancer), so that donors can receive genetic counseling and follow-up testing? Should carriers of severe immunodeficiencies be excluded from stem cell donation even if they are otherwise healthy? Careful study of transplant outcomes will help to answer these questions and clarify whether genetic screening of stem cell donors is warranted.

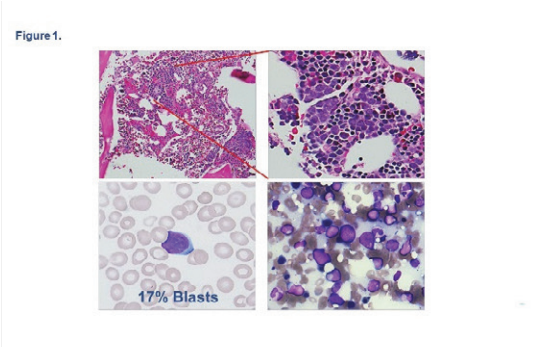

Figure 1. Bone Marrow Biopsy & Touch Prep & Peripheral Smear
Figure 1 shows clonal monotonous atypical proliferation of leukemic cells in the bone marrow biopsy and myeloid blasts on touch prep & peripheral smear, consistent with the "Relapsed AML" 20 months after hematopoietic stem cell transplantation.

H14. Retrospective Assessment of 18 Hematological Malignancy Genomes by Optical Genome Mapping

T. Kelly, A. Korpetinou, P. Pollakis, V. Katsini, D. Iakovaki, G. Christopoulou, P. Constantoulakis
Genotypos MSA, Athens, Greece.

Introduction: For the diagnosis, prognosis, and management of hematological malignancies, the assessment of well-described genomic rearrangements is of critical importance. Conventional methods used for the determination of these genomic aberrations are classical karyotyping, fluorescence *in situ* hybridization (FISH), and molecular karyotyping (aCGH). Optical genome mapping (OGM) is a high-resolution technology rapidly gaining interest for its capacity to detect structural variants (SVs) and copy number variants (CNVs) genome-wide in 1 single assay. Studies have shown that OGM can simplify lab workflow by reducing turnaround time and reducing multiple tests into one. Our objective was to evaluate OGM against standard techniques used in our laboratory in all different kinds of samples and highlight its usefulness in the management of patients with hematological neoplasms. **Methods:** In total, 18 clinical cases from patients with different probable diagnoses were retrospectively assessed. Bone marrow (BM) or peripheral blood samples were processed with karyotype/FISH with standard procedures. Ultra-high molecular weight DNA was isolated from the same samples, labeled, and processed for analysis on the Bionano Genomics Saphyr platform following the manufacturer's protocols (Bionano Genomics, San Diego, US). Genome-wide analyses for SVs and CNVs was performed using the Rare Variant Pipeline Analysis on Bionano Access (v.1.7)/Bionano Solve (v.3.7). Results from conventional chromosomal analyses were compared to those of OGM. **Results:** Results between OGM analysis and conventional techniques were concordant in 13/18 samples. In particular, aneuploidies, deletions or duplications of chromosomal regions, and translocations were accurately determined, whereas in 5 cases, 7 new clinically significant SVs were observed that were not detectable by conventional methods. Interestingly, in 1/18 cases with a normal karyotype, microdeletions in genes of clinical importance (*STIL, CDKN2A, MTAP*) were identified, due to higher OGM resolution. Also, 2 cases were evaluated blindly as part of interlaboratory comparison, resulting in complete agreement. Finally, in 4 cases OGM analysis failed to detect the events described by conventional methods, mainly due to extended BM culture upon stimulation. **Conclusions:** In this study, OGM showed high concordance (72.2%) with our standard-of-care techniques. Excluding samples with culture bias, concordance was >90%, making the method a reliable tool for the detection of abnormalities in hematological malignancies. Furthermore, OGM provided more information in 27.7% of cases, showing 7 new SVs that were missed by routine methods and were of clinical significance, which translates to an increase in diagnostic yield. The increased resolution of OGM analysis is expected to reveal novel genomic aberrations, which may redefine the established prognostic subgroups, and/or lead to better understanding of the pathophysiology and molecular biology of treatment response.

H15. Automated Round Nuclei Selection Improves FISH Analysis in CLL

X. Xu, J. Seheult, S.A. Smoley, K.K. Fisch, R.G. Meyer, C.A. Sattler, M. Shi, P. Greipp, R. Ketterling
Mayo Clinic, Department of Laboratory Medicine and Pathology, Rochester, MN.

Introduction: Fluorescence *in situ* hybridization (FISH) analysis is routinely performed to detect common cytogenetic abnormalities that are key prognostic markers for chronic lymphocytic leukemia (CLL). Low lymphocyte fraction in a subset of CLL cases imposes risk of false-negative FISH results. Since CLL cells typically exhibit round nuclear morphology, scoring round nuclei during FISH analysis can improve the sensitivity for detecting cytogenetic abnormalities. In this study, we evaluated the feasibility of automated round nuclei selection using morphology metrics and its impact on FISH scoring analysis. **Methods:** Sixteen clinical cases with 24 abnormal CLL FISH sites including deletions 13q, 11q, 17p, trisomy 12, and *IGH::CCND1* were selected. Manual scoring of 300 consecutive nuclei regardless of nuclear morphology was performed by technologists to determine the FISH abnormality percentage representative of the abnormal CLL cell fraction in each case. In addition, each nucleus was classified as either round or irregular by technologists. Features of nuclear morphology, including aspect ratio (AR) and irregularity, were obtained from the analysis software for each scanned cell image (Metafer, MetaSystems Inc.) and used to calculate 2 additional parameters: irregularity inverse (II = 1-Irregularity), and a composite of AR and irregularity (IAR = [1-Irregularity]*Aspect Ratio)^2). Empirical cutpoint estimation (Youden method) was used to establish the optimal cut-off of AR, II, and IAR to discriminate between round and irregular nuclei. Sensitivity and specificity for automated round cell selection at the optimal cutpoint for AR, II, and IAR were calculated using the manual nucleus shape classification as ground truth. The percentage of abnormal nuclei in automatically selected round nuclei was compared to that obtained from manual consecutive scoring of all cells. **Results:** Optimal cutpoints, and the corresponding sensitivity and specificity of AR, II, and IAR, as well as the average difference in percentage increase for each FISH site by applying each metric's cutpoint, are summarized in Table 1. The percentage of nuclei with an abnormal FISH pattern was significantly higher with automated round nuclei selection compared to manual consecutive scoring of all cells.

Table 1.

Metrics	Optimal Cut-off	Sensitivity	Specificity	P-value	Average Increase in Percentage of Abnormal Cells				
	del13q	del11q	trisomy 12	*IGH::CCND1*	del17p				
AR	0.9192	80%	68%	0.000028	8.08%	2.76%	6.56%	8.88%	8.38%
II	0.4535	78%	79%	0.000086	8.62%	3.12%	9.59%	17.94%	9.68%
IAR	0.1779	78%	78%	0.00012	9.03%	3.43%	8.23%	17.73%	10.61%

Conclusions: This pilot study demonstrates the feasibility of applying nuclear morphology metrics from a commercially available digital FISH platform to automate round nucleus selection for CLL FISH scoring. This approach results in a higher percentage of abnormal cells and can be used in conjunction with routine analysis in cases with low lymphocyte fraction or concern for false-negative FISH results.

H16. Severe Systemic Auto-Inflammation in an Elderly Woman with Clonal Hematopoiesis

G. George[1], J.L. Liesveld[2], P. McMullen[1], S.El Hussein[1], A. Jajosky[1]
[1]*University of Rochester Medical Center, Department of Pathology and Laboratory Medicine, Rochester, MN;*
[2]*University of Rochester Medical Center, Department of Hematology and Oncology, Rochester, MN.*

Introduction: An 89-year-old woman developed cutaneous Langerhans cell histiocytosis (LCH) (Fig. 1) in association with other severe auto-inflammatory manifestations, including temporal arteritis (Fig. 2), polymyalgia rheumatica, chronic demyelinating polyneuropathy, and malakoplakia. Molecular characterization of her LCH revealed low-level oncogenic *MAP2K1*, *IDH2*, and *SRSF2* mutations. Interestingly, the same *IDH2* and *SRSF2* mutations were highly enriched in her blood, suggesting a common clonal hematopoietic origin and identifying these somatic variants as potential mediators of systemic auto-inflammation. **Methods:** Targeted DNA-based next-generation sequencing (NGS) was performed on her cutaneous LCH using the 35-gene Oncomine Focus Assay and 45-gene Oncomine Myeloid Assay GX, designed for solid tumors and myeloid malignancies, respectively. Targeted DNA-based NGS was also performed on the peripheral blood using the 34-gene Illumina TruSight Myeloid Panel. **Results:** NGS of her LCH revealed oncogenic *MAP2K1* p.C121S (VAF = 4%), *IDH2* p.R140Q (VAF = 8%), and *SRSF2* p.P95L (VAF = 6%) mutations. Since *IDH2* mutations have not been reported in LCH but are well described in hematologic malignancies, myeloid NGS was performed on her blood despite relatively normal blood counts. Both the *IDH2* p.R140Q (VAF = 46%) and *SRSF2* p.P95L (VAF = 51%) mutations were highly enriched in her blood, consistent with clonal hematopoiesis. The *MAP2K1* mutation was not detected in the blood, suggesting that it is a specific acquired

driver of LCH. **Conclusions:** The discovery of clonal hematopoiesis in this elderly woman with a wide spectrum of severe auto-inflammatory conditions supports a potentially intriguing link between somatic blood mutations and her adult-onset rheumatologic disorders. Mechanistically, disrupted *SRSF2*-mediated splicing may be driving aberrant antigen presentation by bone marrow-derived dendritic cells in her skin and other organs. Causal relationships between somatic blood mutations and autoimmune/auto-inflammatory conditions have been established in patients with hematologic malignancies and conditions like VEXAS syndrome. Although this patient does not meet diagnostic criteria for a hematologic malignancy, she will be closely monitored given her mutational profile and dysregulated hematopoiesis that may manifest as a myeloid malignancy. Of note, this is the first reported case of *IDH2*-mutated LCH, raising the potential therapeutic utility of IDH2 inhibitors in this entity. Fortunately, she is responding to treatment with steroids and the anti-IL6R biologic, toclizumab.

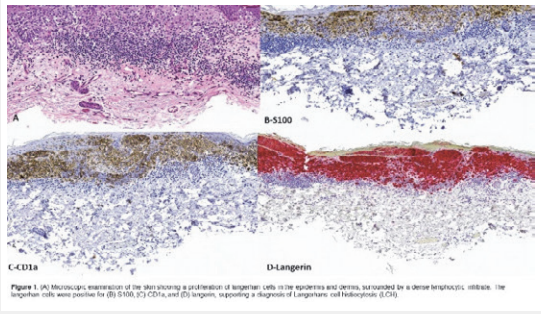

Figure 1. (A) Microscopic examination of the skin showing a proliferation of Langerhans cells in the epidermis and dermis, surrounded by a dense lymphocytic infiltrate. The Langerhans cells were positive for (B) S100, (C) CD1a, and (D) langerin, supporting a diagnosis of Langerhans cell histiocytosis (LCH).

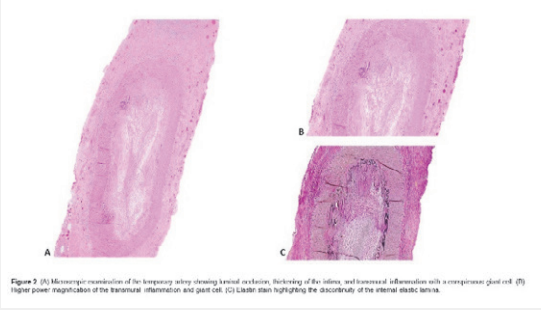

Figure 2. (A) Microscopic examination of the temporary artery showing luminal occlusion, thickening of the intima, and transmural inflammation with a conspicuous giant cell. (B) Higher-power magnification of the transmural inflammation and giant cell. (C) Elastin stain highlighting the discontinuity of the internal elastic lamina.

H17. Genomic Evolution of Philadelphia Negative Myeloproliferative Neoplasms with Double Driver Mutations

R. Sardana[1], L. Boiocchi[1], J. Yao[1], D. Lee[2], R. K. Rampal[3], M. Arcila[1], M. Ewalt[1]

[1]Memorial Sloan Kettering Cancer Center, Department of Pathology and Laboratory Medicine, New York, NY; [2]NewYork-Presbyterian/Weill Cornell, Department of Medicine, New York, NY; [3]Memorial Sloan Kettering Cancer Center, Leukemia Service, New York, NY.

Introduction: Myeloproliferative neoplasms (MPNs) are a group of hematopoietic cancers classified as Philadelphia positive (chronic myeloid leukemia) and Philadelphia negative, of which the most common entities are polycythemia vera, essential thrombocytosis, and primary myelofibrosis. Whereas mutations in driver genes (*CALR, MPL,* and *JAK2*) in these disorders were initially described as mutually exclusive, recent studies have shown rare cases which harbor mutations in 2 or more of these genes, so-called Double Driver Mutant (DDM) MPNs. To date, the effect of these multiple mutations on disease evolution has not been well studied, and we here present a series of patients with DDM MPN and sequential follow-up. **Methods:** Following approval from our institutional review board, patient data was retrieved from clinical records. A total of 1,189 patients were identified who had undergone comprehensive genomic profiling by next-generation sequencing (NGS) and harbored at least 1 mutation in *CALR, JAK2,* and/or *MPL*. In 52 patients, 2 or more alterations were found in these genes. In all, 19 of these patients had 3 or more NGS evaluations over their follow-up. The pathogenicity of the mutations in *CALR, JAK2,* and *MPL* was assessed according to the Clinical Genome Resource, Cancer Genomics Consortium, and Variant Interpretation for Cancer Consortium guidelines. In 11 patients, both mutations were classified as Pathogenic (P) or Likely Pathogenic (LP) and thus represented DDMs for inclusion in this study. The clonal evolution was graphically represented using the fish plot package for R by Miller *et al*. **Results:** Clinical features are described in Table 1. From the point of identification of the DDMs, 2 patterns were noted in this cohort: 1) persistence of DDMs and baseline mutations with minimal change in variant allele fraction (VAF), n = 7/11; and 2) acquisition of additional mutations and changing clonal dynamics with change in VAF, n = 4/11. In the former group with stable clonal dynamics, the patients' clinical status remained relatively stable with only increasing myelofibrosis but stable peripheral blood parameters and bone marrow blast counts. In the latter group, clonal evolution was accompanied by clinical progression characterized by morphologic dysplasia and in 1 patient, transformation to acute myeloid leukemia. Representative

examples of these patterns are shown in Figure 1.

Conclusions: The stable clinical course of the DDM MPN patients in our cohort with stable clonal dynamics is in line with the findings of The FIM study (2017) in that the presence of DDM in itself does not necessarily alter the course of disease. Rather, the correlation of disease progression with additional clonal evolution in our cohort suggests that clinical progression is driven by additional genetic hits outside of *CALR, JAK2,* and *MPL* in the neoplastic clone and that no additional negative prognostic effect should be assumed in patients with DDM in the absence of such additional alterations.

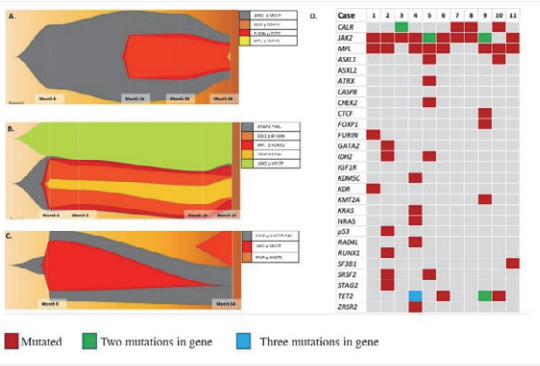

Figure 1
Fish plots showing clonal evolution of various subclones in case 1 (A), 2 (B), and 7 (C), although the order of events depicted can be deduced from the single-clone analysis (the origin of the clones is predicted from the VAF of individual mutation here). **D** shows an oncoprint of the cases in this cohort at the timepoint with the greatest number of mutations.

Case	Age at Dx	Sex	Initial Diagnosis	Spleno-megaly	Reticulin fibrosis at diagnosis	Reticulin Fibrosis at last follow-up	Progression / Transformation	Duration of follow-up (months)
1	75	F	PV	No	0	3+	MDS	47
2	70	F	ET	No	1	3+	AML	28
3	70	M	PMF	Yes	1	2+	MF	56
4	67	F	PMF	Yes	1	2+	MDS/MPN	71
5	73	M	MPN-U	No	2	3+	MDS/MPN – MF	32
6	66	M	PMF	No	2	2+	None	75
7	83	M	PMF	Yes	1	1+	None	67
8	57	M	ET	No	1	1+	None	66
9	68	M	ET	No	1	3+	MDS/MPN – MF	58
10	47	M	ET	Yes	3	3+	MF	52
11	62	M	PMF	Yes	2	3+	MF	27

Table: 1 Clinical Features
Clinical characteristics of patients. PV – polycythemia vera, ET – essential thrombocytosis, PMF – primary myelofibrosis, MPN-U – myeloproliferative neoplasm unclassifiable, MDS – myelodysplastic syndrome, AML – acute myeloid leukemia, MF – myelofibrosis, MDS/MPN – myelodysplastic/myeloproliferative neoplasm.

H18. MYC Status along with *BCL2*, *BCL6* Rearrangements in High-Grade B-Cell Lymphoma

Z. Ansar Ahmed, M. Sharif, S. Siddiqui, F. Faisal, R. Zaki
Aga Khan University, Pathology and Lab Medicine Molecular Pathology section, Karachi, Pakistan.

Introduction: Non-Hodgkin lymphoma (NHL) is the eighth most diagnosed cancer in men and the11th in women. Diffuse large B-cell lymphoma (DLBCL) includes a heterogeneous group of non-Hodgkin lymphoma with different prognoses and molecular and clinical characteristics. *MYC, BCL2*, and *BCL6* are most commonly involved in B-cell lymphomas. Translocations of these oncogenes are associated with an aggressive clinical course. This study aimed to find the distribution of *MYC, BCL2*, and *BCL6* rearrangements in high-grade B cell lymphoma. **Methods:** A total of 110 formalin-fixed, paraffin-embedded blocks were included in our study. The fluorescence *in situ* hybridization (FISH) assay was performed for t(8;14) by probes from Abbott Molecular (US) on 63 Burkitt lymphoma cases, comprising 55 males and 8 females. Moreover, 47 samples, including 24 males and 23 females diagnosed as DLBCL, were evaluated for *MYC, BCL2*, and *BCL6* gene status by break-apart FISH probes. **Results:** Out of 63 samples analyzed, 21 samples of Burkitt lymphoma showed 63% positivity for translocation (8;14), whereas 31% of 42 samples of DLBCL exhibited t(8;14). Furthermore, out of 47 specimens examined for double- and triple-hit lymphoma, 12 cases belonged to double expressor and 35 patients to triple expressor groups. In all, 18% of the total showed positivity for *BCL2* gene rearrangement, 34% showed positivity for *BCL6* gene rearrangement, and 14% showed positivity for *MYC* gene rearrangement. In comparison, 1 sample was positive for triple-hit lymphoma, and 1 was positive for double-hit lymphoma based on FISH studies. **Conclusions:** These data showed the complex nature of molecular events in DLBCL and Burkitt lymphomas. Limited concordance between immunohistochemistry and FISH results reflects these lymphomas' morphologic and clinical heterogeneity

H19. Unraveling the Somatic Mutational Landscape in Myelodysplastic Syndrome: A Single-Center Experience

I. Dey[1], S. Vinarkar[2], M. Parihar[3], K. Patel[1], R. Demde[1], K. Saha[1], S. Banerjee[1], D. Nathi[1], A. Nag[4], J. Kumar[4], R. Nair[4], M. Chandy[4], D. K. Mishra[2]

[1]Tata Medical Center, Kolkata, India, Department of Molecular Genetics, Kolkata, India; [2]Tata Medical Center, Kolkata, India, Department of Molecular Genetics and Laboratory Haematology, Kolkata, India; [3]Tata Medical Center, Kolkata, India, Department of Cytogenetics, Molecular Genetics and Laboratory Haematology, Kolkata, India; [4]Tata Medical Center, Kolkata, India, Department of Clinical Hematology and Bone Marrow Transplant, Kolkata, India.

Introduction: Myelodysplastic syndromes (MDS) are clonal hematological disorders characterized by cytopenia, hematopoietic cell dysplasia, and a predisposition to transform into leukemia. Tremendous interest in the complex genetics of MDS is made evident by the emerging diagnostic, prognostic, therapeutic genetic biomarkers and as highlighted by the recent integration of mutation profile into the prognostic scoring of MDS (IPSS-M). High-throughput next-generation sequencing (NGS) has been instrumental in unraveling this complex genetic landscape of MDS. The aims and objectives were to study the genomic profile of patients with Myelodysplastic syndrome using Next generation sequencing at our center. **Methods:** Routine workflow in assessment of MDS at our center involved peripheral blood, bone marrow examination, cytogenetic study, and comprehensive myeloid panel (NGS). We studied the mutational profile of 46 cases of *de-novo* MDS diagnosed between March 2019 and May 2022. DNA and RNA were extracted from bone marrow samples, followed by library preparation using the Ion Torrent Oncomine Myeloid Research Assay. DNA and RNA sequencing was performed on Ion PGM System. Sequencing reads were aligned using Torrent suite (5.12.1), followed by annotation of .BAM files with Ion Reporter (v 5.18.4.0). **Results:** Over a 3-year period, 46 cases were diagnosed as MDS based on the clinical, morphological, and cytogenetic findings, out of which 56% (n = 26/46) patients were ≥60 years of age, M:F ratio was 1.8:1, and 78% (n = 32/46) had good cytogenetic risk (IPSS-R). In all, 61% (n = 28/46) of cases had ≥1 pathogenic variant, and 36% (n = 10/28) of mutated cases had a single gene variant, whereas the rest had multiple (2 to 4) mutations. MDS-MLD (46%, n = 21/46) was the most common morphological classification and most frequent mutated subgroup, followed by MDS-EB (30%, n = 14/46). According to functional genetic categories, the majority of the mutated genes belonged to DNA methylation (50%, n = 14/28), followed by RNA splicing regulators (46%, n = 13/28), and transcription regulating genes (39%, n = 11/28). The most frequently mutated gene was *TET2* (39%, n = 11/28), followed by *RUNX1* (21%, n = 6/28), and most commonly co-mutated genes were *TET2* and *SRSF2* (29%, n = 5/17). Three patients transformed to acute myeloid leukemia, out of which 1 had *TP53* gene variant. Five patients (11%) succumbed to disease/therapy-related complications, out of which 2 harbored mutations in *TP53* gene. **Conclusions:** We studied the genetic profile of 46 MDS cases using NGS. The mutation frequency of MDS at our center was 61%, which was concordant with published literature. *TET2* and *RUNX1* genes were the most frequently mutated genes, and *TP53* gene-mutated patients showed progression and poor outcomes. We could hence conclude that targeted NGS panels can help in detecting recurrent mutations associated with this rare disorder.

H20. Acquired *GATA2* Mutations in CSF3R-Negative Chronic Neutrophilic Leukemia

M. Jin, J. Gomez-Gelvez, B. Shaw, O. Kis, Y. Shen

Henry Ford Hospital, Detroit, MI.

Introduction: Chronic neutrophilic leukemia (CNL) is a *BCR::ABL1*-negative myeloproliferative neoplasm (MPN) characterized by sustained neutrophilia with ≥80% segmented neutrophils and bands, bone marrow (BM) granulocytic proliferation, activating *CFS3R* mutations, and absence of dysplasia or monocytosis. Acquired *GATA2* mutations have previously been found in myeloid neoplasms. In acute myeloid leukemia, somatic *GATA2* gain-of-function mutations have correlated with poor outcome. *GATA2* mutations are rarely found in CNL. Here, we describe a patient with CSF3R-negative CNL and acquired *GATA2* mutations. **Methods:** Peripheral blood and BM samples were collected from the patient after obtaining informed consent. Flow cytometric analysis, chromosome analysis, and fluorescent *in situ* hybridization (FISH) were performed on BM aspirates. Next-generation sequencing (NGS) analysis was performed on DNA extracted from the patient's BM on Illumina NextSeq Dx 550. **Results:** The 95-year-old female patient presented with slight leukocytosis. The white blood cell count at diagnosis was 25.2 × k/uL, 82% neutrophils, and <10% granulocytic precursors on manual differential, with anemia (8.1 g/dL) and thrombocytopenia (64 × k/uL). BM biopsy showed hypercellular marrow (80% to 90%) with marked granulocytic hyperplasia, high M:E ratio (13:1), 4% myeloid blasts, and no overt dysplasia in all lineages. Flow cytometry showed abnormal myeloblasts with aberrant CD5 expression, and polytypic plasma cells. Chromosome analysis showed a normal female karyotype, and MDS/MPN FISH showed normal results for all loci studied. Of note, FISH was negative for *BCR::ABL1* t(9;22) translocation. Myeloid NGS panel

analysis demonstrated multiple pathogenic/likely pathogenic mutations including *ASXL1* E635Rfs*15 with variant allele frequency of 40.7%, *U2AF1* R156H (47.9%), *GATA2* L138Hfs*81 (36.5%), and *GATA2* G292Rfs*93 (5.4%). The 2 acquired *GATA2* mutations in this patient are predicted to be in *trans* and thus will lead to loss of GATA2 protein function due to the loss of functional zinc finger domains. Morphologic features associated with GATA2 deficiency, namely monocytopenia and atypical megakaryocytes with separated lobes, were identified in this patient. Following diagnosis in July 2022, the patient progressed with marked monocytopenia, anemia, and thrombocytopenia, requiring frequent supportive transfusions. She passed away 5 months after CNL diagnosis. **Conclusions:** CSF3R-negative CNL is a challenging diagnosis, as it does not carry the mutation that classically defines the entity. Whereas *CSF3R* mutations may be most common in CNL, this case showed that it might not always be the central factor in development of this disorder. This case also demonstrated morphological features of GATA2 deficiencies found previously, monocytopenia, and atypical megakaryocytes with separated lobes. Acquired *GATA2* mutations in CNL, an entity which rarely carries them, increase the complexity of disease presentation and may have prognostic value.

H21. Co-existence of *CALR* and *JAK2* or *MPL* Mutations in Myeloid Disorders: A Reference Laboratory Experience

X. Zhang, J. Yuan, M. Shi, K. Bessonen, D. Viswanatha, R. He

Mayo Clinic, Department of Laboratory Medicine and Pathology, Rochester, MN.

Introduction: *JAK2*, *CALR,* and *MPL* mutations are the most frequent driver events in *BCR-ABL1*-negative myeloproliferative neoplasms (MPNs). These mutations are generally considered mutually exclusive, due to their convergent roles in the activation of the JAK/STAT signaling pathway. Although co-mutated cases are occasionally encountered clinically, the incidence and clinical significance of the co-occurrence of these mutations have not been thoroughly explored in a large cohort. We aimed to investigate molecular features of co-existing MPN-associated mutations in our reference lab based on next-generation sequencing (NGS) data. **Methods:** Peripheral blood or bone marrow specimens submitted for myeloid NGS analysis in our institute were collected. A myeloid neoplasm-targeting, 35- or 42-gene panel with capture-based chemistry on an Illumina HiSeq or Novaseq sequencer (San Diego, US) was used. Molecular data of cases with co-existing *CALR* and *JAK2* mutations, or *CALR* and *MPL* mutations were selected and analyzed. **Results:** Out of 25,191 specimens submitted for NGS evaluation of known or suspected myeloid neoplasms, 410 (1.6%) harbored a pathogenic *CALR* mutation with a variant allele frequency (VAF) ranging from 3% to 69%. Thirteen out of 410 (3%) *CALR*-mutated cases had a co-existing pathogenic *JAK2* or *MPL* mutation: 5 (5/13, 38%) with a *JAK2* V617F mutation (VAF range 6% to 22%), and 8 (8/13, 62%) with an *MPL* mutation (W515R/L, S505N, Y591D, VAF range 5% to 39%). Co-existence of *JAK2*, *CALR,* and *MPL* mutations were not identified. Seven (7/13, 54%) cases showed clonal VAF of greater than 10%. The VAF differences of the 2 driver mutations ranged from 2% to 45%, with 8 and 5 cases showing higher and lower *CALR* VAFs, respectively. In 8 cases, the VAF difference was greater than 10%, suggesting that 1 mutation likely occurred in a founder clone and the other mutation occurred during clonal evolution. The other 5 cases with similar VAFs of the co-existing mutations may reflect co-existence of similarly sized, distinct clones or mutational co-existence in the same clone. Detailed information of the 13 cases is listed in Table 1. **Conclusions:** Although *JAK2, CALR,* and *MPL* mutations are considered mutually exclusive, double mutations occurred in 3% of *CALR*-mutated cases in our large NGS study cohort. Our findings accentuate the clonal complexity, heterogeneity, and evolution in myeloid disorders. The stepwise approach for sequential testing of *JAK2, CALR,* and *MPL,* until a mutation is identified in MPN, may not identify all the 3 drivers in some cases. The biological mechanism and clinical significance of co-existing MPN-associated driver mutations deserve further studies.

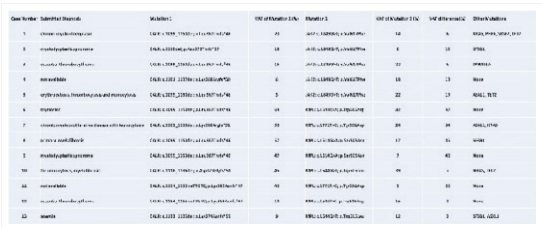

Table 1. Summary of cases with co-existing MPN-associated driver mutations.

H22. Discovery of a Germline *EZH2* Variant, and Underlying Weaver Syndrome, during Sequencing of an Adult B-Cell Acute Lymphoblastic Leukemia

C. R. Syposs[1], K. H. Seymour[2,3], M. Buldo[1], K. O'Dwyer[2], A. N. Jajosky[1]

[1]University of Rochester Medical Center, Department of Pathology and Laboratory Medicine, Rochester, MN; [2]University of Rochester Medical Center, Department of Medicine, Rochester, MN; [3]University of Rochester Medical Center, Department of Pediatrics, Rochester, MN.

Introduction: A 44-year-old woman with intellectual disability and a history of childhood acute lymphoblastic leukemia (ALL) presented with fatigue, night sweats, and easy bruising. She was found to have leukocytosis with 93% circulating B-lymphoblasts. Given her remote history of chemotherapy and radiation treatment for childhood ALL, she was diagnosed with therapy-related B-cell ALL (B-ALL). **Methods:** Targeted DNA-based next-generation sequencing (NGS) was performed at both diagnosis and remission using the Illumina TruSight Myeloid Panel designed to detect substitutions and small insertions/deletions within the mutational hot spots of 34 genes recurrently altered in hematologic malignancies. **Results:** At diagnosis, NGS of a peripheral blood sample containing 93% leukemic blasts identified 2 pathogenic variants: 1) *TET2* p.R1516Ter at 53% variant allele frequency (VAF), and 2) *EZH2* p.E745K at 45% VAF. To investigate the suspected germline origin of the *EZH2* variant, NGS performed during complete remission confirmed the *EZH2* p.E745K mutation was still present at 48% VAF. **Conclusions:** Identification of an *EZH2* p.E745K mutation about 50% VAF during tumor-only sequencing prompted careful review of the medical literature. Somatic *EZH2* mutations are not well described in B-ALL, although germline *EZH2* variants have been reported in Weaver syndrome, a rare autosomal dominant overgrowth disorder documented in 50 individuals to date. Close review of her medical record confirmed she had many clinical features of Weaver syndrome: tall stature (5'11"), a distinctive facial appearance, intellectual disability, a history of developmental delay, and signs of pre- and postnatal overgrowth (99th percentile for childhood growth). She was referred to a genetic counselor, and we are awaiting results of definitive germline testing of skin fibroblasts. Hematologic malignancies developing in infancy and childhood, including ALL, have been described in 2 patients with Weaver syndrome; however, heightened cancer surveillance is not currently recommended. This unusual case of ALL arising in both childhood and adulthood supports a potential link between Weaver syndrome and susceptibility to hematologic cancers. Since we could not obtain her childhood ALL specimen, it is unknown whether the adult B-ALL is a late relapse of her childhood leukemia or a clonally unrelated disease. The working diagnosis of underlying Weaver syndrome (clinically unrecognized for more than 40 years) likely explains her intellectual disability, which appears to have been misattributed to "cerebral palsy" in childhood. By explaining her constellation of seemingly unrelated clinical findings, a genetic diagnosis can provide answers and emotional relief to patients and their families.

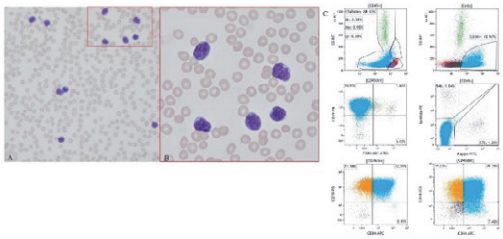

Adult therapy-related B-ALL

Figure 1. Circulating leukemic blasts at initial presentation (A: 10X magnification, B: 50X magnification). C: Immunophenotyping of circulating blasts by flow cytometry establishes a diagnosis of B-ALL. Flow cytometry identified 93% lymphoblasts expressing CD34 (partial, 75%), CD10, CD19, CD22, CD38, CD123, CD200, HLA-DR, and cytoplasmic 79a; TdT was indeterminate.

Persistence of EZH2 p.E745K during complete remission

Figure 2. During complete remission of her B-ALL, NGS of her bone marrow showed persistence of EZH2 p.E745K at 48% VAF, supporting a germline origin.

H23. Validation of a New Next-Generation Sequencing Library Prep Kit for the Detection of Mutations in Hematological Neoplasms

M. S. Basqueira, P. H.S. Rodrigues, R.C. Petroni, S. E.A. da Rosa, R.S. Reis, K.O. Pelegrino, M.C. Cervato, R. A.F. Santana, R. Sitnik, N.H. Muto, P.V. Campregher
Hospital Israelita Albert Einstein, São Paulo, Brazil.

Introduction: Myeloid malignancies are clonal diseases affecting hematopoietic stem or progenitor cells driven by genomic abnormalities. Detection of mutations responsible for these diseases has an impact on diagnosis, prognosis, and therapy. Next-generation sequencing (NGS) technology can achieve this goal because it allows detection of a comprehensive mutation repertory using massively parallel sequencing. However, NGS technology has challenges on detecting highly important genes, such as *CEBPA*, due to high GC content. NGS kit manufacturers have developed different library preparation and analysis strategies to address these challenges. The Archer VariantPlex Myeloid Panel could be a promising kit, since it utilizes Anchored Multiplex PCR (AMP) that enables deep strand-specific amplification of molecular barcoded DNA fragments for sequencing and allows DNA copy number variation, DNA SNP/indel, and DNA structural variation detection. **Methods:** For performance evaluation of VariantPlex Myeloid Panel (Archer), we selected 21 samples with previous results obtained with TruSightMyeloid Sequencing Panel (Illumina). The 21 samples were intended for an accuracy test, and 5 of them were also used for reproducibility assay, 2 samples for duplicate intra-assay, and 3 samples for triplicate inter-assays. For test sensitivity, a pool was prepared with 4 equimolar positive samples to obtain a total of 23 variants with allele frequency ranges from 1.03% to 15.78% and tested 16 times to establish the assay limit of detection (LOD). The Illumina panel includes 54 genes and does not have molecular barcodes, whereas Archer panel targeted 75 genes and has molecular barcodes in methodology. For the Ilumina panel, amplification of the *TP53* and *CEBPA* genes was also performed in parallel to complement the test. Library sequencing was performed on Nextseq 550 platform (Illumina). Data and variant analysis were performed on an online platform from the manufacturer. **Results:** The overall sequencing metrics of both methodologies were satisfactory, with a better coverage uniformity in Archer panel. In accuracy, 21 of 21 (100%) samples presented concordance with the previous results, and 76/76 (100%) variants reported were identified with an allele frequency coefficient of variation of 0.0003 to 0.5521. Intra- and inter-assay reproducibility showed 100% correlation between replicates. The test LOD was established in 5% based on the lowest allelic frequency detected in 100% of the replicates. **Conclusions:** The Archer panel presented high performance and good coverage in GC-rich regions as *CEBPA* gene being a promising test in accuracy of somatic analysis and was validated in our laboratory.

H24. Validation of an Ultra-Sensitive Genomic NGS Assay for Hematological Malignancies (Selected for Oral Presentation, O-04-01)

S.E. DiNapoli[1], E. Gedvilaite[1], A. Bowman[1], F. Xu[1], A.D. Parikh[1], M. Diosdado[1], J. Cassanova-Murphy[1], S. Rana[1], M.H. Haque[1], C. Hale[3], Y-T. Lin[1], Y. Hu[1], G.A. Salles[2], M.F. Berger[1,3], B. Loomis[1,3], M.D. Ewalt[1], M. Arcila[1], A.R. Brannon[1]
[1]Memorial Sloan Kettering Cancer Center, Department of Pathology, New York, NY; [2]Memorial Sloan Kettering Cancer Center, Department of Medicine, New York, NY; [3]Memorial Sloan Kettering Cancer Center, Center for Molecular Oncology, New York, NY.

Introduction: In recent years, analysis of cell-free DNA (cfDNA) by next-generation sequencing has shown clinical utility in non-invasive assessment and monitoring of solid cancer mutations. Preliminary data in lymphoma patients suggest that patients with hematologic malignancies could also benefit from the more sensitive approach that had been developed for cfDNA sequencing. Therefore, we developed and validated MSK-ACCESS Heme (Memorial Sloan Kettering-Analysis of Circulating cfDNA to Examine Somatic Status), a unique molecular indexing (UMI) ultra-deep sequencing assay that examines select exons of 117 genes recurrently mutated in hematological cancer. The assay was designed based upon the New York State Department of Health-approved MSK-IMPACT HEME and MSK-ACCESS SOLID assays, but with the flexibility to interrogate either plasma from lymphoma patients or whole blood samples from leukemia patients. Moreover, the assay was designed to be performed either fully matched or as an unmatched hotspot analysis to enable flexibility around sample collection and turnaround time needs. Herein we present the results of the assay's validation. **Methods:** UMI tagged and dual-barcoded libraries were constructed from 92 plasma or whole blood samples, captured with IDT baits targeting 420kb across select exons of 117 genes, then sequenced on an Illumina NovaSeq 6000. Additionally, 75 healthy donor samples were collected to aid in removing recurrent artifacts and to assess and control for noise at each base of the targeted region. *De novo* variant calling was performed using Vardict, MuTect, Mutect2, and SomaticIndelDetector, and known alterations were genotyped using an internally developed tool, gbcms, to mimic a tumor-informed approach. Results were compared against the same samples sequenced with the already validated and NYS-approved MSK-ACCESS solid assay. **Results:** The average deduplicated consensus sequencing of

the 92 validation samples was 1,509X, with a mean of 1,471X for the plasma samples and 1,673X for the whole blood samples. Background error rate patterns for plasma versus whole blood were notably different, which underscored the need for healthy donor controls to be collected for both plasma and whole blood extraction. A genotyping accuracy of 97% and *de novo* accuracy of 87% were achieved for the 326 mutations identified in the orthogonal assay. The limit of detection analysis using a commercial standard demonstrated the ability to reliably call mutations *de novo* down to 0.5%. **Conclusions:** The analytical validation results demonstrate that MSK-ACCESS Heme is a robust and reliable tool that sensitively and accurately detects clinically relevant alterations in hematological malignancies. Further work will focus on confirming the clinical utility of this assay.

Selected Infectious Diseases Abstracts

ID01. The Long Pentraxin PTX3 Is an Early Prognostic Biomarker of Bacterial or Fungal Co-infections in COVID-19 Patients

F. Scavello[1], E. Nappi[1], I.D. García Martín[1], M. Sironi[1], R. Leone[1], S. Mapelli[1], P. Morelli[2], F.M. Tordato[2], B. Bottazzi[1], A. Mantovani[1,4], C. Garlanda[1,3]
[1]IRCCS Humanitas Research Hospital, Rozzano, Italy; [2]IRCCS Humanitas Research Hospital, Infectious Diseases Unit, Hospital Health Direction, Rozzano, Italy; [3]Humanitas University, Department of Biomedical Sciences, Pieve Emanuele, Italy; [4]Queen Mary University of London, London, United Kingdom.

Introduction: Clinical records show that broad-spectrum antimicrobial prescriptions in COVID-19 dramatically outnumbered the estimated rate of bacterial co-infections in these patients. Distinguishing COVID-19 with and without secondary co-infections is a clinical issue, because the massive use of broad-spectrum agents can result in detrimental emergence of antimicrobial resistance. Currently, procalcitonin (PCT) and C-reactive protein (CRP) are considered the most suitable biomarkers of COVID-19-associated co-infections, but both of them have limitations. Pentraxin 3 (PTX3) is a soluble pattern recognition molecule (PRM), and its plasma concentration rapidly increases in infectious and inflammatory diseases earlier than CRP. In COVID-19 patients, increased plasma concentrations of PTX3 were observed compared to healthy individuals and they were a strong independent predictor of mortality. In this study, we assessed whether PTX3 could be of help in early identification of co-infections in COVID-19 patients. **Methods:** We analyzed, by ELISA tests, the circulating levels of PTX3 and several inflammatory markers in 37 patients with a COVID-19 laboratory-confirmed diagnosis and a concomitant bloodstream infection (BSI) with a fungal or bacterial pathogen. We next enlarged our study to a cohort of 119 COVID-19 co-infected patients, with pneumonia or urinary tract infection, stratified in Community and Hospital-Acquired Infections (CAI or HAI). The presence and relevance of co-infections was supported by laboratory and clinical data. All these patients were compared with a control group of COVID-19 patients with no evidence of a concomitant secondary infection. **Results:** In BSI patients PTX3 plasma levels at diagnosis of co-infection were significantly higher compared to COVID-19 patients without evidence of co-infection. PTX3 concentration correlated with other serum biomarkers of infection (PCT, CRP, ferritin, D-dimer, and interleukin-6) at the co-infection time point, and was positively associated with mortality. Also, in our second cohort, PTX3 plasma levels at diagnosis of CAI or HAI were significantly higher compared to COVID-19 patients without secondary infections, and the increase of PTX3 plasma levels preceded that of PCT and CRP. In COVID-19 patients with HAIs, PTX3 increased at admission and co-infection time points, decreasing in the other phases of the hospitalization. Furthermore, PTX3 levels remained elevated throughout the hospitalization in deceased patients with HAIs. PTX3 levels at hospital discharge positively correlated with mortality and inflammatory status at the confection time point. **Conclusions:** Our study demonstrates that PTX3 is a promising biomarker for the early identification and risk stratification of COVID-19 patients with bacterial or fungal co-infections.

ID02. Extensive Validation of a Saliva-Based PCR Diagnostic Test Designed to Reduce Costs and Increase Access to Testing

A. Wyllie
SalivaDirect, New Haven, CT.

Introduction: The COVID-19 pandemic presented an unprecedented demand for diagnostic testing. Testing was essential for identifying infected individuals and preventing further virus spread, but was significantly strained by high costs, inadequate infrastructure, and supply chain disruptions. To overcome these challenges and increase testing equity, we developed a low-cost solution: An open-source, saliva-based PCR test for SARS-CoV-2. Over the course of the pandemic, we have further validated this approach for the detection of additional infectious diseases. **Methods:** Identifying the potential of saliva early in the pandemic, we simplified testing by: 1) demonstrating the sensitivity of saliva for SARS-CoV-2 detection; 2) developing clear self-collection instructions; 3) negating the need for healthcare worker-assisted collection; 4) eliminating collection tubes with

propriety buffers and/or preservatives; 5) replacing nucleic acid extraction with a simple heat and/or enzymatic step; 6) validating each protocol step with reagents and instruments from multiple suppliers; and 7) establishing a novel emergency use authorization (EUA) regulatory model. More recently, we also validated this approach (SalivaDirect) for the detection of influenza, respiratory syncytial virus, and mpox. **Results:** We observed stable detection of virus RNA in raw unsupplemented saliva for prolonged periods at elevated temperatures. The lower limit of detection ranges from 1.5 to 12 virus RNA copies/μl of saliva, workstream-depending, comparable to many sensitive PCR tests. Since August 2020, >8 million SalivaDirect tests have been performed by 201 designated labs in 42 US states. SalivaDirect has also been independently validated in at least 13 countries. The flexible protocol allows labs to utilize existing infrastructure and vendor relationships for greater supply chain resilience and lower costs. The streamlined PCR process reduces test turnaround time and increases lab throughput. Expansion of the protocol (e.g., unsupervised self-collection, at-home collection kits, pooled testing) extends its utility to numerous patient profiles and clinical scenarios. **Conclusions:** Advances in testing during the pandemic created new possibilities for respiratory pathogen detection. Since, we have found that saliva can be used as a sensitive, reliable option for PCR testing for not only SARS-CoV-2 detection, but also other viruses. Compared to other sample types, saliva supports more equitable diagnostic and surveillance testing programs, particularly in low-resource and remote environments. Our innovative regulatory framework and resulting laboratory network produced a low-cost, high-quality public health model capable of national impact.

ID03. SARS-CoV-2 Infection Is Associated with Age- and Gender-Specific Changes of the Nasopharyngeal Microbiome

C. Costantini, S. Bozza, E. Nunzi, A. Frías Mazuecos, A. Mencacci, V.N. Talesa, L. Romani, C. Antognelli, P. Puccetti
University of Perugia, Department of Medicine and Surgery, Perugia, Italy.

Introduction: The recent COVID-19 (coronavirus disease 2019) pandemic was caused by the severe acute respiratory syndrome coronavirus 2 (SARS-CoV-2), an airborne pathogen that exploits air transmission to infect potential hosts and cause significant morbidity and mortality in susceptible populations. The initial steps in COVID-19 pathogenesis involve the binding of SARS-CoV-2 with angiotensin-converting enzyme 2 (ACE2) followed by virus release inside susceptible cells. The ensuing host-pathogen interaction drives the evolution of the clinical picture, which may range from asymptomatic to potentially fatal multi-organ failure. It is increasingly being recognized that the early interactions between the host and the virus in the upper respiratory tract are critical in disease evolution. Indeed, the nose shows the highest expression of ACE2 along the respiratory tract, and the nasopharyngeal (NP) microbiome plays a major role in the regulation of both local and systemic immunity. Therefore, the identification of NP microbial signatures of SARS-CoV-2 infectivity would be critical in a diagnostic/prognostic perspective with the potential to identify personalized therapeutic approaches. **Methods:** An observational study with a cross-sectional and monocentric design was carried out. NP swabs from individual adults referring to the Hospital of Perugia for SARS-CoV-2 molecular testing were collected from January 2021 to March 2021. The swabs were processed for SARS-CoV-2 testing according to standard procedures/CDC guidelines. The residual sample was used for DNA extraction and 16S rRNA sequencing. A total of 540 NP swabs were collected and stratified into 18 groups based on age (18 to 40, 40 to 60, >60 years), gender (male, female), and viral load according to cycle threshold value (Ct) (negative, >35 Ct; low viral load, 25 to 35 Ct; high viral load, <25 Ct). **Results:** The taxonomic composition of the NP microbiome revealed that Firmicutes, Bacteroidota, Proteobacteria, Actinobacteriota, and Fusobacteriota were the most abundant phyla, while *Prevotella*, *Streptococcus,* and *Veillonella* dominated at the genus level, in line with previous studies. Age, gender, and viral load had distinct effects on both richness and evenness of genera, and influenced the compositional structure of the NP microbiome. Upon applying the Adonis test when a multifactorial model of age, gender, and viral load was used, all the variables were found to interact with each other. **Conclusions:** The results indicate the age, gender, and viral load variably affect NP microbial composition, indicating that the effect of viral infection on the microbiome must be considered in the context of the individual variability set by demographic factors. Unraveling the microbial signatures resulting from the interactions between infection and demographic factors will be instrumental for personalized diagnosis and prognosis. This study was supported by Fondazione Cassa di Risparmio di Perugia.

ID04. Development of a Syndromic Molecular Diagnostic Assay for Tickborne Pathogens Using Barcoded Magnetic Bead Technology

S. Mir, E. Kahang, S. Rowan
Western University of Health Sciences, Pomona, CA.

Introduction: The infectious disease diagnostics often depends on costly serological testing with poor sensitivity, low specificity, and long turnaround time. Here in this manuscript, we demonstrate the proof of the principle for simultaneous detection of 2 tickborne pathogens from a single test sample using barcoded magnetic bead technology on the BioCode 2500 system. **Methods:** Specific primer sets complementary to the conserved genes of *Anaplasma phagocytophilum* and *Borrelia burgdorferi* were used in PCR amplification of the target, followed by the hybridization of the resulting biotinylated PCR products with specific probes tethered to the barcoded magnetic beads for simultaneous detection, using a fluorophore with high quantum yield. The assay has extremely high signal-to-background ratio and detects up to 2 copies of the target in a test reaction with high sensitivity and specificity. **Results:** The assay demonstrated 100% positive and negative agreements on performance evaluation using patient specimens and blood samples spiked with tittered pathogens. No cross-reactivity was observed with other related tickborne pathogens and genomic DNA of human, cattle, and canine origin. **Conclusions:** The assay can be upgraded to a sensitive and cost-effective multiplex diagnostic approach that can simultaneously detect multiple clinically important tickborne pathogens in a single sample with a short turnaround time.

ID05. Plasmatic 8-OH-dG Levels and O-GlcNAcase Activity as Additional Tools in the Oxidative Stress Evaluation in COVID-19 Infection

L. Massaccesi[1], E. Galliera[1,2], M.M. Corsi Romanelli[1,3]
[1]Università degli Studi di Milano, Dipartimento di Scienze Biomediche per la Salute, Milano, Italy; [2]IRCCS Orthopedic Institute Galeazzi, Milan, Italy, Milano, Italy; [3]U.O.C SMEL-1 Patologia Clinica IRCCS Policlinico San Donato, San Donato, Milan, Italy, San Donato, Italy.

Introduction: Oxidative stress (OS) plays an important role within the COVID-19 infection. Recently the degree of proteins O-GlcNAcylation has been showed as able to influence the stress response pathway; cellular levels of O-GlcNAc, regulated by O-GlcNActransferase and O-GlcNAcase (OGA), are thought to be OS sensors and are implicated in the aetiology of various diseases. OGA is a ubiquitous enzyme also present in the cytosol and plasma; alteration in its activity has been observed in several pathologies related to strong OS, such as Down syndrome or erectile dysfunction. For these reasons its use as a new marker of cellular OS has been suggested. In recent years, several OS markers have gained increasing attention. Among them, a new method for the evaluation of total plasma antioxidant defenses, known as lag-time, proved to be a valid marker of OS in different diseases including COVID-19. It is well known that OS is closely related to levels of advanced glycation end products (AGEs). AGEs interact with their receptors, receptor for advanced glycation end products (RAGE), which can be bound to the membrane or in soluble form (sRAGE). Interaction of AGEs with membrane-bound RAGE leads to massive inflammatory cytokine and ROS production. sRAGE acts as a decoy receptor performing a protective action against the harmful effects resulting from the activation of the AGEs-RAGE axis. Several studies proposed soluble RAGE as an OS circulating biomarker in several diseases, including COVID-19. Oxidized guanine nucleoside, 8-oxo-7,8-dihydro-2'-deoxyguanosine (8-OH-dG) is a metabolite derived from oxidative damage to DNA. The plasmatic evaluation of 8-OH-dG is used to investigate the effects of OS on nucleic acids in several pathologies. Therefore, we analysed a panel of OS parameters to better characterize the OS in COVID-19. **Methods:** In 13 COVID-19 (58.6 ± 18.8 years), 52 non-COVID-19 patients presenting COVID-19-like symptoms (60.8 ± 20.6 years) at hospital emergency admission, and 30 age-matched non-infected controls (56.9 ± 14.3 years), plasmatic sRAGE and 8-OH-dG levels (by ELISA assay), total antioxidant defenses, and OGA activity (by fluorimetric method) were evaluated. **Results:** 8-OH-dG were significantly increased in COVID-19 patients compared to the other subjects ($P < 0.05$). sRAGE was significantly lower in all patients compared to controls ($P < 0.001$). OGA was significantly lower in COVID-19 patients compared to non-COVID-19 patients ($P < 0.05$). In COVID-19 patients 8-OH-dG showed a significant ($P < 0.05$) negative linear correlation with lag-time ($r^2 = -0.614$) and OGA activity ($P < 0.05$) ($r^2 = -0.674$). **Conclusions:** Our results give a deeper picture of the role of OS in COVID-19 and emphasize the importance of a global redox characterization as a potential tool to monitor conditions of COVID-19 patients under therapies aimed to regain a correct redox balance and to counter the harmful systemic effects of this pathology.

ID06. Diagnostic Potential of the Long Pentraxin 3 in Hip and Knee Periprosthetic Joint Infections

M. Loppini[1,2], M. Di Maio[1], R. Avigni[1], R. Leone[1], A. Inforzato[1,2], G. Grappiolo[1,3], A. Mantovani[1,2], B. Bottazzi[1]
[1]IRCCS Humanitas Research Hospital, Rozzano (MI), Italy; [2]Humanitas University, Department of Biomedical Sciences, Pieve Emanuele (MI), Italy; [3]Università degli Studi di Genova, Fondazione Livio Sciutto Onlus, Campus Savona, Savona, Italy; [4]Queen Mary University of London, Harvey Research Institute, London, United Kingdom.

Introduction: Preoperative diagnosis of periprosthetic joint infections (PJIs) poses an unmet clinical challenge. The long pentraxin PTX3 is a member of the innate immune system produced by stromal and immune cells in response to inflammatory and infectious stimuli and is a candidate biomarker of inflammation and infections. The aim of this study was to evaluate the potential of synovial and plasmatic PTX3 in the diagnosis of hip and knee PJIs. **Methods:** The study was approved by the Institutional Review Board of IRCCS Humanitas Research Hospital. Plasma, synovial fluid, and intra-operative periprothesic tissue samples were collected prospectively before surgery from consecutive revisions of total hip and knee arthroplasty (THA/TKA). Each revision was classified as septic or aseptic according to the European Bone and Joint Infection Society (EBJIS) and Musculoskeletal Infection Society (MSIS) criteria. PTX3 levels were measured in collected plasma and synovial fluid samples by a sandwich ELISA based on reagents (i.e., antibodies and recombinant protein) developed in-house. The assay was not reacting with CRP and had a sensitivity of 75 pg/ml. CRP, D-dimer, ESR, and synovial fluid leukocyte count were measured by standard procedures in use in the Institutional Clinical Laboratory. Presence and identity of aerobic and anaerobic microorganisms were assessed following culture in appropriate selective media. The area under the curve (AUC), threshold value, sensitivity, specificity, and positive and negative likelihood ratios were calculated using the ROC (receiver operating characteristic) curve method. **Results:** The study population included 128 patients (94 THAs; 34 TKAs) enrolled at Humanitas Research Hospital. Patients with a confirmed infection were between 41% (according to EBJIS criteria) and 27% (according to MSIS criteria) of the enrolled patients. The most frequent pathogens isolated in infected patients were coagulase-negative Staphylococci, *Staphylococcus aureus,* and Streptococci. Synovial PTX3 and plasmatic CRP were significantly higher in the infected patients compared to the non-infected ones when either EBJIS or MSIS criteria was considered for diagnosis of PJI ($p < 0.0001$). Plasmatic PTX3, ESR, and D-dimer did not discriminate infected from non-infected patients. When patients were stratified based on the explanted implant (THA or TKA), the synovial levels of PTX3 remained significantly higher in the infected individuals compared to the ones who had aseptic revision, regardless of the criteria used for diagnosis of PJI. The AUC of the synovial PTX3 based on EBJIS criteria was 0.85 ($p < 0.0001$), with a sensitivity of 81.13% and a specificity of 93.33%. The AUC based on MSIS criteria was 0.95 ($p < 0.001$), with a sensitivity of 91.43% and a specificity of 89.25%. **Conclusions:** Synovial PTX3 demonstrated an excellent diagnostic potential in hip and knee PJIs, with a very high specificity irrespective of the diagnostic criteria for PJI.

ID07. Innate Immunity and Bone Infections: Emerging Roles of the Long Pentraxin PTX3 in *Staphylococcus aureus*-Dependent Osteomyelitis

A. Inforzato[1,2], R. Parente[2], V. Possetti[1,2], V. Granata[2,3], F. Davi[2], M.L. Schiavone[3,2], D. Strina[3,2], M. Filipović[4,5], D. Grčević[4,5], B. Bottazzi[2], A. Mantovani[2,6], C. Sobacchi[3,2]
[1]Humanitas University, Department of Biomedical Sciences, Pieve Emanuele, Italy; [2]IRCCS Humanitas Research Hospital, Rozzano, Italy; [3]National Research Council-Institute for Genetic and Biomedical Research (CNR-IRGB), Rozzano, Italy; [4]University of Zagreb School of Medicine, Department of Physiology and Immunology, Zagreb, Croatia; [5]University of Zagreb School of Medicine, Croatian Institute for Brain Research, Zagreb, Croatia; [6]Queen Mary University of London, Harvey Research Institute, London, United Kingdom.

Introduction: Osteomyelitis (OM) is a debilitating infection of the bone primarily caused by the opportunistic pathogen *Staphylococcus aureus* (SA). SA exploits several strategies to evade the immune response, acquire antibiotic resistance, and chronically colonize the musculoskeletal tissue, yet the underlying molecular and cellular processes are largely unclear. This study aimed to characterize the pathogenetic mechanisms of SA-OM with a focus on the long pentraxin 3 (PTX3), a soluble pattern recognition molecule and bone tissue component that is emerging as a new player in osteoimmunology and a diagnostic marker of periprosthetic joint infections (PJIs), a common form of OM. **Methods:** A murine model of OM based on intra-femur injection of SA was developed that closely mimicked surgery-/trauma-related OM in humans and allowed addressing the role of PTX3 in gene-modified (*Ptx3*$^{-/-}$) animals. Local and systemic infection and inflammation were assessed via microbiology, flow cytometry, histochemistry, and microCT techniques. **Results:** SA-injected mice developed chronic infection with measurable levels of viable bone-resident bacteria up until 30 days from microbial challenge. The infection was confined to the treated limbs only and accompanied by extensive tissue remodeling. The bacterial load was higher in wild-type (WT) than *Ptx3*$^{-/-}$

animals at 6 and 14 days from SA injection. Accordingly, WT mice had enhanced systemic inflammation with expanded innate immune compartment in the spleen and increased serum levels of inflammatory cytokines and chemokines. PTX3 levels were higher in SA- than vehicle (PBS)-injected WT animals, both in the serum and bone tissue. Furthermore, administration of a PTX3-targeting antibody reduced the bacterial burden in the bones of SA-injected WT mice. **Conclusions:** In a mouse model of SA-OM, genetic deficiency of PTX3 protected from infection and inflammation, pointing to this pentraxin as a crucial player in OM pathogenesis and a novel therapeutic target in bone infections.

ID08. The Two Faces of IFN-g in the Immune Challenge against Fungi

V. Oikonomou, G. Renga, M. Pariano, C. Stincardini, F. Donofrio, C. Costantini, M.M. Bellet, L. Romani
University of Perugia, Department of Medicine and Surgery, Pathology Section, Perugia, Italy.

Introduction: Fungi can cause diseases in humans, from mucocutaneous (*Candida* spp.) to life-threatening systemic infections (*Aspergillus* spp.). Interferon-gamma (IFN-g) has emerged as an extremely versatile cytokine mediating protection against a wide array of pathogens. Undoubtedly, such an important immune mediator is under stringent regulatory control. However, IFN-g is a double-edged sword: It can have therapeutic as well as aberrant effects depending on the type of disease. Two clear examples are: 1) chronic granulomatous disease (CGD), a genetic disorder of the NADPH oxidase characterized by increased susceptibility to *Aspergillus* infections and hyperinflammation associated with defective autophagy and increased inflammasome activation; and 2) autoimmune polyendocrinopathy–candidiasis–ectodermal dystrophy (APECED), an autoimmune disease of impaired central immune tolerance characterized by selective susceptibility to mucosal but not systemic fungal infection. **Methods:** First, we monitored DAPK1 expression and its modulation by IFN-g *in vivo* $p47^{phox-/-}$ in infected mice and *in vitro* in both $p47^{phox-/-}$ lung macrophages and monocytes from CGD patients. Second, we broadly investigated oral mucosal immune responses both in a model of oropharyngeal candidiasis in $Aire^{-/-}$ mice and in a large cohort of APECED patients. **Results:** In mouse models and patients with CGD, we have described an IFN-g/DAPK1 signaling that mediates LC3-associated phagocytosis (LAP), critical for dampening *Aspergillus*-triggered immunopathology. Of interest, DAPK1 activity was defective in murine and human CGD, a finding suggesting that the LAP/DAPK1 axis may represent a druggable pathway in CGD. Indeed, IFN-g, the only FDA-approved treatment option in CGD, restored reduced DAPK1 activity and dampened fungal growth. Activated by IFN-g, DAPK1 not only mediated *A. fumigatus*–LAP but also concomitantly inhibited NOD-like receptor protein 3 (NLRP3) activation, thus restraining pathogenic inflammation. In contrast, in AIRE deficiency, we have shown that excessive IFN-g–dependent responses at the mucosal level lead to susceptibility to oral mucosal infection by *Candida albicans*. Concordantly, genetic and pharmacologic inhibition of IFN-g or JAK-STAT signaling ameliorated mucosal fungal disease and multi-organ autoimmunity. Thus, aberrant T-cell-dependent, type 1 mucosal inflammation is a critical tissue-specific pathogenic mechanism that promotes mucosal fungal infection susceptibility. **Conclusions:** Together, our data suggest that the bright side of IFN-g in CGD in which it is beneficial is counteracted by the exaggerated IFN-g/STAT1 response leading to tissue-specific autoimmune manifestations in APECED. Thus, IFN-g-mediated host-pathogen interactions are critical for both understanding disease pathogenesis and IFN-g optimization by disease-oriented therapy.

ID09. Innate Immune Responses to Malaria Parasites: Role of the Malaria Pigment Hemozoin in Macrophage Polarization

F. Perego[1], S. Parapini[2], E. Calvo Alvarez[3], M. Dolci[1], P. Rebuffini[3], K. Maina[1], R. Ticozzi[1], S. Delbue[1], P. Misiano[3], D. Taramelli[3], N. Basilico[1], S. D'Alessandro[3]
[1]University of Milan, Department of Biomedical, Surgical and Dental Sciences, Milan, Italy; [2]University of Milan, Department of Biomedical Sciences for Health, Milan, Italy; [3]University of Milan, Department of Pharmacological and Biomolecular Sciences, Milan, Italy.

Introduction: Malaria is a parasitic, vector-borne disease causing millions of cases every year. The importance of innate immunity to malaria infection is well recognized. Hemozoin (HZ), or malaria pigment, is the detoxification product of heme, produced by parasites during their intra-erythrocytic stages following hemoglobin digestion in the so-called food vacuole. HZ is released into the circulation during asexual replication of parasites, when merozoites are released from red blood cells to infect new erythrocytes. HZ has been found in postmortem samples of malaria patients, especially in the spleen, liver, bone marrow, lungs, brain, and placenta. Once phagocytized by host cells, especially macrophages, HZ may induce different, often opposite responses such as the production of pro-inflammatory or anti-inflammatory cytokines. The aim of this work was to investigate whether HZ can affect M1/M2 macrophage polarization induced by known stimuli. **Methods:** THP-1

monocytes were differentiated into macrophages by 48 h incubation with 10 nM PMA. M1 and M2 macrophage polarization was obtained by 24 h treatment with IFN-γ and LPS or IL-4 and IL-13, respectively. HZ at the physiologically relevant concentrations of 1.5 or 10 μM was co-incubated with the M1/M2 stimuli. The activation of macrophages was evaluated by measuring the production of IL-1β, TNF-α, IL-10 in cell supernatants by ELISA, and by measuring the expression of the corresponding genes by RT-PCR. Two markers of M2 phenotype were examined: PPARγ expression by RT-PCR and STAT6 activation by Western blot (phosphorylated STAT6 normalised on total STAT6 protein levels). **Results:** Both naïve (M0, unstimulated) and M1 or M2 polarized macrophages avidly phagocytosed HZ. HZ mainly induced pro-inflammatory cytokines, namely IL-1β and TNF-α, by unstimulated macrophages. However, in the presence of M1 stimuli, HZ reduced the expression and production of IL-1β and TNF-α. HZ had no effect on cytokine production in M2 polarized macrophages, whereas it decreased STAT6 phosphorylation. The same trend has been observed for PPARγ expression. **Conclusions:** This work represents one of the first investigations about the effect of HZ on macrophage polarization. The differential response of M1 versus M2 macrophages to HZ may help reconcile the controversial and often opposite responses obtained *in vitro* with HZ and different macrophage population. Further work is necessary to better characterize the effective *in vivo* role of HZ during the different phases of innate immunity in malaria.
Acknowledgement: PR and KM were supported by a young scientist fellowship from the GSA-IDEA project (PSRL621CBAND_01) funded by University of Milan.

ID10. Human Papillomavirus Typing in Liquid-Based Pap Tests in Israel

S. Aviel-Ronen[1,2], R. Yacobi[1], H. Tabibian-Keissar[1], I. Barshack[1,3]
[1]Sheba Medical Center, Pathology, Ramat Gan, Israel; [2]Ariel University, Adelson School of Medicine, Ariel, Israel; [3]Tel Aviv University, Sackler Faculty of Medicine, Tel Aviv, Israel.

Introduction: The types of human papillomavirus (HPV) related to the development of uterine cervix dysplasia, carcinoma, and genital warts are well characterized. We aimed to study the distribution of HPV types in Israel and compare it to the prevalence reported in the literature. **Methods:** HPV typing was performed in 977 cervical ThinPrep samples at the Sheba Medical Center, Israel, from 2019 to 2021. The Pap tests were taken for several medical indications, including screening, post-coital bleeding, and various degrees of epithelial dysplasia. HPV typing was done using Master Diagnostics HPV Direct Flow CHIP on the eBRID automated system. This PCR amplification and reverse dot blot hybridization-based method identifies 36 types of HPV (18 high-risk, 18 low-risk) and the presence of unspecified HPV genotype (using a universal HPV probe detecting L1 consensus region). **Results:** The median patient age in our cohort was 43 years (range 17 to 80 years, average 43.3 years). HPV typing failed in 31 (3.2%) samples (15 due to insufficient material and 16 for other pre-analytical reasons). Of the 421 (44.5%) samples positive for HPV, high-risk HPV alone was found in 160 patients (16.9%), both high- and low-risk HPV were detected in 119 patients (12.6%), only low-risk HPV was present in 108 patients (11.4%), unspecified HPV was found in 34 patients (3.6%), and 525 (55.5%) were negative for HPV. The relative prevalence we found for each of the 36 types is presented and shows differences from the traditionally accepted distribution (e.g., high prevalence of types 53, 66, and 31). **Conclusions:** The relative prevalence of the HPV types we found in our cohort of patients deviates from the recognized distribution in the literature. The type of epithelial abnormality (low-grade intra-epithelial lesions [LSIL] and high-grade intra-epithelial lesions [HSIL] vs. atypical squamous cells-undetermined significance [ASC-US]), method of HPV detection, geography, and HPV vaccination may all contribute to these differences.

ID11. Single-Cell Transcriptome and Epigenomic Alterations in Enterovirus and Parechovirus Systemic Illness in Infants

R. Selvarangan, D. Louiselle, A. Sasidharan, J. Johnston, W. Cheung, B. Yoo, M. Gibson, A. Walter, T. Bradley, E. Grundberg, T. Pastinen
Children's Mercy Kansas City, Kansas City, MO.

Introduction: Enterovirus (EV) and parechovirus (PeV) are leading viral causes of systemic illness in infants, manifesting as aseptic meningitis and sepsis-like illness. Although clinical symptoms for EV and PeV systemic illness overlap, the plasma cytokine/chemokine profile during PeV infections is more robust than EV. The basis for the difference in host response to EV and PeV is not well understood. We describe the single cell transcriptome and epigenome alterations in EV and PeV infected infants in comparison to control infants with similar clinical presentation testing negative for both viruses. **Methods:** EV and PeV real-time RT-PCR testing was performed on cerebrospinal fluid samples submitted from infants suspected of central nervous system infections. We enrolled EV-positive (n = 3), PeV-positive (n = 6), and EV/PeV-negative (control) infants (n = 6), and collected whole blood for peripheral blood mononuclear cell (PBMC) isolation and buccal swab for genotyping using the Illumina Global Screening Array (GSAMD-24v1-0). PBMC samples were

pooled in 2 groups, and approximately 21,000 cells were loaded into a 10x Genomics Single Cell A Chip and tested by kit v2 for scRNA-seq. Approximately 15,300 nuclei were loaded into 1 well of a Chromium Chip E (10x Genomics Cat No. 1000155), and scATAC-seq was performed using the scATAC Library & Gel Bead Kit (10x Genomics Cat No. 1000110). Differentially expressed genes were determined within each cell cluster and pathogen classification using Seurat v3.1.4's default Wilcoxon Rank Sum test, followed by Bonferroni correction of resulting p-values. **Results:** The clinical presentation and laboratory findings of enrolled children are presented in **Table 1**. In unsupervised annotation analyses we found overall high predominance of CD4+/CD8+ T-lymphocyte cells, but also characterized B-cells, NK cells, monocytes, and dendritic cells. Following cell deconvolution to PeV, EV, and negative groups, respectively, we noted very distinct patterns across the groups. Specifically, we identified complete polarization (i.e., >10-fold difference in relative cell abundance between infected infants and negative controls) of cells in T-cell clusters that together defined systemic response to PeV and EV compared to control group infants requiring hospitalization. Differential expression analysis of marker genes across the clusters revealed PeV eliciting increased overexpression of a wide variety of interferon pathway/antiviral genes in T-cells as compared to EV infection, and this difference was primarily manifested in CD4 and CD8 T-cells. **Conclusions:** We demonstrate distinct gene expression changes in immune cell populations in infants with systemic viral infection, with remarkably distinct immune cell profiles noted for EV and PeV infection, with canonical interferon pathway activation and shutdown of protein translation.

Table: Demographics and laboratory findings of hospitalized EV, PeV and control infants

Range (Median ± STD)	EV (n=3)	PeV (n=6)	Neg (n=6)	P value**
Demographics:				
Age (in days)	3 - 45 (5 ± 19.3)	6 - 48 (24 ± 13.4)	16 - 145 (45 ± 44.9)	0.07
Gender	3 M ; 0 F	4 M ; 2 F	3 M ; 3 F	
Hospital Course:				
LOS	2 -7 (4 ± 2)	0 -5 (2 ± 1.7)	0 -18 (2 ± 6.7)	0.70
Tmax	38 - 39 (39 ± 0.4)	38 - 40 (39 ± 0.4)	37 - 38 (37 ± 0.2)	0.08
CSF Findings:				
*CSF pleocytosis	0	2	1	0.38
CSF WBC	2 - 17 (3 ± 6.8)	2 - 57 (3 ± 20.3)	1 - 8 (2 ± 2.4)	0.28
CSF RBC	0 - 23 (3 ± 10.2)	0 - 27,000 (10 ± 10364.6)	0 - 247 (1 ± 95.5)	0.21
CSF Glucose	40 - 54 (42 ± 6.1)	34 - 53 (49 ± 6.7)	36 - 68 (47 ± 11.6)	0.09
CSF Protein	47 - 127 (98 ± 33)	49 - 108 (63 ± 19.6)	33 - 135 (112 ± 37.0)	0.28
Hematology findings:				
Blood WBC	7 - 18 (14 ± 4.3)	3 - 8 (6 ± 1.6)	8 - 18 (12 ± 3.8)	0.51
ANC	4 - 14 (11 ± 4.3)	1 - 3 (3 ± 0.8)	1 - 6 (5 ± 2.0)	0.40
ALC	2 - 3 (3 ± 0.3)	2 - 4 (2 ± 0.6)	4 - 11 (6 ± 2.5)	0.08
CBC %Lymph	16 - 65 (36 ± 19.9)	31 - 57 (46 ± 9.1)	33 - 67 (56 ± 12.5)	
CBC %Mono	2 - 15 (11 ± 5.6)	14 - 25 (11 ± 4)	5 - 14 (10 ± 3.4)	

Table 1: Demographics and laboratory findings of hospitalized EV, PeV, and control infants

ID12. Choice of *Candida auris* DNA Extraction Method Is Crucial to PCR Assay Performance

N.A.L. Supandi, X.L.K. Chan, L.E.L. Oon, K.S. Chan
Singapore General Hospital, Molecular Pathology, Singapore, Singapore.

Introduction: *Candida auris* (CAU) is a multi-drug-resistant yeast causing healthcare-associated infection with high mortality worldwide. Rapid identification of colonization status through early patient screening is recommended to control its spread. Polymerase chain reaction (PCR) can yield results within a day compared to 7 days for culture. The presence of a complex, tough, chitinous cell wall that is resistant to chemical lysis used by conventional extraction methods impairs effective DNA extraction. This study aims to compare the performances of 4 commercially available extraction methods on CAU: one with bead-beating step followed by chemical lysis (QIAGEN DNeasy PowerSoil Pro [PSP] on QIAcube/QIAcube Connect), and three using purely chemical lysis (bioMérieux NucliSens easyMAG/eMAG, Promega Maxwell RSC Viral Total Nucleic Acid Purification Kit and QIAGEN EZ1&2 Virus Mini Kit v2.0). **Methods:** A clinical isolate of CAU was cultured and suspended in 1x phosphate buffered saline to 0.5 McFarland turbidity before serial dilution to 96 CFU/mL and 960 CFU/mL using combined nose, axilla, and groin swab media (ESwab, Copan Diagnostic Inc.) matrix (previously tested negative) followed by DNA extraction and PCR testing. Plate counts were done to establish the inoculum. Five replicates were performed for each dilution per extraction method. All extractions were performed based on manufacturer's instructions, using maximum recommended input volumes and minimum elution volumes for highest DNA extract concentrations. PCR was performed using primers and probes, described by Leach *et al.* (2018) on Bio-Rad CFX96 instrument. Results were analysed using Bio-Rad Manager 3.1, and cycle threshold (Ct) values were determined using regression. One-way ANOVA by IBM SPSS 25.0 software package was used to compare the results. A *P*-value of <0.05 was considered statistically significant. **Results:** There was a significant difference in the Ct values (P <0.05) at 960 CFU/mL between the different extraction methods. The 95% confidence interval of Ct values attained on PSP was 22.75 to 25.57; on easyMAGä/eMAG it was 28.89 to 29.94; on Promega it was 37.49 to 40.51; and on EZ1&2 it was 32.83 to 35.09. Extraction using PSP had the highest DNA yield, followed by easyMAG/eMAG, EZ1&2, and Promega. Of note, only with PSP extraction was the PCR assay able to pick up CAU DNA at 96 CFU /mL (all 5 replicates detected). **Conclusions:** Extraction with PSP on QIAcube/QIAcube Connect, which included bead-beating, resulted in a CAU

PCR assay with a much higher analytical sensitivity compared to the other 3 extraction methods. This was despite PSP extraction method requiring the lowest input volume. Our findings highlight the importance of including a bead-beating component in CAU extraction. Highly sensitive screening assay with rapid turnaround time is the cornerstone for early detection of CAU colonization, facilitating infection control efforts to stamp out nosocomial spread.

ID13. HIV-1 Exploits CD32-Driven Autoantibody-Enhanced Trogocytosis to Facilitate Infection of Resting CD4 T-Cells

M. Albanese[1,2], H.-R. Chen[1], M. Gapp[1], M. Muenchhoff[1], D. Peterhoff[3], K. Hoffmann[4], H. Hengel[4], R. Wagner[3], O.T. Fackler[5], A. Lanzavecchia[2], O.T. Keppler[1]

[1]Ludwig Maximilian University (LMU) of Munich, Max von Pettenkofer Institute and Gene Center - Faculty of Medicine - Virology, München, Germany; [2]National Institute of Molecular Genetics (INGM), Human Immunology, Milan, Italy; [3]University of Regensburg, Institute of Medical Microbiology and Hygiene, Molecular Microbiology (Virology), Regensburg, Germany; [4]University Medical Center, Albert-Ludwigs-University Freiburg, Institute of Virology, Freiburg, Germany; [5]University Hospital Heidelberg, Department of Infectious Diseases, Integrative Virology, Heidelberg, Germany.

Introduction: The replication-competent HIV-1 reservoir persists despite antiretroviral therapy, but knowledge gaps on the mechanisms regulating its size limit rational approaches to HIV cure. The identification of biomarkers expressed selectively on the surface of resting CD4 T-cell subsets harboring replication-competent HIV-1 would facilitate the targeting and elimination of the latent viral reservoir in infected individuals. The Fcγ receptor CD32 has been reported to serve as such a biomarker for resting CD4 T-cells, but its role has remained controversial. **Methods:** We established a CRISPR/Cas9 model system using *ex vivo* co-cultures of primary human macrophages together with autologous resting CD4 T-cells, as well as a cell line-based donor-target model system. We combined microscopy, flow cytometry, and other state-of-the-art techniques including the Amnis ImageStream technology to characterize CD32 exposed on CD4 T-cells. The transient expression of different CD32 isoforms, chimeras, and mutants, together with other surface receptors expressed as well as the addition of modulating antibodies provided unprecedented mechanistic insight into a process called “trogocytosis," in which T-cells acquire receptors from the macrophages’ cell surface. Finally, HIV-1 binding, fusion, and infection assays were used to study the infection in CD4 T-cells which acquired CD32 patches from macrophages. **Results:** Thanks to this co-culture system, we identified the Fcγ receptor CD32 as driver and cargo of a cell contact-dependent, unidirectional trogocytotic transfer of distinct plasma membrane patches from macrophages to resting CD4 T-cells that render these non-permissive reservoir cells transiently susceptible to HIV-1 infection. T-cell-reactive autoantibodies in plasma from a subset of chronic HIV-1 patients, forming a “bridge” between donor and recipient T-cells, enhanced the trogocytotic transfer of membrane patches via highly dynamic, filamentous nanoprotrusions. Surprisingly, we identified a long list of other receptors that are transferred from macrophages to T-cells via trogocytosis. **Conclusions:** On CD4 T-cells, trogocytosed CD32 membrane patches recruited the CD4 receptor, creating hot spots of preferential binding and fusion for HIV-1 particles, resulting in increased infection. Additional trogocytosed receptors conferred new migration and adhesion functions, potentially creating a more infection-prone environment. Thus, Fcγ receptor-mediated trogocytosis expands the proteomic and functional plasticity of immune cells and is exploited by HIV-1 to persist. In HIV patients, this process can enhance HIV-1 susceptibility of resting CD4 T-cells and may thus contribute to expanding the latent HIV-1 reservoir *in vivo*.

ID14. Evaluation of a Meta-Genomics Next-Generation Sequencing (mNGS) Assay with Novel Host Depletion Method for Pathogen Identification in Sepsis Patients (Selected for Oral Presentation, O-02-02)

Y-C. Chen[2,3], D.H-T. Yen[4], M. Chan[1], H. Hung[1], K. Chao[1], M. Wu[1]

[1]Micronbrane Medical, Taoyuan, Taiwan; [2]Taipei Veterans General Hospital, Emergency Department, Taipei, Taiwan; [3]School of Medicine, National Yang Ming Chiao Tung University, Emergency Department, Taipei, Taiwan; [4]Chang Bing Show-Chwan Memorial Hospital, Changhua, Taiwan.

Introduction: Sepsis is a life-threatening condition arising from the human immune response to the bloodstream infection. It can progress into septic shock, organ failure, and death if diagnosis and correct treatment are not timely made. The traditional diagnosis of sepsis by microbial blood culture (BC) suffers from 1) long culture cycle leading to delay of results, and 2) low diagnostic yields. Metagenomic next-generation sequencing (mNGS) methods have the potential to overcome these issues. In this study, an mNGS workflow utilizing a novel filter to specifically capture white blood cells and deplete host DNA background was evaluated against BC results, as well as mNGS without the filter, for pathogen identification from blood samples. **Methods:** Patients admitted to Taipei Veterans General Hospital with suspected sepsis were recruited to the study approved by the IRB. Blood sample was taken for BC (designated as first BC) before any antibiotic exposure. Upon patient enrollment, blood was taken again and divided into 3 portions, with one used for the second BC. The other two were used for mNGS with one processed with the filter and the other without filtering, to assess the effectiveness of host depletion by the filter. **Results:** A total of 50 patients were recruited, among which 39 had results for all 4 tests. The mNGS with filter had the highest positive rate of 64.1%, followed by first BC (51.3%) and mNGS without filter (46.2%), whereas the second BC had the lowest positive rate of 25.6%. It strongly suggested that

mNGS was less sensitive to antibiotics exposure as compared to BC. The overall correlation between samples with versus without filtration (R^2 = 0.99) confirmed that filtration does not affect microbial composition in a sample. For the BC positive samples, the effect of host depletion by filtration increased microbial target reads/million QC reads from 41 reads to 209 reads on average. Microbial reads enrichment by the filter appeared to be more effective for the samples with lower microbial concentration, thus increasing the test sensitivity over mNGS without filter. Using the second BC results as a reference, mNGS with filter and mNGS without filter exhibited sensitivities of 90.0% and 50.0%, and specificities of 41.4% and 55.2%, respectively. **Conclusions:** The mNGS with filter was able to recover most of the pathogens identified by clinical BC and achieved the highest diagnostic yield. With the clinical implementation to complete the workflow within 24 hours, it has the potential to overcome slow turnaround and low diagnostic yield issues of traditional BC.

ID15. A New High-Throughput Viral Integration Sequencing Method Coupled to a New Bioinformatic Pipeline Revealed That Mitochondrial DNA Can Be Targeted by Hepatitis B Virus (HBV) Integration in Tumour and Non-Tumour Liver Cells Showing Active HBV Replication (Selected for Oral Presentation, O-02-01)

D. Giosa[1], D. Lombardo[1], C. Musolino[1], V. Chines[1], F. Casuscelli di Tocco[1], D. Daliberti[1], G. Caminiti[1], C. Saitta[1], A. Alibrandi[3], R. Aiese Cigliano[4], O. Romeo[5], G. Navarra[2], G. Raimondo[1], T. Pollicino[1]
[1]University of Messina, Clinical and Experimental Medicine, Messina, Italy; [2]University Hospital of Messina, Human Pathology, Messina, Italy; [3]University of Messina, Economics, Messina, Italy; [4]Sequentia Biotech Sl, Barcelona, Spain; [5]University of Messina, ChiBioFarAm, Messina, Italy.

Introduction: Although research on hepatitis B virus (HBV) DNA integration has made relevant progress, important aspects remain unclear. Development of new integration detection methods may help in improving knowledge in the field and in better understanding HBV-related tumorigenesis. Our aim was to conduct a high-throughput integration detection on tumour (T) and non-tumour tissues (NT) from HBsAg-positive patients using a highly sensitive method for assaying HBV integration. **Methods:** We studied T from 7 patients with HBV-related hepatocellular carcinoma (HCC) and paired NT from 6 of the 7 cases. HBV integration sites were recovered by semi-nested ligation-mediated PCR from host DNA (fragmented by sonication and ligated to asymmetric DNA linkers) and the use of forward or reverse HBV-specific primers. Targeted sequences were further enriched by nested-PCR with forward or reverse MiSeq HBV primers and forward or reverse MiSeq plinkers. PCR products were subjected to paired-end sequencing, and reads were aligned to a hybrid genome including human genome (GRCh38.p10) and HBV genome (NC_003977). **Results:** A total of 3,339 unique HBV integration sites were detected in the 7 patients: 2,913 integrations in T and 426 in NT. The average numbers of integration sites in T and NT were 416 and 71, respectively. All patients had HBV integrations, with an average of 256.8 integrations per individual patient. The detected integration sites were randomly distributed across the whole genome and no hotspot was detected. Compared to individual chromosomes, a significant enrichment of virus integration sites was observed in mitochondrial DNA (mtDNA) both in T (P <0.0001) and NT (P <0.0001), after normalization of the number of integrations to chromosome length. We found a total of 20 unique HBV integrations in mtDNA from the tissue samples obtained from 4/7 patients (17 breakpoints in T from 4/4 patients and 3 breakpoints in NT from 2/4 patients). HBV integration in mtDNA was associated with HBV DNA (P = 0.01) and pregenomic RNA amounts (P = 0.02). In mtDNA, the integration breakpoints were preferentially located in mitochondrial genes in T (17/17 vs. 0/3; P <0.0001) and in the D-loop region in NT (2/17 vs. 3/3; P = 0.001). *RNR2, ATP6, ND4*, and *ND5* mitochondrial genes were identified as recurrent sites of integration in T. Moreover, in T of individual patients, HBV integrations were detected in *CYTB, COX1, ND1*, and *ND2* genes. Furthermore, we found that HBV RNAs are imported into mitochondria. **Conclusions:** The new HBV integration sequencing method importantly increased the detection efficiency of HBV integration breakpoints. We detected an enrichment of virus integrations in mtDNA from both T and NT. HBV integrations in mtDNA preferentially involved OXPHOS mitochondrial genes in T, suggesting that there is selection for mitochondria harboring HBV integration in these genes or for cells containing these mitochondria during hepatocarcinogenesis. Our data suggest a novel mechanism by which HBV insertion might contribute to HCC development.

ID16. Postbiotics as Mediators of the Host-Microbiota Front Line

M. Pariano[1], M. Puccetti[2], G. Renga[1], F. D'Onofrio[1], S. Giovagnoli[2], M. Ricci[2], L. Romani[1]
[1]University of Perugia, Department of Medicine and Surgery, Perugia, Italy; [2]University of Perugia, Department of Pharmaceutical Science, Perugia, Italy.

Introduction: Alterations of the microbiome occur in a number of immune-mediated diseases, a finding consistent with the role of the microbiome in the maintenance of the immune system homeostasis. In this regard, L-tryptophan

metabolites of microbial origin, referred to as postbiotics, are crucial regulators of the host-microbial symbiosis by acting as aryl hydrocarbon receptor (AhR) ligands. A number of studies have highlighted the capacity of AhR to respond to indoles postbiotics, thus positioning AhR as a candidate indole receptor. The intestinal and respiratory barriers are very sensitive to AhR activity, suggesting that AhR modulation could be a therapeutic option to maintain the microbial and immune homeostasis at the epithelial barrier, which has substantial implications for health even beyond the mucosal site. However, the context- and ligand-dependent activity of AhR requires one to resort to suitable biopharmaceutical formulations to enable site-specific drug delivery in order to achieve therapeutic effectiveness, decrease unwanted toxicities, and prevent off-target effects. **Methods:** We resorted to biopharmaceutical technologies to deliver the microbial-derived indole-3-aldehyde (3-IAld), known to act as guardian of epithelial barrier integrity via the AhR/Il-22 pathway, directly into the lung via dry powder inhalation, or into the gut via dry powder encapsulation, in preclinical models of lung or gut inflammation. **Results:** We found that site-specific delivery of 3-IAld is an efficient strategy to mitigate lung and gut inflammatory pathology, by restoring immune and microbial homeostasis at mucosal surfaces. Specifically, 3-IAld dry powder prevented lung inflammatory pathology in murine cystic fibrosis; restrained epithelial injury and the consequent microbial dysbiosis, immune, and metabolic dysregulation in intestinal and liver inflammatory diseases; and protected from immune check-point inhibitor adverse events without affecting the antitumoral activity. No systemic effects were observed upon each targeted delivery. **Conclusions:** These studies provide proof-of-concept demonstration of how pharmaceutical technology helps translating the new frontiers of microbial drug discovery into human therapeutics.

ID17. Role of *Leishmania infantum* Infection and Hypoxia in Modulating the Crucial Fate of Arginine in Macrophages

F. Perego[1], S. D'Alessandro[2], S. Parapini[3], M. Dolci[1], L. Signorini[1], S. Delbue[1], D. Taramelli[2], N. Basilico[1]
[1]Università degli Studi di Milano, Dipartimento di Scienze Biomediche, Chirurgiche e Odontoiatriche, Milano, Italy; [2]Università degli Studi di Milano, Dipartimento di Scienze Farmacologiche e Biomolecolari, Milano, Italy; [3]Università degli Studi di Milano, Dipartimento di Scienze Biomediche per la Salute, Milano, Italy.

Introduction: Leishmaniasis is a neglected tropical disease caused by infection with *Leishmania* parasites and transmitted by the bite of a phlebotomine sand fly. Infected tissues are characterized by a hypoxic inflammatory environment where macrophages are the final hosts of the intracellular parasite *Leishmania*. In macrophages, arginine is the common substrate of the inducible nitric oxide synthase (NOS) and of the 2 arginase isoforms, arginase 1 (Arg1) and arginase 2 (Arg2). The balance among these enzymes is critical for the outcome of the disease; indeed, a major consumption of arginine by NOS leads to a higher amount of the microbiocidal nitric oxide (NO), whereas a predominant activity of arginases induces intracellular survival of *Leishmania* through polyamines production. Since their regulation by *Leishmania* infection and hypoxia is still not fully understood, the aim is to evaluate how the metabolism of arginine is orchestrated in an *in vitro* model of *Leishmania*-infected macrophages in normoxia or hypoxia. **Methods:** Mouse bone marrow-derived macrophages (BMDMs) were activated to a pro-inflammatory phenotype with mIFNγ and LPS, and infected with *Leishmania infantum* (*L. infantum*) MHOM/TN/80/IPT1 promastigotes (MOI 1:10). After 6 hours of incubation in normoxia (20% O_2) or hypoxia (1% O_2) Nitric Oxide Synthase 2 (*NOS2*), Arginase 1 (*ARG1*), and Arginase 2 (*ARG2*) gene expression was evaluated by RT-PCR. After 24 hours of incubation, NO and urea levels were evaluated in cell supernatants as a measure of the activity of NOS or arginases, respectively. **Results:** In normoxia, *L. infantum* infection reduced *NOS2* expression and NO secretion induced by BMDM activation, whereas it induced *ARG1* expression and the activity of arginases, despite a reduction of *ARG2* expression. Although hypoxia strongly induced *NOS2* in uninfected macrophages, NO production was completely abrogated. Concomitantly, the activity of arginases was increased in the hypoxic environment. *L. infantum* infection reduced the expression of both *NOS2* and *ARG1* induced by hypoxia, although with no significant effects on the final products, NO and urea. **Conclusions:** Our data suggest that in normoxia the infection of macrophages with *L. infantum* parasites preserves their own survival by promoting the arginase-mediated pathway to the detriment of arginine metabolism by inducible NOS. Even a hypoxic environment, typical of an inflammatory state, seems to modulate arginine metabolism in favor of arginases. A clearer comprehension of the interplay between hypoxia and *Leishmania* infection in the main macrophage defense mechanism is essential not only for a better knowledge of leishmaniosis pathogenesis, but also in the perspective of new possible tools for leishmaniosis treatment.

ID18. Extracellular Vesicle Biomarker Detection for COVID-19 Diagnostics Using MALDI-Based Screening

D. Stefanizzi, F. Caponnetto, R. Del Sal, E. Sozio, C. Tascini, F. Curcio, A.P. Beltrami
Università degli studi di Udine, Department of Medical Area, Udine, Italy.

Introduction: Multi-omic approaches have been implemented under COVID-19 pressure for the identification of biomarkers of patient outcome. In this setting, matrix-assisted laser desorption/ionization-time of flight (MALDI-TOF) is being studied to identify specific proteomic and lipidomic fingerprints of biological samples that could be associated with disease outcome. Exosomes are small, cell-derived bioactive nanovesicles (50 to 200 nm) increasingly recognized as a promising source of circulating biomarkers for non-invasive diagnostics from body fluids. For this reason, the aim of this work is to create a fingerprint of circulating extracellular vesicles (EVs) associated with COVID-19 outcome. **Methods:** Platelet-poor plasma of 20 COVID-19 patients was dichotomized based on disease severity and collected at hospital admission. Patients who were either paucisymptomatic or affected by a mild to moderate form of the disease were referred to as “non-severe,” whereas patients who were either affected by severe to critical COVID-19 at disease onset or who had moderate disease and worsened requiring admission to the ICU were referred to as “severe." The same mutational variant of concern was maintained for reproducibility of data. Biological samples underwent exosomal enrichment using SelectEV kit (Exosomics) to obtain an exosomal pellet, which was processed for protein isolation using 2-D Clean-up kit (Bio-Rad). Proteins, together with intact EVs, were desalted and concentrated using C18-ZipTips and spotted directly on the MALDI plate in duplicate. We performed analysis using the MALDI-7090. **Results:** Protein extracts were analyzed by MALDI-TOF in the range of m/z 2,000 to 20,000, and using mMass software for peak picking we could identify 82 peaks in non-severe patients’ protein extracts and 90 peaks in severe patients’ protein extracts. Analyzing intact vesicles, we detected 67 peaks in non-severe patients’ and 77 peaks in severe patients. As expected, we found that 38 peaks were shared among all the spectra, while 26 were shared only in extracted vesicles and 17 were present only in the intact vesicles. Lastly, once we compared the peaks obtained, correlating them with disease severity, 23 peaks were exclusive of severe patients’ protein extracts and 16 peaks exclusive of non-severe patients’, whereas considering intact vesicles, 14 peaks were detected in severe patients’ intact vesicles and only 4 peaks were found in non-severe patients. **Conclusions:** This work shows the great potential of MALDI-based technology for the identification of a specific proteic exosomal fingerprint to identify potential clinical biomarkers. The presence of the peaks, as well as their intensities, were found to vary greatly depending on the type of sample analyzed. More generally, MALDI could be promising to establish a high-throughput screening platform for clinical purposes in several pathologies.

ID19. Determination of a Ct Cut-off Value for Optimization of SARS-CoV-2 Detection via CDC Protocol

M.T. Tada, E.M. Silva, N.C. Melo, D.A. Nociti, J.S.L. Silva, A.S. Lima, C.F.A. Cavalcanti, R.A. Coudry
UnitedHealth Group, Laboratory of Molecular Biology, São Paulo, Brazil.

Introduction: The World Health Organization (WHO) on March 11, 2020, declared the novel coronavirus outbreak a global pandemic. The Centers for Disease Control and Prevention (CDC) has released in February 2020 a SARS-CoV-2 detection protocol, which detects 2 viral targets (N1/N2) and RNaseP (endogenous control). However, some RT-PCR results can be classified as inconclusive due to the detection of only 1 viral target. These results may confound the laboratory result of SARS-CoV-2 viral infection. Despite this, few studies have explored the obtaining of Ct cut-off to determine positive results in a large cohort. Thus, the aim of this study was to evaluate the outcome of inconclusive results using the CDC method for detecting SARS-CoV-2 using the multiplex technique that evaluates 3 viral targets. **Methods:** We selected 1,487 nasopharyngeal/oropharyngeal swab samples with an undetermined result (detection of only 1 target) by CDC protocol (RT-PCR TaqMan SARS-CoV-2 – CDC) between July and December of 2020. All patients signed an informed consent form. Samples were reprocessed with the same amount of RNA input into a multiplex detection kit (TaqPath COVID-19 CE-IVD RT-PCR Kit, Thermo Fisher) to confirm the result. This kit consists of 3 SARS-CoV-2 targets: *S*, *N,* and *ORF1ab* genes, and an exogenous control (MS2 bacteriophage). The results were compared using receiver operating characteristics (ROC) curves and Youden index to determine the better cut-off considering its sensitivity and specificity. SARS-CoV-2 detection procedures were performed according to the manufacturers' recommendations. Statistical analysis was made using SPSS software. **Results:** Reprocessed samples using the multiplex kit with undetermined results by the CDC showed 98.12% negative (n = 1,459) and 1.88% (28) positive results. All tested samples had RNaseP identification, showing that the RNA extraction step was efficient. In positive samples, the mean Ct was 36.3 ± 3.04 for N1/N2 and 26.9 ± 2.09 for RNaseP for

undetermined samples by CDC protocol, whereas positive samples with multiplex kit showed a mean Ct of 30.1 ± 5.20, 30.2 ± 5.30, and 33.0 ± 5.30 in *S*, *N*, and *ORF1ab* targets, respectively. The Youden index determined the best cut-off point for Ct of 35.15, corresponding to 75.0% of sensitivity and 85.2% of specificity. ROC curve analysis showed a statistically significant curve (AUC = 0.845; SE = 0.039; p <0.01; 95% CI = 0.769 to 0.921). **Conclusions:** Using a large number of samples with an undetermined result in the CDC protocol and comparing with the multiplex detection kit by analyzing the ROC curve and the Youden index demonstrated that the best cut-off point for Ct for undetermined results from the CDC protocol is 35.15, considering 75.0% of sensitivity and 85.2% of specificity.

ID20. Validation of SARS-CoV-2 Detection in Saliva Samples by Real-Time PCR (RT-PCR)

N.C. Melo, E.M. Silva, M.T. Tada, J.S.L. Silva, D.A. Nociti, A.S. Lima, C.F.A. Cavalcanti, R.A. Coudry
UnitedHealth Group, Laboratory of Molecular Biology, São Paulo, Brazil.

Introduction: The detection of viral RNA in respiratory specimens such as nasopharyngeal/oropharyngeal swabs (NP/OP) by real-time PCR (RT-PCR) for SARS-CoV-2 infection is recommended by the World Health Organization. However, the need to increase the capacity for SARS-CoV-2 testing in different realities associated with the availability of collection supplies has motivated the search for alternative specimen types. In this context, the objective of the current study was to validate the detection of SARS-CoV-2 in saliva samples in comparison with NP/OP specimens using RT-PCR. **Methods:** This multicenter retrospective study included 3 medium-sized hospitals and collected samples from 253 patients from April 2021 to May 2021. All patients signed an informed consent form. The MagMAX Viral/Pathogen Nucleic Acid Isolation kit (Thermo Fisher) and the saliva lysis protocol were used to obtain RNA from swab and saliva samples, respectively. For swab viral detection we used multiplex detection kit (TaqPath COVID-19 CE-IVD RT-PCR, Thermo Fisher), which targets ORF1ab, N, and S viral regions, whereas the saliva RT-PCR kit TaqMan SARS-CoV-2-CDC targets 2 regions of the *N* gene (N1/N2) and RNaseP. SARS-CoV-2 detection procedures were performed according to the manufacturers' recommendations. Statistical analysis was performed using SPSS software. **Results:** The incidence of SARS-CoV-2 was 38% (70/253) by 2 tests (saliva and NP/OP swab by RT-PCR). The population consisted of 61.26% (155/253) females with a mean age of 39 ± 12.27 years. The limit of detection observed was of 100 copies/μL in saliva samples performed in 20 replicates by detection curve and reproducibility. In saliva samples, the mean Ct values of *N1* and *N2* genes were 27.8 and 28.0, respectively, whereas in swab samples, the mean Ct values of *S*, *N*, and *ORF1ab* targets were 20.2, 20.2, and 20.0, respectively. We verified a strong positive correlation for both CDC and for the multiplex targets, suggesting homogeneity in the analysis. The detection of SARS-CoV-2 using saliva samples showed sensitivity of 95.7% and specificity of 98.4% when compared to the gold standard method. The accuracy obtained was 97.63%, with a Cohen's kappa coefficient of 0.941 (p <0.001) and classified as "almost perfect." All tested samples had RNaseP identified, showing that the saliva lysis step was efficient. **Conclusions:** The RT-PCR test on a saliva sample showed high sensitivity and specificity for the detection of SARS-CoV-2. These findings provide supporting evidence for recommending saliva as an alternative modality that is safer, comfortable, and convenient to collect, and sufficiently accurate for making a clinical diagnosis. Thus, the direct saliva sample showed good applicability in the laboratory routine by reducing costs with extraction methods and practicality in collection.

ID21. Evaluation of SARS-CoV-2 Genomic Mutations Potentially Conferring Resistance to Antiviral Drugs in Viral Populations Isolated from Untreated SARS-CoV-2-Infected Subjects (Selected for Oral Presentation, O-04-04)

D. Lombardo, G. Caminiti, C. Musolino, V. Chines, C. Palermo, G. Raffa, T. Pollicino
University Hospital "G. Martino" of Messina, Clinical and Experimental Medicine, Messina, Italy.

Introduction: The development of safe and effective antiviral drugs has been a crucial issue since the outbreak of the severe acute respiratory syndrome coronavirus-2 (SARS-CoV-2) global pandemic. Currently, only three antiviral drugs are approved for the treatment of SARS-CoV-2-infected patients. Remdesivir and molnupiravir are two nucleoside analogs that target non-structural protein 12 (nsp12), the catalytic subunit of the RdRp complex. Paxlovid (a nirmatrelvir and ritonavir combination) blocks the activity of SARS-CoV-2 Nsp5/Main Protease/3C-like protease. Given the adaptive potential of SARS-Cov-2 and the ongoing selection of viral variants, it is conceivable that natural selection of mutant viruses might jeopardize the efficacy of new developed antiviral agents. The aim of this study was to analyze the SARS-CoV-2 genetic variability of the RdRp complex subunits and Nsp5 in SARS-Cov-2 populations isolated from a large series of subjects naïve to antiviral therapy. **Methods:** Viral RNA from 4,155 nasopharyngeal swabs from subjects from Southern Italy, collected from April 2021 to October 2022, was

extracted using an automated nucleic acid purification platform. Viral genomes were amplified with a SARS-CoV-2-specific primers pool. The amplicons were used to prepare the libraries that were sequenced on Illumina MiSeq platform, producing 151 bp paired-end reads. The SARS-CoV-2 complete genomes were reconstructed using the pipeline SARS-CoV-2 RECoVERY (REconstruction of COronaVirus gEnomes & Rapid analYsis). Phylogenetic relationship between viral isolates was obtained using the Molecular Evolutionary Genetics Analysis X (MEGAX) software. **Results:** Analysis of nsp12 SARS-CoV-2 sequences identified 84 aa substitutions. Among these, the P323L substitution was detected in 3,777/4,155 (91%) of the samples and the G671S substitution was detected in 2,906/4,155 (69.9%) of the isolates, 2,904/2,906 (99.9%) belonging to Delta variant and 2/2,906 (0.1%) belonging to Omicron BA.5 subvariant. In addition, 457/4,155 (11%) of the samples showed the L838I substitution, which is associated with remdesivir resistance. Sequencing analysis of the nsp7 and nsp8 SARS-CoV-2 genomic regions identified 14 and 24 different aa substitutions, respectively, which have not been characterized to date. The analysis of nsp5 identified 28 different aa substitutions. Among these, the A191V substitution, flanking the active site cavity of nsp5, has been detected in 3/4,155 (0.07%) of the cases. Phylogenetic analysis showed that, compared to nsp12 and nsp5 genomic regions, nsp7 and nsp8 have a lower genetic variability. **Conclusions:** This study demonstrates that both nsp12 and nsp5, targeted by currently available antiviral therapies, may accumulate several naturally selected aa substitutions, which may potentially affect antiviral drug efficiency, and suggests that nsp7 and nsp8 might be considered as new potential targets for the development of new antiviral drugs because of their low genetic variability and essential role in SARS-CoV-2 replication.

ID22. Evaluation of SARS-CoV-2 Positivity by RT-PCR in a Clinical Laboratory in São Paulo during 2022

E.M. Silva, M.T. Tada, N.C. Melo, J.S.L. Silva, D.A. Nociti, C.R.M. Pereira, C.F.A. Cavalcanti, R.A. Coudry
UnitedHealth Group, Laboratory of Molecular Biology, São Paulo, Brazil.

Introduction: In Brazil, in March 2020, the Ministry of Health characterized COVID-19 as a pandemic. After the first case had been verified a dynamic of positivity involved several factors, including socio-demographic aspects, vaccination, and the presence of different variants of SARS-CoV-2. Knowledge of the extent of infection is critical to developing an effective public health response to COVID containment. In this context, the objective of the current study was to evaluate positivity of SARS-CoV-2 by RT-PCR in a clinical laboratory in São Paulo during 2022. **Methods:** This was a multicenter retrospective study that included 17 hospitals, involving patients who received at least 1 interpretable SARS-CoV-2 RT-PCR result from January 1 to December 31 of the year of 2022. For the detection of SARS-CoV-2, samples of nasopharyngeal/oropharyngeal swabs (NP/OP) or saliva were analyzed by real-time PCR (RT-PCR). In NP/OP swabs, we used MagMAX Viral/Pathogen Nucleic Acid Isolation kit for RNA isolation and TaqPath COVID-19 CE-IVD RT-PCR (Thermo Fisher) kit for multiplex SARS-CoV-2 viral detection, whereas for saliva, we used TaqMan SARS-CoV-2 Fast PCR Combo Kit 2.0 for direct multiplex SARS-CoV-2 detection. A descriptive analysis of the variables (genus and age) was made by absolute and relative frequencies. Statistical analyses were performed using SPSS and GraphPad Prism software. **Results:** During the study period, 75,226 cases were analyzed; 27.74% (n = 20,865) were positive for SARS-CoV-2 in 2022. In Brazil, we had 2 peaks of infections, one in January and another in June, presenting a positive rate of 51.1% and 40.0%, respectively. Positive cases were characterized by presenting 64.85% (n = 13.532) of female patients and 19.91% (n = 4.155) of vulnerable patients (764 children ≤5 years old [mean age 2.1 ± 1.4] and 3,391 people aged ≥60 years old [mean age 73.6 ± 9.8]). Positivity decreased during the year as expected, with a significant difference between the first and second semesters $p < 0.05$, 3,096.0 ± 3,390.0 and 381.0 ± 396.9, respectively. Positivity in vulnerable patients represented 19.1% (4,155/20,865) of positive attendances in 2022. The average positivity in vulnerable patients was 346.3 ± 398.0 per month, with minimum values from 13 (September) to 1,407 (January), showing no differences between the first and second semesters ($p > 0.05$). **Conclusions:** The mean positivity found in our study was high both in the general population (27.74%) and in vulnerable patients (19.91%). The peaks of positive cases in January and June were consistent with the positivity curve in Brazil in the year 2022. As expected, there was a reduction in the number of cases over the course of the year, probably due to the vaccination adherence of the population analyzed in this study.

ID23. Hantavirus Detection in a Private Hospital in São Paulo, Brazil, Using a Metagenomic RNA Diagnostic Test

R. Petroni, R. Santana, N. Muto, D. Amgarten, E. Dorlass, B. Oliveira, A.P. Salles, A. Santos, A. Takara, M. Menezes, R. Sitnik, J.R. Pinho, A. Doi
Hospital Israelita Albert Einstein, São Paulo, Brazil.

Introduction: Hantaviruses (family Hantaviridae, genus *Orthohantavirus*) are enveloped zoonotic RNA viruses hosted by rodents that can cause diverse potentially fatal syndromic diseases. In the Americas, they are responsible for hantavirus pulmonary syndrome (HPS). In Europe and Asia, they cause hemorrhagic fever with renal syndrome. Laboratory diagnosis is often conducted by detection of IgG- and IgM-specific antibodies in blood; in addition, immunohistochemistry can be used to detect viral antigens, and viral RNA can be detected through RT-PCR. However, all of these laboratory techniques are rarely available in clinical laboratories. We report a case of hantavirus detection in a private hospital in São Paulo, Brazil, using a metagenomic RNA diagnostic test. **Methods:** We developed and validated a new routine metagenomic test for RNA viruses, a virome enrichment technique using metagenomic next-generation sequencing (NGS) technology. Briefly, total RNA was extracted from plasma and human rRNA was depleted. Reverse transcription of RNA was performed with a 2-step cDNA random synthesis, followed by PCR amplification, a protocol adapted from Greninger *et al*. The generated data were used as input for an in-house bioinformatics pipeline. **Results:** After the bioinformatics analysis, it was possible to recover 99 reads of Andes orthohantavirus. NGS average coverage was 32X with an abundance of 62,6%. No other potentially clinical pathogen was detected in our metagenomic test. Considering the consistency between clinical history and metagenomic genetic finding, we reported the result as positive. **Conclusions:** Andes orthohantavirus is a type of hantavirus found in rodents in South America which leads to a severe and potentially fatal respiratory illness called HPS. These can develop quickly and therefore a rapid medical intervention is necessary. There is no specific treatment, cure, or vaccine for HPS. However, patients can receive supportive care in the hospital to help with symptoms. Through the technique used in this study, it was possible to recover the partial genome of the Andes orthohantavirus. This case demonstrated the importance of using metagenomics in the clinical laboratory for the detection of rare pathogens, which normally do not have specific tests in the laboratory menu. Moreover, a non-targeted test can also help in potentially new emerging infectious disease.

ID24. Direct from Specimen Species Identification: Urinary Tract Microbiota Assay

C. Ledesma, J. Garcia
Marquis Labs, Oklahoma City, OK.

Introduction: Urinary tract infections (UTIs) are very common, especially in women, and consist of an infection of the urinary system, including the bladder, urethra, and/or kidneys. If treated promptly, no serious condition arises, but if not treated or treated with the wrong medicines, more serious conditions like kidney infection may occur. Although widely used, culture-based methods for the detection of pathogens involved in urinary tract infections lack sensitivity, are subjective, have longer turnaround times, and have been shown to miss a significant percentage of positive cases. Molecular solutions for UTI analysis can take as little as 5 hours from DNA extraction to results reporting, with increased accuracy in reporting of detected organisms. **Methods:** The purpose of this validation is to demonstrate the acceptable analytical and clinical performance of the Thermo Scientific Custom Urinary Tract Microbiota (UTM) Assay on a QuantStudio 12k Flex (QS12k). **Results:** The method validation is composed of the following studies: precision, accuracy, limits of detection, analytical sensitivity, stability, and interference studies. Precision data for all targets and all replicates were 95% to 100% concordant. Accuracy: All targets for all specimens were 100% concordant. Limits of detection (LOD): The experimental data consistently showed successful PCR for all targets contained in the Custom UTM Amplification Control at all tested concentrations except 100 and 500 copies/µL. The LOD for this validation is considered to be a concentration of 1,000 copies/µL (103). Analytical sensitivity: All targets on this assay produced a specificity value of 100% Interference; no significant PCR interference was detected for blood, rash cream, zinc, or benzalkonium chloride. **Conclusions:** Molecular solutions can expedite the process of organism identification. The validation of this assay could be beneficial to antibiotic stewardship, as it promotes the earlier detection of organisms.

Selected Informatics Abstracts

I01. Predicting Immunotherapy Response by Inferring Tumor Neoantigen Load (Selected for Oral Presentation, O-01-03)

R. Burns, C.C. Palsuledesai, N. Friedman, M.C. Liu, M. Rabinowitz, A. Aleshin, H.A. Costa
Natera, Inc., Austin, TX.

Introduction: Tumor mutational burden (TMB), which reflects the number of cancer mutations, has emerged as a predictive biomarker of immunotherapy (IO) response. Although high TMB status leads to increased neoantigen presentation and

enables T-cell recognition, not all mutations produce neoantigens or elicit an immune response. TMB is therefore an imperfect biomarker. In this study, we sought to analyze whether neoantigen load and immune diversity inferred from tumor whole-exome sequencing (WES) and/or RNA sequencing (RNAseq) data could improve the prediction of patient response to IO when compared with TMB alone. **Methods:** In this study, we built an immune response prediction model by analyzing publicly available WES and RNAseq data from 257 patients with high-risk muscle-invasive bladder cancer (MIBC) who received adjuvant IO. Protein coding somatic mutations identified using WES from each patient were processed by several open-source neoepitope and neoantigen classifiers working as an ensemble for maximum predictive power. Tumor bulk RNAseq data were used to deconvolute proportions of immune cells present within the tumor, assemble B- and T-cell receptors, and calculate the receptor alpha diversity within each patient. The model was then trained using the above dataset, pre-IO circulating tumor DNA (ctDNA) results (Signatera), and clinical characteristics (age, cancer stage, previous therapies, and metastases). The training was conducted using 80% of the patients, whereas testing was conducted using 20% of the patients. **Results:** We analyzed the performance of our model by predicting response to IO. Predicted responders had significantly better disease-free survival (DFS) (HR: 0.15; 95% CI: 0.06 to 0.39; p = 0.001; area under the curve = 0.79) compared to predicted non-responders. TMB (high/low) alone was observed to be less predictive of DFS (HR: 0.60; 95% CI: 0.40 to 0.88; p = 0.007) than the immune response prediction model. The presence of neoantigens (inferred by PRIME and DeepImmuno) was predictive of IO response, whereas a higher number of nodal metastases, ECOG score, and pre-IO ctDNA-positivity status were predictive of non-response to IO. Additionally, higher immune diversity was found to be predictive, wherein monocytes C and pDCs were associated with higher risk of recurrence. Interestingly, TMB status was not found to be a predictive factor by the model. **Conclusions:** Our results indicate that the incorporation of neoantigen load, immune diversity, and other clinical variables significantly improved the prediction of IO response in patients with MIBC, compared to TMB status alone. For patients undergoing tumor-informed ctDNA monitoring and/or comprehensive tumor profiling, neoantigen load and immune diversity information can be inferred without the need for any additional tests. Further studies in other cancer types are warranted to establish the clinical utility of the immune response prediction model.

I02. Identification of Potential Gut Microbiota Biomarkers of Predisposition to Inflammatory Bowel Disease in Healthy Subjects from Northern Italy

G. Taurino[1,2], L. Mancabelli[1,2], M.G. Bianchi[1,2], G. Longhi[3], M. Chiu[1], F. Turroni[2,3], R. Cecchi[2,4], M. Ventura[2,3], O. Bussolati[1,2]

[1]University of Parma, Laboratory of General Pathology, Department of Medicine and Surgery, Parma, Italy; [2]University of Parma, Microbiome Research Hub, Parma, Italy; [3]University of Parma, Laboratory of Probiogenomics, Department of Chemistry, Life Sciences, and Environmental Sustainability, Parma, Italy; [4]University of Parma, Laboratory of Forensic Medicine, Department of Medicine and Surgery, Parma, Italy.

Introduction: Inflammatory bowel disease (IBD) is an heterogeneous group of chronic pathologies of the gastrointestinal tract, including Crohn disease (CD) and ulcerative colitis (UC). The main biomarkers used to diagnose and monitor IBD are faecal calprotectin (FC) and serum C-reactive protein. FC is released by recruited neutrophils and, in smaller quantity, monocytes, thus reflecting local inflammatory status, and can reach very high levels in IBD patients (CD ~3,200 µg/g, UC ~1,900 µg/g). It is known that gut microbiota composition of IBD patients is characterized by an enhancement and/or depletion of specific microbial groups such as *Fusobacterium* and *Faecalibacterium*, respectively. Hence, the gut microbiota can also be a potential IBD biomarker, although profiling data available so far do not consider possible confounding host "extrinsic" (diet, geographical location, drug therapy) and "intrinsic" (stress, immunity status, psychopathologies) factors. In this study, we have evaluated the presence of potential microbial biomarkers in healthy subjects of a specific area of northern Italy as part of a larger project (i.e., the Parma Microbiota study), correlating taxa composition with FC levels and considering a number of extrinsic/intrinsic factors. **Methods:** Healthy subjects (n = 500, age 18 to 70 yrs) resident in the Parma area (Emilia-Romagna, Italy) were enrolled, and their extrinsic/intrinsic factors were obtained through questionnaires. Faecal samples were collected and 15 mg of each sample were picked up with specific devices to quantify FC levels through ELISA analysis. At the same time, bacterial DNA was extracted and purified from faecal samples to perform next-generation metagenomics analysis (deep shotgun metagenomics attempts). **Results:** Median FC in the 500 healthy subjects was 23.4 µg/g of faeces (Q1 11.8 µg/g to Q3 46.9 µg/g). More than 70% of donors show FC levels below the normal cut-off (50 µg/g), whereas about 10% of subjects present FC levels higher than 100 µg/g, showing an elevated inflammatory, IBD-related status. Studies of the correlation between FC levels and age or gender of donors such as the analysis of the different microbiome taxa are

ongoing. **Conclusions:** The results of FC levels show that at least 10% of the adult healthy population in northern Italy display laboratory indexes indicative of an intestinal inflammatory condition, suggesting a possible predisposition of this "IBD-cluster" to develop the intestinal pathology. These data will be correlated with host extrinsic/intrinsic factors and with gut microbiota composition to identify putative microbiome biomarkers associated to a higher risk of IBD.

I03. Predicting the HER2 Receptor Amplification and Its Implementation in Routine Clinical Diagnostics of Breast Cancer Using Machine Learning and RNA-seq Data

S.P. Kuntia, N.A. Tanwar, R. Malhotra, S. Reddy P, K.D. Rishi, H. Goswami, V.H. Veldore
4baseCare Onco Solutions Pvt. Ltd., Bangalore, India.

Introduction: About ~15% to 20% of breast malignancies have an overexpression/amplification of HER2, which is often referred to as HER2-positive and makes these cancers more aggressive. This also serves as a biomarker for targeted anti-HER2 therapies. In clinical practice, assays such as immunohistochemistry (IHC), fluorescence *in situ* hybridization (FISH), and DNA-seq-based analyses are used to determine a patient's HER2 amplification status by evaluating different aspects of the HER2 receptor. Here, we are presenting a new method for predicting HER2 status using machine learning (ML) algorithms applied to RNA-seq data. The aim of the study is to compare the performance of this ML-based approach to traditional DNA and protein-based methods, and develop a more efficient and accurate way of predicting HER2 status, which could potentially improve patient outcomes. **Methods:** We have used the TCGA-BRCA dataset (n = 1,098) to train an ML pipeline using the SVM algorithm. The training set consisted of 736 samples, and the HER2 status was trained based on concordant IHC and FISH results, which served as the dependent variables. The remaining TCGA data, which comprised about 33% of the total dataset, were used to evaluate the performance of the algorithm. The robustness of the algorithm was further validated using tumor profiling data from 150 cancer patients, which included RNA-seq, DNA-seq (amplification), and IHC results from 4baseCare. To ensure accurate predictions, the raw data were normalized for library sizes using the TMM approach and was batch corrected to avoid any biases. **Results:** The ML pipeline used in the study was able to accurately predict the HER2 receptor status with 89.2% accuracy using data from the TCGA dataset and 88.8% accuracy using data from the 4baseCare dataset. The results showed a high concordance among the results of IHC, RNA-seq, and DNA-seq data. **Conclusions:** The ML approach has helped in better stratification of patients with HER2 amplification, as it provided a clear binary distribution, unlike the difficulties experienced with patients who have IHC3+ results and ambiguous HER2 results from FISH testing. To summarize, incorporating AI/ML techniques into the routine clinical testing workflow adds tremendous value in the selection of patients who would be potential responders to targeted therapies.

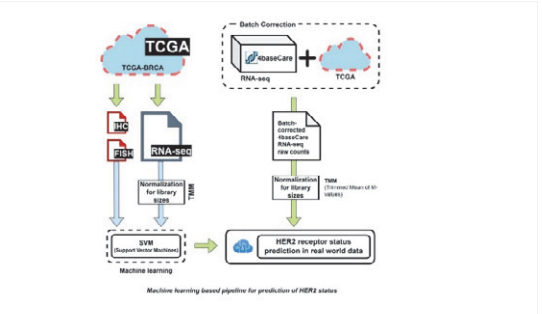

Machine learning pipeline for prediction of HER2 status.

I04. The Development of a Genomic Variant "Truth Set" to Aid Next-Generation Sequencing-Based Cancer Diagnostics (Selected for Oral Presentation, O-01-04)

G. C.J. Mackenzie[1,2], P. Roxburgh[1], G. Hamilton[1], L. Lo-Cascio[2], A.P. Sanzone[3], F. Lescai[4]
[1]University of Glasgow, Institute of Cancer Science, Glasgow, United Kingdom; [2]Medicines and Healthcare Products Regulatory Agency, Division of Diagnostics, Genomics Team, South Mimms, United Kingdom; [3]Formerly Medicines and Healthcare products Regulatory Agency, Division of Diagnostics, Genomics Team, South Mimms, United Kingdom; [4]University of Pavia, Laboratory of Computational Genomics, Pavia, Italy.

Introduction: Exhaustive characterisation of cancer patient genomes can only be achieved by accurate detection of somatic variants and quantification of their variant allele frequencies (VAFs). Overcoming the difficulties in distinguishing low VAFs from sequencing and analysis errors is essential to the successful implementation of precision medicine in healthcare. The lack of appropriate standards and calibrated methods is a critical gap. In 2018, NIBSC created the first WHO international standard (IS) panel for somatic variants in cancer, containing 5 highly characterised variants across 3 cell lines: HCT15, MOLT4, and ATDB102. Project aims were to expand upon the original standard by characterising structural variants (SVs) present in original cell lines' genome, study potential biases introduced by PCR during library preparation, and ensure reproducibility of the results. **Methods:** Whole-genome sequencing was performed by BGI Sequencing, using both PCR and PCR-free library preparations, allowing biases from PCR to be detected by comparing each pair of cell line datasets. Since the cell lines

lack matched normal samples, a Panel of Normals (PON) was generated using publicly available sequencing data from the Sequence Read Archive. We wrote a custom Nextflow workflow as currently, nf-core/Sarek does not support PON generation. Variant calling was performed using the nf-core/Sarek somatic and joint germline workflows. nf-core/Sarek was chosen as it follows the widely adopted GATK best practices, being written in Nextflow makes it easily portable, and is available on the nf-core repository for easy installation. Analysis was run on the Google Cloud Platform (GCP). **Results:** To start, modules necessary for GATK best practices not on nf-core were written and submitted to nf-core These helped create the joint germline workflow introduced in the 3.0 release of nf-core/Sarek and to write the PON workflow. Sequencing data selected for PON generation was the closest technical match in terms of sequencing conditions publicly available. This was limited by the sequencing platform, but an appropriate match was found. Using the GCP to run nf-core/Sarek allowed for flexible storage of large quantities of data and access to the processing power that would otherwise be unavailable. For each cell line, annotated variants were generated covering the whole genome, for both PCR and PCR-free library preps. Joint germline variants were also generated using all cell line sequencing data. Newly discovered variants will be validated by digital PCR. **Conclusions:** We expanded the analysis of the original WHO IS to cover the whole genome, focusing on SVs. Since the original cell lines are available from NIBSC and each step of the bioinformatic analysis uses publicly available, easy-to-run workflows, the results generated can be reproduced and the methods used can be applied as a standard workflow for data analysis and future standards generation.

Selected Solid Tumors Abstracts

ST01. Mutational-Copy Number Variation Profile and Immunotherapy Drivers in Neuroendocrine Lung Carcinomas: PD-L1, Microsatellite Instability, DNA Mismatch Repair Genes Expression and Tumor Mutational Burden in a Series of 30 Cases

N. Rodon[1], C. Pubill[1], Y. No[1], E. Garcia[2], E. Saigi[2], X. Puig[1,3]
[1]BIOPAT. Biopatologia Molecular SL. Grup Assistència., Barcelona, Spain; [2]Servicio de Oncologia, SCIAS-Hospital de Barcelona, Grup Assistència., Barcelona, Spain; [3]Histopat Laboratoris SL, Barcelona, Spain.

Introduction: Immunotherapy, with treatments aimed at inhibiting immune checkpoints, has meant a paradigm shift in the therapeutic approach to solid neoplasms. The biomarkers postulated to indicate this type of treatment have been the PD-L1 expression, the presence of microsatellite instability (H-MSI), loss of DNA mismatch repair gene (dMMR) expression, and tumor mutational burden (TMB), interpreted as the number of mutations detected per megabase of DNA analyzed (mut/Mb). In the current study, these 4 biomarkers as well as the mutational profile and copy number variation (CNV) status have been analyzed in a series of lung neuroendocrine carcinomas. **Methods:** A retrospective study was designed. Lung neuroendocrine neoplasms analyzed in our center between 2019 and June 2022 were included. The morphological and MMR expression diagnosis included the immunohistochemical study of TTF-1 (Novocastra), chromogranin (Cell Marque), synaptophysin (Cell Marque), INSM1 (Santa Cruz), PANK (Biolegend), PD-L1 (Roche), and MLH1, MSH2, MSH6, and PMS2 (BD Pharmingen). The molecular study was performed with 2 NGS panels: one for the analysis of alterations in 52 genes at DNA and RNA level (FOCUS, Thermo Fisher); and a second NGS panel for TMB analysis (Oncomine TML, Thermo Fisher). Mutations, CNV, and gene fusions were recorded. The microsatellite instability study was performed by PCR and fragment analysis of 13 markers (TrueMark MSI Assay, Thermo Fisher). **Results:** Thirty lung neuroendocrine tumors were included (7.5% of all lung neoplasms studied in the indicated period): 27 small cell tumors and 3 large cell tumors. None were negative for synaptophysin and chromogranin simultaneously. Only 3 tumors showed PD-L1 expression (20%, 20%, and 5%); all of them presented a combined pattern of squamous cell carcinoma and TMB values of 11, 4, and 7 mut/Mb, respectively. In 2 of these cases neither mutation nor CNV was detected. The third one showed a *TP53* mutation and *MYCL* amplification. In the global series, non-informative NGS panel results were obtained in 1 case due to the presence of deamination in the DNA extracted. Mutations in *TP53, RB1, HNF1A, NOTCH1, PTEN, ARID1A,* and *STK11* genes were detected in 72.4%, 17.2%, 10.3%, 10.3%, 6.9%, 6.9%, and 6.9% of patients, respectively. Mutations in 13 more genes were detected with a frequency of less than 4%. Ten patients (34,5%) showed a CNV involving *MYC, RICTOR, TERT, PIK3CA, PDGFRA, KIT*, and *MYCL* genes. No alteration was detected at RNA level. None of the analyzed tumors presented H-MSI or dMMR. The range of TMB values was from 0 to 18.8 mut/Mb with a mean of 7.8 mut/Mb. Eleven cases (37.9%) presented a TMB ≥ 10 mut/Mb. **Conclusions:** In this series of lung neuroendocrine carcinomas, *TP53* and *RB1* mutations were the most prevalent. No tumors showed H-MSI or dMMR. Only 3 expressed PD-L1. TMB can predict a potential response to immunotherapy in 38% of the cases analyzed.

ST02. Next-Generation Sequencing-Guided Therapy for *BRAF V600E* Mutant Glioblastoma Results in Stable Disease

S. Bannykh, J. Hu, C. Patil, E. Vail
Cedars-Sinai Medical Center, Pathology and Laboratory Medicine, Los Angeles, CA.

Introduction: Glioblastoma multiforme (GBM) is an aggressive infiltrative brain tumor with poor outcome and only a 14-month overall survival. The molecular makeup varies for individual tumors. Next-generation sequencing (NGS) offers a multiplex analysis of mutations in hundreds of genes, yet the clinical applicability of these findings is limited. Here we report a case of a GBM with sarcomatoid morphology and a presence of *BRAF* V600E mutation. The tumor was treated with *BRAF*-targeted therapy, resulting in a stable disease. **Methods:** Tissue diagnosis was obtained using WHO (2021) criteria using routine histology of formalin-fixed, paraffin-embedded (FFPE) tissue supplemented by immunohistochemical studies. Genomic DNA and RNA were extracted from macro-dissected areas on FFPE tissue sections. Concurrent DNA and RNA libraries were constructed using Oncomine Comprehensive Plus Assay library preparation kits (Thermo Fisher Scientific, Waltham, US) and the library pools were sequenced using the Ion GeneStudio S5 Prime system (Thermo Fisher Scientific). The sequencing data were analyzed by Ion Reporter Software v5.18 and in-house-developed bioinformatic pipelines. The assay detects single nucleotide variants, small insertion-deletions, copy number variants, and select fusions from more than 500 genes and accurately assesses tumor mutation burden and microsatellite instability. **Results:** The patient presented with worsening headaches, confusion, altered mental status, and ataxia on June 12, 2021. Imaging revealed centrally necrotic enhancing 6.4 cm right frontal mass. Near complete resection was obtained. Pathology revealed an isocitrate dehydrogenase 1/2-wild-type GBM. NGS revealed *SMARCB1* p.R40 (75.9%), *TERT* promoter mutation (44.4%), and *BRAF* p.V600E (28.6%). Tumor mutation burden was 5 muts/Mb (intermediate), and there was no PD-L1 expression by immunohistochemistry. O^6-methylguanine-DNA methyltransferase promoter showed presence of methylation. The patient underwent a standard post-operative treatment with radiation and 12 cycles of temozolomide. Magnetic resonance imaging (MRI) of the brain from October 6, 2022, showed increased enhancement along cerebellum (presumed recurrence). Given the presence of *BRAF* V600E mutation, the patient was started on dabrafenib 150mg BID and trametinib 2mg (10/07/2022). Follow-up MRIs from November 3, 2022, and January 5, 2023, showed no evidence of progression and slight decrease in tumor's size. **Conclusions:** NGS can provide useful data for successful targeted therapy of patients with GBM.

ST03. Diagnosis of Metastatic SHH-Activated Medulloblastoma in Adult via Bone Biopsy and Next-Generation Sequencing

S. Bannykh, B. Balzer, X. Fan, E. Vail, J. Hu
Cedars-Sinai Medical Center, Pathology and Laboratory Medicine, Los Angeles, CA.

Introduction: Establishing a primary site for a bony metastasis of tumor of unknown origin relies on multiple modalities, including demographics, PET scan, histology, and immunohistochemistry. Commonly, advanced clinical stage dictates the need for targeted therapy. Here we report a case of SHH-activated medulloblastoma metastatic to bone, diagnosed through next-generation sequencing (NGS). **Methods:** Tissue diagnosis was rendered based on WHO (2021) criteria using routine histology of formalin-fixed, paraffin-embedded (FFPE) tissue supplemented by immunohistochemical studies. Genomic DNA and RNA were extracted from macro-dissected areas on FFPE tissue sections. Concurrent DNA and RNA libraries were constructed using Oncomine Comprehensive Plus Assay library preparation kits (Thermo Fisher Scientific, Waltham, US) and the library pools were sequenced using the Ion GeneStudio S5 Prime system (Thermo Fisher Scientific). The sequencing data were analyzed by Ion Reporter Software v5.18 and in-house-developed bioinformatic pipelines. The assay detects single nucleotide variants, small insertion-deletions, copy number variants, and select fusions from more than 500 genes. **Results:** Fifty-one-year-old woman presented with headaches in October 2022. Brain MRI revealed a 3.8 x 3.2 cm dural-based lesion along the paramedian transverse sinus with remodeling of the occipital bone. Subsequent MRI of the spine and whole-body PET CT from December 2022 showed more than 10 hypermetabolic lytic axial bony metastases. The differential diagnosis included metastatic carcinoma, melanoma, lymphoma, or histiocytosis. Stereotactic iliac biopsy on December 27, 2022, disclosed histologically and immunophenotypically poorly differentiated primitive small round cell malignant neoplasm, negative for histiocytic markers, and also of a carcinoma, lymphoma, or melanoma. Neuroendocrine marker: Insulinoma Associated Protein 1, was strongly positive and Ki-67 was 45%. NGS demonstrated mutation pattern of SHH activated, *TP53*-wild-type medulloblastoma. The mutations included: *PTCH1* splice site alteration chr9:g.98268688C>A NM_000264.3:c.394+1G>T (allele frequency (AF) of 84%), *PIK3CA* p.E545K (AF 40%), *MYCN* p.P44L (AF 42%), *KDM6A* p.L981Nfs*17 (AF 40%),

and *TERT* promoter site alteration (AF 36%). The findings were therefore consistent with metastatic medulloblastoma. Clinically, there was no evidence of Gorlin syndrome. Mutations in Patched (PTCH) with loss of protein function release tonic inhibition of Smoothened (SMO), which in turn result in abnormal activation of the Hedgehog pathway. Potent inhibitor of SMO can suppress proliferation of cells of medulloblastoma, driven by SHH pathway activation. Vismodegib, an inhibitor of SMO, was therefore administered in combination with temozolomide. **Conclusions:** NGS can play a pivotal role in providing a definitive diagnosis and guide therapeutic efforts in central nervous system tumors.

ST04. Using Chromosome Microarray to Resolve Difficult ERBB2 FISH Results: Example Cases

J. Dong
University of Texas Medical Branch, Pathology, Galveston, TX.

Introduction: Erb-b2 receptor tyrosine kinase 2 (ERBB2) fluorescent *in situ* hybridization (FISH) assay is routinely used to measure ERBB2 DNA copy numbers in immunohistochemistry (IHC) equivocal (2+) tumor samples. ERBB2 IHC and FISH results have prognostic and predictive values for breast, gastroesophageal adenocarcinoma (GEA), and other cancers. FISH results can be complicated by equivocal ERBB2 status and by intra- and inter-tumor genetic heterogeneity. This study examined the use of whole-genome chromosome microarray (CMA) to help resolve difficult ERBB2 results. **Methods:** FISH assay was conducted by using PathVysion HER-2 DNA Probe Kit (Abbott Laboratories) according to the manufacturer's instructions. ERBB2 and chromosome enumeration probe 17 (CEP17) signals were observed under a fluorescent microscope (CytoVision, Leica Biosystems Inc). ERBB2 status was evaluated by the most updated ASCO/CAP guidelines for breast and GEA cancers. Cases with challenging ERBB2 FISH results were examined by CMA using OncoScan CNV Assay Kit (Affymetrix). A copy number variant profile was generated and analyzed using Chromosomal Analysis Suite (ChAS, Affymetrix). **Results:** CMA detected cases with false ERBB2 FISH signal due to larger size of FISH probe covering amplified flanking sequences of ERBB2 and clonal differences of primary and metastatic samples from the same patients with different ERBB2 results. **Conclusions:** CMA can help us understand and resolve challenging ERBB2 results. Further studies are warranted to examine the utility of CMA in facilitating ERBB2 testing, especially in cases with unusual results.

ST05. Validation and Clinical Implementation of a Pan-Cancer Circulating Tumor DNA-based Next-Generation Sequencing Assay (Selected for Oral Presentation, O-01-01)

G. Zheng, A. Schneider, M. Campion
Mayo Clinic, Rochester, MN.

Introduction: Cell-free tumor DNA (ctDNA) enables non-invasive diagnostic assays for precision medicine, and it could provide similar comprehensive molecular mutation profile information as tumor tissue biopsies. In this study, we validated and clinically implemented a 33-gene Pan-Cancer ctDNA next-generation sequencing (NGS) assay (PGDx Elio Plasma resolve [EPR] assay). **Methods:** In the validation study, 40 clinical plasma samples, 10 healthy donor plasma samples, 20 contrived samples using DNA derived from formalin-fixed paraffin-embedded tumor tissue, and 3 commercial reference materials were used. CfDNA was extracted from whole blood using KingFisher Presto Nimbus automated platform. Ten to 40 ng of cfDNA was used to prepare genomic libraries using the EPR kit. The sequencing was performed on the Illumina Nextseq. PGDx EPR software performs alignment, variant calling, and filtering. The alterations detected included single nucleotide variants, small insertions and deletions (indels), amplifications, microsatellite instability (MSI) status, and translocations. Detected DNA variants were compared to orthogonal NGS testing results if available, and digital droplet PCR for amplifications or 2-Step PCR for SNVs and indels were used as confirmation tests. Clinical experience after test implementation was summarized, focusing on clinical actionability. **Results:** Both within-run and between-run reproducibility studies showed >99% concordance across different types of alterations. The assay showed a limit of detection of at least 0.5% variant allele frequency (VAF) for hotspot SNVs, and 1% for non-hotspot SNVs; 2.5% for indels, 1.2- to 1.6-fold change for gene amplification depending on specific genes and the number of single nucleotide polymorphisms available to assess allelic imbalance, 2% for MSI status detection, and 2 supporting reads for fusion detection. Hotspot mutation reportable range can be as low as 0.1% with positive prediction value of 100% between 0.1% to 0.5% VAF. In accuracy study, sensitivity for SNVs and indels was 97% (97/100) and specificity was 100% (123/123), and overall concordance was 99% (220/223). Concordance for gene amplification was 95% (20/21), fusions 100% (17/17), and MSI status 88% (30/34). Clinically the assay shows an average turnaround time of 7 to 8 days and 100% success rate. A total of 52.5% of clinical samples were from patients with metastatic non-small cell lung cancer, 62% of which had

tier 1 variants detected, and 18% with tier 2. Overall, 57.5% of cases showed either tier 1 or tier 2 variants detected (Fig. 1). **Conclusions:** This 33-gene ctDNA NGS assay shows high reproducibility, accuracy, and sensitivity, which enable the assay to be applied clinically in cancer mutation profiling to aid clinical decision making for oncology patients. In addition, our clinical experience strongly supports clinical feasibility and utility of ctDNA panels for advanced cancer patients.

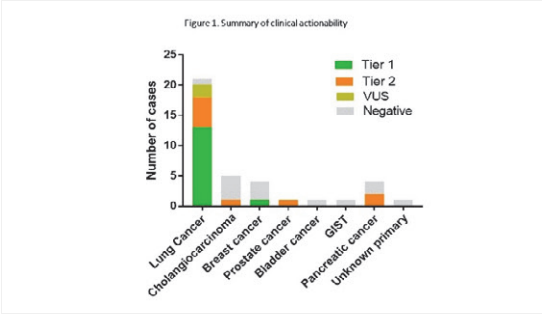

Figure 1. Summary of clinical actionability
Summary of clinical actionability of the MCLBP (Mayo Complete Liquid Biopsy Panel) with real-world data.

ST06. Multiple Alterations of *TP53* Predict Worse Clinical Outcome for Oral Cavity Squamous Cell Carcinoma

M. Afkhami[1], N. Haghighi[1], H. Ma[1], A. Guerrero[2], M. Telatar[1], M. Gust[1], T. Dyer[1], H. Yew[1], L. Chang[1], T. Gernon[3], R. Bakkar[4], E. Massarelli[2], E. Maghami[3], D. Bell[4], V. Villaflor[2]
[1]City of Hope Comprehensive Cancer Center, Pathology, Molecular Pathology and Therapy Biomarker Division, Duarte, CA; [2]City of Hope Comprehensive Cancer Center, Medical Oncology, Head and Neck Division, Duarte, CA; [3]City of Hope Comprehensive Cancer Center, Surgical Oncology, Head and Neck Division, Duarte, CA; [4]City of Hope Comprehensive Cancer Center, Pathology, Anatomic Pathology Division, Duarte, CA.

Introduction: This study evaluated the prognostic significance of *TP53* mutations and shedded light on the prognostic value of TERT promoter mutations and other genes exclusively in oral cavity squamous cell carcinoma (OCSCC). **Methods:** Retrospective review of 388 head and neck SCC from December 2017 to 2022 was performed. After exclusion of oropharynx and nasopharynx cases, 63 cases of OCSCC with available samples were identified. Tumor primary sites were 2 groups of tongue/floor of mouth versus other, which includes buccal mucosa, gingiva, and retromolar trigone. Thirty-three, 29, and 3 cases were sequenced, respectively, with Oncomine V3, TSO500, and whole-exome sequencing. PD-L1 22C3- CPS score by immunostains was evaluated in 61 cases. Biostatistical analysis was performed using SAS 9.4 (SAS Institute, Cary, US). Overall survival (OS) and disease-free survival (DFS) stratified by each factor of interest were examined using Kaplan-Meier curves and log-rank test in the univariate analysis (2-sided at a significance level of 0.05). Hazard ratio for mortality risk and its 95% confidence interval (95% CI) were estimated using univariate Cox proportional hazards regression models. **Results:** Thirty-six females and 27 males ranged from 19 to 83 years of age, with 55 patients at least 40; the median age of diagnosis was 63. In all, 43/63 patients were still alive by the end of follow-up. All cases were negative for human papillomavirus (HPV) either by p16 or HPV high-risk immunohistochemistry. Our univariate analysis showed that higher pN, ever smoking, and double/triple *TP53* mutations were associated with worse OS (all LR test p <0.04); higher PD-L1 expression was associated with better OS (LR p = 0.039). All-cause mortality risk (ACMR) was approximately 11 times (HR = 10.58, 95% CI = 2.14 to 52.17) for pN = 3 vs. pN ≤1, 3 times for ever smoking vs. never smoking (HR = 3.35, 95% CI = 1.35 to 8.31), and double/triple *TP53* mutations (HR = 2.87, 95% CI = 1.02 to 8.07). Patients with at least 20% of PD-L1 expression had 68% (HR = 0.32, 95% CI = 0.11 to 1.00) lower ACMR than those with <20% PD-L1 expression. No statistically significant association with ACMR was observed for other factors examined. Our data also showed that tongue/floor of mouth demonstrated better DFS- than other group (LR test p = 0.002). The most common alterations were *TP53, TERT PM, CDKN2A, HRAS, PIK3CA, NOTCH1,* and *CASP8* mutations. The most common amplifications found were *FGF19, FGF3, CCND1, EGFR*, and *IGF1R*. TERT PM was positive in 68.3% (43/63), with equal -124 and -146 distribution. *TP53* was positive in 84.1% (53/63) mainly in exon 4 to 8 (Fig. 1), with 12/53 having double or triple mutations. **Conclusions:** Other than *TP53* double or triple mutations, other gene alterations did not show any clinically significant ACMR or DFS including TERT PM. Limitations of this study include small size of the cohort and relatively short duration of follow-up. The predictive roles of more than 1 *TP53* are under further investigation for a larger cohort with multivariant analysis and functional studies.

Figure 1. TP53 mutation distribution.

ST07. SARS-CoV-2 Humoral Immunity in a Cohort of Patients with Head and Neck Carcinoma

L.G. Marutescu[1,2], A.G. Enea[5,4], E. Dragu[1,2], M. Popa[2], D.A. Costea[1], M. Neculae[1], C.M. Chifiriuc[1,2], E. Codrici[6], S.G.-V. Bertesteanu[5,4], V. Ristoiu[2,3], V. Lazar[1,3], R. Grigore[5,4], P. Ancuta[7,8],

[1]University of Bucharest, Department of Botanics and Microbiology - Faculty of Biology, Bucharest, Romania; [2]University of Bucharest, Department of Anatomy, Animal Physiology and Biophysics - Faculty of Biology, Bucharest, Romania; [3]University of Bucharest, Institute of Research, Bucharest, Romania; [4]Coltea Clinical Hospital, Ent Department, Bucharest, Romania; [5]Carol Davila University of Medicine and Pharmacy, Coltea Clinical Hospital - Ent Department, Bucharest, Romania; [6]Victor Babes, National institute of Pathology, Bucharest, Romania; [7]Université de Montréal, Centre de recherche du Centre hospitalier de l'Université de Montréal, Montreal, Canada; [8]Université de Montréal, Montréal, Département de microbiologie, infectiologie et immunologie, Faculté de médecine, Montreal, Canada.

Introduction: The COVID-19 pandemic caused by SARS-CoV-2 infection was associated with increased mortality in relationship with aging and comorbidities. The duration of natural and vaccine-induced immunity was largely studied in the general population, but investigations in cancer patients remain scarce. Here, we aimed to monitor the humoral immunity upon SARS-CoV-2 infection or vaccination in patients with head and neck cancer (HNC) recruited at Colțea Hospital, Bucharest, Romania. **Methods:** Peripheral blood was collected from HNC participants (n = 50; 44 males, 6 females; median age: 65 years; body mass index [BMI]: 25 kg/m^2), convalescent (n = 17; mild/moderate symptoms) or vaccinated (n = 34; Pfizer/Moderna RNA or AstraZeneca/Johnson&Johnson adenoviral vector vaccine), and non-cancer controls (n = 14; 5 males, 9 females) between August 2021 and January 2022. The anti-Spike (S1, S2), anti-receptor binding (RBD) and anti-nucleocapsid (NC) IgG antibodies (Abs) were detected in the plasma using MILLIPLEX (EMD Millipore) technology; the results were expressed by the average fluorescence intensity parameter. Total and memory (CD27$^+$) CD19$^+$ B-cells producing SARS-CoV-2-specific Abs of IgM, IgG, or IgA isotype were identified by polychromatic flow cytometry analysis of peripheral blood mononuclear cells *ex vivo*, using the SARS-CoV-2 RBD B-cells kit (Miltenyi Biotec). Finally, a panel of 25 cytokines was quantified using the MILLIPLEX technology. The Mann-Whitney test and the Spearman correlation model were used for statistical analysis. **Results:** Based on vaccination status, SARS-CoV-2 PCR, and plasma NC Abs, participants were classified in vaccinated, hybrid immunity, and convalescent groups similar in age, BMI, and time since immunization. The S1, S2, and RBD Abs were detected in the majority of participants up to 300 days post-immunization, whereas NC Abs were only detected in convalescent/hybrid immunity groups. SARS-CoV-2 Abs levels were significantly higher in convalescent/hybrid versus vaccinated HNC, but did not differ between HNC and controls, and did not correlate with the time since infection, age, or BMI. RBD-specific B-cells exhibited similar frequencies in HNC versus controls and vaccinated versus convalescent/hybrid immunity HNC, but positively correlated with plasma SARS-CoV-2 Abs levels and time since infection. RBD-specific B-cells were enriched in cells with a memory CD27$^+$ phenotype and IgG/IgA isotype, with no differences between vaccinated versus convalescent/hybrid immunity HNC. Finally, the frequency of RBD-specific B-cells negatively correlated with plasma levels of IL-6, a marker of systemic inflammation. **Conclusions:** Our results reveal that HNC patients mount efficient humoral memory responses upon SARS-CoV-2 vaccination or natural infection. These results also point to the deleterious effects of systemic inflammation on the quality of antiviral responses. Subsequent longitudinal studies will inform on the duration/quality of SARS-CoV-2 humoral immunity in HNC patients.

ST08. Secretogranin II Could Be a Biological Indicator and Potential Target for Bladder Cancer

Q.-X. Yu[1], D.-X. Li[2], L.-X. Ye[1], H.-H. Zheng[1]

[1]Taizhou Hospital, Wenzhou Medical University, Department of Pathology, Taizhou, China; [2]West China Hospital, Sichuan University, Department of Urology, Chengdu, China.

Introduction: Secretogranin II (SCG2) is involved in the development of many cancers. However, the function of SCG2 in bladder cancer (BC) remains unclear. This study aimed to clarify the role of SCG2 in BC through bioinformatics analysis and immunohistochemical analysis. **Methods:** The data of bioinformatics analysis were downloaded from online database and analyzed by R version 3.6.3 and relative packages. Immunohistochemical staining (IHC) was performed in the samples from our institution with the approval of the Institutional Ethics Committee (K20220830). **Results:** The expression of SCG2 in BC tissues was significantly higher than that in adjacent tissues according to the results of TCGA dataset and IHC data. Patients in the high-SCG2 expression group were statistically associated with poor overall survival in TCGA dataset, GSE31684 dataset, and IHC data. Furthermore, SCG2 had independently prognostic value for patients with BC in TCGA dataset and IHC data. The function analysis identified that SCG2 was involved in immune-related and metabolism-related pathways. There was a significant positive correlation between SCG2

expression and some immune checkpoints, such as CD274, PDCD1, and CTLA4. Referring to the results of the CIBERSORT algorithm, the low-SCG2 expression group contained a higher proportion of B-plasma cell, CD4+T naïve cell, and T follicular helper cell infiltration. Meanwhile, SCG2 expression was positively correlated with tumor mutation burden score and stemness index, suggesting that patients with low-SCG2 expression were more likely to benefit from immunotherapy. In the TIDE algorithm, compared with the high-SCG2 expression group, the low-SCG2 expression group had a significantly lower TIDE score. Meanwhile, responders to immunotherapy had statistically lower SCG2 expression than no-responders. Patients in the high SCG2 expression group were sensitive to docetaxel and gemcitabine, according to the results of the "pRRophetic" algorithm. **Conclusions:** According to the results of bioinformatics and IHC analyses, SCG2 can predict the prognosis, immunotherapy, and chemotherapy response of BC patients, indicating that SCG2 is a biomarker and target of BC.

ST09. Allele-Specific *CDKN2A/B* Loss Worsens Overall Survival in *IDH*-Mutant Astrocytomas

R.A. Hickman[1,2], E. Gedvilaite[1], R. Ptashkin[3], R. Cimera[1], C. Vanderbilt[1], J. Benhamida[1], T. Fahy[4], R. Young[4], A. Miller[5], I. Mellinghoff[5], M. Rosenblum[1], M. Ladanyi[1], M. Arcila[1], R. Brannon[1], Y. Zhang[1], T. Bale[1]

[1]Memorial Sloan Kettering Cancer Center, Pathology, New York, NY; [2]Henry M. Jackson Foundation for the Advancement of Military Medicine, Surgery and Pathology, Bethesda, MD; [3]C2i Genomics, New York, NY; [4]Memorial Sloan Kettering Cancer Center, Radiology, New York, NY; [5]Memorial Sloan Kettering Cancer Center, Neurology, NY.

Introduction: *IDH*-mutant gliomas represent the most common glioma subtype in patients younger than 50 years of age. The World Health Organization Classification for central nervous system tumors recommends that *IDH*-mutant astrocytomas with homozygous deletion (HOMDEL) of *CDKN2A/B* be designated as grade 4 irrespective of histologic appearance; however, there is no recommended testing method for determining HOMDEL, and current guidelines do not include other mechanisms of *CDKN2A/B* inactivation. Using an FDA-authorized next-generation sequencing pipeline, we examined whether mutations and somatic copy number alterations (SCNA) of *CDKN2A/B* could influence overall survival (OS) and whether allele-specific copy number alterations (ASCNA) of *CDKN2A/B* might better stratify OS. **Methods:** Matched tumor-normal targeted sequencing of all exons and select introns of 341 to 505 genes was performed using MSK-IMPACT of 382 *IDH*-mutant astrocytomas. Point mutations and indels were detected using MuTect, Vardict and SomaticIndelDetector. SCNA were determined using loess normalized sequence coverage of targeted regions in each tumor sample compared with a standard diploid nontumor sample (SCNA analysis). We used the FACETS algorithm (Fraction and Allele-Specific Copy Number Estimates from Tumor Sequencing), which uses a single nucleotide polymorphism-based approach for allele discrimination, to perform ASCNA across genomic targets. **Results:** Somatic copy loss of *CDKN2A/B* was the most frequent SCNA in *IDH*-mutant astrocytomas and conferred shorter OS than copy neutral samples (13.6% [n = 52], median OS: 1.9 versus 12.6 years, P <0.01). In samples considered *CDKN2A/B* copy neutral by SCNA analysis, 24% (n = 78) had a *CDKN2A/B* ASCNA by FACETS, which conferred worse OS than otherwise (median OS: 7.0 vs. 15.4 years, P = 0.01). FACETS assessment of *CDKN2A/B* revealed intermediate OS between heterozygous loss (HETLOSS, median survival: 6.9 years, n = 89), HOMDEL/copy neutral loss of heterozygosity (median survival: 2.3 years, P = 0.02, n = 37), and neutral states (median survival: 15.4 years, P <0.01, n = 256). In samples with *CDKN2A/B* HETLOSS, additional gains in the related RB pathway genes, *CCND2* and/or *CDK4*, conferred worse OS than otherwise (median OS: 1.4 years, P = 0.01). Finally, 12 samples, all of which considered neutral by SCNA analysis, harbored a *CDKN2A/B* somatic mutation, which was associated with shorter OS than wild-type samples (1.6 vs. 11.8 years, P <0.01). No mutation was recurrent; however, most were considered oncogenic or likely oncogenic by OncoKB (n = 7) and included single nucleotide variants, truncating variants, and in-frame deletions. Five of these samples were *CDKN2A/B* HETLOSS and 2 had copy neutral loss of heterozygosity. **Conclusions:** Other *CDKN2A/B* genetic alterations beyond HOMDEL associate with shortened OS. Comprehensive analysis of *CDKN2A/B* genetic alterations and relevant RB pathway genes using tumor-matched normal sequencing data allows for further prognostication of IDH-mutant astrocytomas beyond current guidelines.

ST10. Adhesion-Regulating Molecule 1 (ADRM1) Can Be a Potential Biomarker and Target for Bladder Cancer

Q.-X. Yu[1], D.-X. Li[2], Y.-Q. Guo[1], H.-H. Zheng[1]
[1]Taizhou Hospital, Wenzhou Medical University, Department of Pathology, Taizhou, China; [2]West China Hospital, Sichuan University, Department of Urology, Institute of Urology, Chengdu, China.

Introduction: Adhesion-regulating molecule 1 (ADRM1) can regulate tumor development. However, the function of ADRM1 in bladder cancer (BC) remains unclear. We wanted to identify the role of ADRM1 in BC by bioinformatic analysis and immunohistochemical analysis (IHC). **Methods:** R version 3.6.3 and relative packages were used to analyze the data from the online database and IHC data with the approval of the Institutional Ethics Committee (K20220830). **Results:** In paired and unpaired comparisons, the expression of ADRM1 in BC tissues was significantly higher than that in adjacent tissues. Patients with high ADRM1 expression had statistically worse overall survival than those with low ADRM1 expression. Functional analysis enriched immune-related pathways. There was a significant positive correlation between ADRM1 expression and some important immune checkpoints. Samples with high ADRM1 expression contained a significantly higher proportion of CD8+ T-cells and macrophage infiltration, and had significantly higher tumor mutation burden scores and stemness indices. Patients with low ADRM1 expression were sensitive to cisplatin, docetaxel, vinblastine, mitomycin C, and methotrexate. **Conclusions:** Based on the results of bioinformation and IHC analyses, ADRM1 had prognostic value in BC patients and could predict immunotherapy and chemotherapy responses, indicating that it is a biomarker and target of BC.

ST11. Role of GREM1 in Bladder Cancer: A Biological Indicator and Potential Target

Q.-X. Yu[1], D.-X. Li[2], L.-X. Ye[1], H.-H. Zheng[1]
[1]Taizhou Hospital, Wenzhou Medical University, Department of Pathology, Taizhou, China; [2]West China Hospital, Sichuan University, Department of Urology, Institute of Urology, Chengdu, China.

Introduction: Gremlin 1 (GREM1), a secreted protein, can regulate the development of many cancers. However, no studies have revealed the role of GREM1 in bladder cancer (BC). We aimed to identify the function of GREM1 in BC. **Methods:** R version 3.6.3 and relative packages were used to analyze the data. Samples from our institution were assessed by immunohistochemical staining (IHC) with the approval of the Institutional Ethics Committee (K20220830). **Results:** GREM1 was highly expressed in BC tissues according to the TCGA and IHC data. GREM1 had significant prognostic value for patients with BC in the TCGA, GSE32584, GSE31684, and GSE32894 datasets. Our IHC data also indicated that GREM1 could predict the prognosis of BC patients. GREM1 was involved in immune-related and metabolism-related pathways according to the results of functional analysis. In immune-related analysis, compared with the low-GREM1 group, many immune checkpoints, including CD274, PDCD1, and CTLA4, were differentially expressed in the low- and high-GREM1 groups. The low-GREM1 group had significantly higher T follicular helper cell and monocyte cell infiltration than the high-GREM1 group. Meanwhile, GREM1 expression was negatively associated with the stemness index. In the TIDE algorithm, 61.0% (119/195) of patients in the low-GREM1 group were effective for immunotherapy, higher than 13.3% (26/195) in the high-GREM1 group. Patients in the high-GREM1 group were sensitive to cisplatin, docetaxel, gemcitabine, and vinblastine. **Conclusions:** GREM1 can predict the prognosis, immunotherapy, and chemotherapy responses of BC patients, indicating that it may be a biomarker and target of BC.

ST12. Identification of a Cross-Talk between the MEK5/ERK5 and the Hedgehog/GLI Pathways in Melanoma

I. Tusa[1], A. Tubita[1], A. Menconi[1], S. Gagliardi[2], M. Lulli[1], B. Stecca[2], E. Rovida[1]
[1]University of Florence, Department of Experimental and Clinical Biomedical Sciences, Florence, Italy; [2]ISPRO, Core Research Laboratory - Institute for Cancer Research and Prevention (ISPRO), Florence, Italy, Florence, Italy.

Introduction: Malignant melanoma is among the most aggressive cancers, and its incidence is increasing worldwide. Available treatments for melanoma, especially in its intermediate or advanced stages, are unsatisfactory. We have recently reported that the MAPK ERK5 is required for the Hedgehog/GLI (HH/GLI)-dependent melanoma cell proliferation and that GLI1, the major downstream effector of HH/GLI signaling, positively regulates ERK5 expression by binding to a functional non-canonical GLI consensus sequence at the *ERK5* promoter. We have also observed that activation of the HH/GLI pathway induces a marked increase of the upstream kinase MEK5, pointing to an additional HH/GLI-dependent mechanism that could contribute to the activation of the ERK5 pathway in melanoma. Additionally, since the HH/GLI pathway may be activated in a non-canonical way by the MAPK ERK1/2, we also explored whether ERK5 positively regulates the HH/GLI signaling. **Methods:** Melanoma cell lines used: SSM2c (wild-type B-RAF) and A375 (*BRAF* V600E). Activation of the HH/GLI pathway was obtained by silencing the negative regulator

PATCH1 using lentiviral vectors expressing a specific short hairpin RNA (shRNA), whereas genetic inhibition of GLI1 or ERK5 was achieved using lentiviral vectors expressing GLI1- or ERK5-targeting shRNA. Luciferase assay using the GLI-binding site luciferase reporter was performed to evaluate GLI1 transcriptional activity. A constitutively active form of MEK5 (MEK5DD) was used to induce ERK5 activation. **Results:** Activation of the HH/GLI pathway by genetic inhibition of PTCH1 increased the expression and phosphorylation of MEK5. Chromatin immunoprecipitation experiments performed in SSM2c, in which the HH/GLI pathway is constitutively active, showed that GLI1 silencing determined a reduction of RNA Polymerase Type II recruitment at and of GLI1 binding to a functional non-canonical GLI consensus sequence at *MAP2K5* promoter, the gene encoding for MEK5 protein. In further support of a positive regulation of *MAP2K5* by GLI1 transcription factor, GLI1 silencing resulted in the reduction of *MAP2K5* mRNA. To test whether ERK5 regulates the expression of components of the HH/GLI pathway, we evaluated the mRNA and protein expression levels of GLI transcription factors in melanoma cells following genetic inhibition of ERK5. ERK5 knockdown reduced the amount of GLI1 and GLI2 mRNA and protein. Moreover, MEK5DD overexpression further increased transcriptional activity of the HH-GLI signaling, whereas ERK5 silencing reversed this effect. These results confirmed that ERK5 positively regulates the HH/GLI signaling. Consistently, MEK5DD overexpression increased GLI1 protein level. **Conclusions:** These findings highlight the existence of a consistent bidirectional cross-talk between the ERK5/MEK5 and the HH/GLI pathways. Regarding a possible translational impact of this study, combined inhibition of the 2 pathways may prevent resistance mechanisms frequently observed upon monotherapy in melanoma.

ST13. Withdrawn

ST14. A Multisite Study of Molecular Profiles of Brain Metastasis in Non-Small-Cell Lung Cancer

M. Kokabee[1], Y.-R. Wuu[4], M. Vojnic[2], R.S.D'Amico[3], A.G. Wernicke[4], M. Harshan[1]

[1]Donald and Barbara Zucker School of Medicine at Hofstra/Northwell, Department of Pathology and Laboratory Medicine at Lenox Hill Hospital, New York, NY; [2]Donald and Barbara Zucker School of Medicine at Hofstra/Northwell, Department of Medical Oncology, Northwell Health Cancer Institute at MEETH, New York, NY; [3]Donald and Barbara Zucker School of Medicine at Hofstra/Northwell, Department of Neurosurgery at Lenox Hill Hospital, New York, NY; [4]Donald and Barbara Zucker School of Medicine at Hofstra/Northwell, Department of Radiation Medicine at Lenox Hill Hospital, New York, NY.

Introduction: Lung cancer is a leading cause of cancer death globally. Despite advances in therapies, up to 50% of brain metastases (BrM) will originate from lung cancer. Advances in sequencing have improved outcomes for non-small-cell lung cancer (NSCLC), with targetable alterations identified in genes such as *EGFR, BRAF, MET, RET, ROS1, NTRK*, and *ALK*. Programmed death-ligand receptor 1 (PD-L1) tumor proportion score (TPS) ≥50 allows for chemotherapy-free options in the first-line setting, with several immune checkpoint inhibitors approved. High tumor mutation burden (TMB) (>10 mutations/Mb) predicts improved response to immunotherapy. Despite these advances, there are limited data on molecular profiles of BrM from NSCLC. This report presents molecular findings from our database and provides a foundation for future studies aimed at improving treatment and outcomes for these patients. **Methods:** Northwell Health's pathology and clinical systems were queried for NSCLC patients with BrM who underwent neurosurgical resection between 2011 and 2022. Tumor molecular profiles were reviewed. PD-L1 expression testing for BrM NSCLC began in 2015, and detailed lung cancer panel testing in 2020. Data were entered in cBioPortal, which uses a one-sided Fisher's Exact Test to assess if observed events are random or due to biological phenomena. cBioPortal also uses the Log2 Odds Ratio to assess the direction of association. **Results:** A total of 149 cases of NSCLC with BrM were identified across 5 hospitals. Of these, 124 (83%) were adenocarcinomas, 17 (11.5%) were squamous cell carcinomas (SCC), 7 (4.7%) were NSCLC NOS or poorly differentiated, and 1 (0.7%) was sarcomatoid carcinoma (Fig. 2). Median age at diagnosis of BrM was 65.2 years for females (53%) and 66.3 years for males (47%). Among patients with SCC, 5 were females (29%) and 12 were males (71%) with mean age at diagnosis

of BrM 70 years and 62.5 years, respectively. PD-L1 expression was tested in 69% of cases, of which 59% were positive (TPS ≥1). Of these, 30% had high PD-L1 expression (TPS ≥50). *TP53* mutations were identified in 81% of 63 tested samples, *KRAS* in 52% of 80 tested, *EGFR* in 21% of 85 tested, and *ALK* rearrangements in 2.6% of 76 tested. No *RET*, *NTRK,* or *ROS1* fusions were found. In the SCC subgroup, *TP53* mutations were found in 100% of 3 tested, *EGFR* in 67% of 3 tested, *ALK* rearrangements in 34% of 3 tested, and no *RET, NTRK*, or *ROS1* fusions were found. The most frequent *KRAS* alteration was G12C (20/80), followed by G12V (6/80). In *EGFR* mutated tumors, E746-A750del was present in 5/85 tested tumors. Mutual expression of genes was calculated, and *EGFR* and *KRAS* were mutually exclusive (p-Value <0.001 and Log 2 Odds ≤3).

Conclusions: Identification of actionable tumor drivers is important both for prognosis and treatment of patients with BrM. Our molecular profile database may serve as a major step in identification of BrM-specific drivers, which may lead to better understanding of BrM biology and consequently improvement in therapeutic strategies.

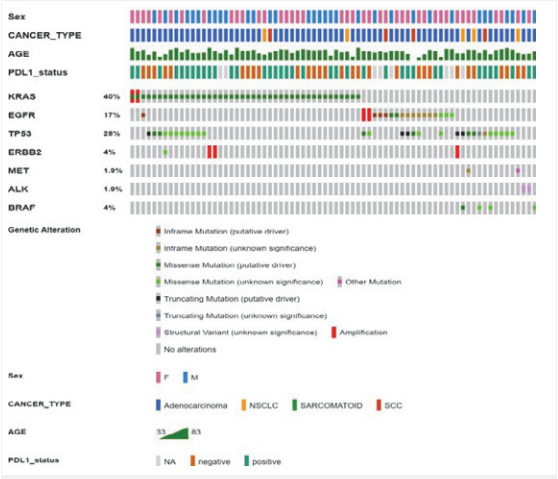

Figure 1. Oncoprint
Detailed Oncoprint of cases with molecular alteration.

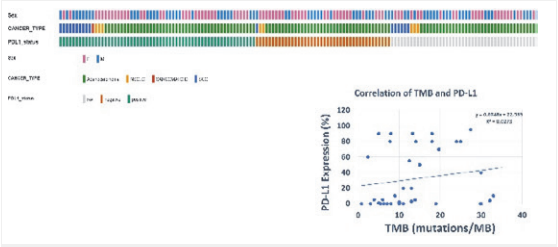

Figure 2. PD-L1 and TMB
Detailed PD-L1 expression and correlation with TMB.

ST15. Clinical Significance of IDH Mutations and MGMT Promoter Methylation among WHO Classified CNS Tumors in Major Tertiary Care Unit of Pakistan

Z. Ansar Ahmed, S. Naz, A. Ujala, T. Moatter
Aga Khan University, Pathology and Lab Medicine Molecular Pathology section, Karachi, Pakistan.

Introduction: In the revised World Health Organization (WHO) classification of tumors of the central nervous system (CNS), molecular genetic alterations have been incorporated into the classic histology of primary brain tumors (PBT), including isocitrate dehydrogenase 1 and 2 (IDH1 and IDH2) mutations and methylation of the O-6-methylguanine-DNA methyltransferase (MGMT) promoter. Glioblastoma, the most common malignant PBT, is characterised by aggressive behaviour and poor survival. Combined assessment of IDH1 mutations and MGMT methylation status is suggested to predict survival in glioblastoma better than either IDH1 or MGMT alone. Multiplex ligation-dependent probe amplification (MLPA) can detect the methylation status of the *MGMT* gene and identify the 4 most predominant IDH1 (R132H and R132C) and IDH2 (R172K and R172M) point mutations in glioma. Assessment of IDH mutation status in central nervous system tumors may assist in tumor classification and provide prognostically relevant information for subgroups of patients with diffuse gliomas. **Methods:** The Methylation Specific MLPA (MS-MLPA) assay has been used to detect IDH type 1/type 2-point mutations and MGMT methylation. In the MS-MLPA assay the sequence targeted by specific probes contains a restriction site for the HhaI endonuclease, able to recognize the unmethylated GCGC sequence on formalin-fixed, paraffin-embedded tissue sections. **Results:** This study investigated 30 patients with primary brain tumors enrolled January 2021 to February 2022 at the Aga Khan University Hospital. The male-to-female ratio was 2:1. Mean age was 38 years, and patients' ages ranged from 19 to 70 years. Fourteen cases (47%) were positive for isocitrate dehydrogenase mutation. Among IDH Positive patients, 12 cases exhibited IDH1 (P. R132H/P. R132C) point mutation and 2 cases exhibited IDH2 (R172K) point mutation. Sixteen (53%) of the cases had no mutation detected, whereas methylation of MGMT was detectable in 18 out of the 30 patients examined (60%). According to the WHO classification of tumors of the CNS: Six patients had glioblastoma and MGMTp methylation (20%); 4 patients had glioblastoma but no MGMTp methylation (13.3%); 3 patients had glioma and MGMTp methylation (10%); 1 patient had glioma but no MGMTp methylation (3.3%); 9 patients had oligodendroglioma and MGMTp methylation (30%); 3 patients had oligodendroglioma but no MGMTp methylation (10%).

Conclusions: Practical implementation of routine molecular work-up of CNS tumors is compromised by impractically long turnaround times and economic restraints. Based on our results, we advocate a stepwise approach, providing fast-track results obtained by MLPA for first-line therapy decisions within a week after surgery.

ST16. Diagnostic and Prognostic Value of Circulating Tumor Cells in Indian Women with Suspected Ovarian Cancer

S. Singh
Netaji Subhas Medical College and Hospital, Biochemistry, Patna, India.

Introduction: "Liquid biopsy," where body fluids are screened for biomarkers, is gathering substantial research. We aimed to examine women with suspected ovarian cancer for the presence of circulating tumor cells (CTCs) and study their role in prediction of chemoresistance and survival. **Methods:** Magnetic powder labeled monoclonal antibodies for epithelial cell adhesion molecule (EpCAM), Mucin 1 cell surface associated (MUC1), mucin 16, cell surface associated MUC16, or CA-125 were prepared according to the manufacturer's protocol. Expression of 3 ovarian cancer-related genes were detected in CTCs using multiplex reverse transcriptase-polymerase chain reaction (Multiplex RT-PCR). CTCs and serum CA-125 were measured in 100 patients with suspected ovarian cancer. Correlations with clinicopathological parameters and treatment were analyzed. **Results:** CTCs were detected in 18/70 (25.7%) of women with malignancy compared to 0/30 (0.0%) in those with benign gynecologic diseases (p = 0.001). The sensitivity and specificity of the CTC test for predicting a malignant histology in pelvic masses was 27.7% (95% CI:16.3%, 37.7%) and 100% (95% CI: 85.8%, 100%), respectively. The number of CTCs correlated with stage of ovarian cancer (p = 0.030). The presence of $EpCAM^{+}CTC$ at primary diagnosis in ovarian cancer was found to be an independent predictor of a poor progression-free survival (HR,3.3; 95% CI, 1.3 to 8.4; p = 0.010), overall survival (HR, 2.6; 95% CI,1.1 to 5.6; p = 0.019), and resistance to chemotherapy (OR 8.6; 95% CI, 1.8 to 43.7; p = 0.009). **Conclusions:** Expression of $EpCAM^{+}CTC$ in ovarian cancer predicts platinum resistance and poor prognosis. This information could be further utilized in investigating anti-EpCAM targeted therapies in ovarian cancer.

ST17. A European Newcomer's Experience with NGS-Based Proficiency Testing Offered by the College of American Pathologists

S. Laßmann[1,2], S. Kral[1], M. Kunz[1], X. Ungefug[1], M. Werner[1,2]
[1]Institut für Klinische Pathologie, Universitätsklinikum Freiburg, Freiburg, Germany; [2]Comprehensive Cancer Center Freiburg, Freiburg, Germany.

Introduction: Next-generation sequencing (NGS) molecular pathology testing requires continuous quality assurance for the entire work process from pre-analytics, sample processing for NGS, and diagnostic bioinformatics to reporting. So far, few external quality assurance programs covering these aspects are offered in Europe. Here we report on our experiences with the College of American Pathologists (CAP, US) NGS-based proficiency testing (PT) programs in 2022. **Methods:** Enrollment was for 5 PT programs, including 3/5 starting from a given DNA sample ("NGS-exome," "tumor mutation burden [TMB]," "copy number variant [CNV]") and 2/5 starting from own modified or provided fastq-files for diagnostic bioinformatics ("NGS-BV" exome, "NGSB" panel). PT programs were for certification (1/5 "NGS-exome") or for educational challenge (4/5). For each PT program, testing was performed in 2 phases (spring and autumn 2022). The laboratory processes included hybrid-capture NGS panel (TSO500, Illumina) and/or whole-exome sequencing (SureSelect All Human Exon V8; Agilent). Diagnostic bioinformatics included commercial pipelines (TSO500 local app, Illumina; CLC Genomic Workbench, Qiagen) and/or custom in-house pipelines (for whole-exome sequencing [WES]). **Results:** Registration and enrollment for CAP PT, shipment schedules, and e-Lab Solution Suite (ELSS) results/interaction were professionally organized and readily usable. Initial delays of shipment due to unforeseen airport customs/tax issues were resolved. Subsequent to laboratory processing and/or diagnostic bioinformatics, all results were entered manually into ELSS. For the users' benefit, interim result evaluations and program statistics were provided after the first phase for potential laboratory adjustments and overview of the NGS community's procedures: For the PT "NGS-exome" correct results were obtained in 92.5% and a specificity of 98.9%, resulting in a good overall assessment. For the "TMB" challenge (DNA provided: Seven mut/Mb) our results (9.5 and 9.6 mut/Mb by TSO500 and WES) and those of the NGS community (n = 50 participants: 8.39+/- 3.2 mut/Mb) were higher. For the "CNV" challenge, 10/14 alterations were correctly called (TSO500). For the "NGSB" challenge, all 16/16 alterations were correctly called (TSO500). For the "NGS-BV" challenge, interim results are currently awaited. Challenges experienced were 1) manual entering of detected variants into ELSS, 2) lack of hg19 and

hg38 flexibility for all PTs and 3) in part provision of old-type fastq-files. Opportunities experienced were 1) availability of several comprehensive NGS PT programs, 2) twice a year PTs with few samples, and 3) comprehensive results requested and evaluated (such as correct variant description). **Conclusions:** NGS-based proficiency testing by the CAP is a highly valuable quality assurance resource for European molecular pathology diagnostic laboratories for ensuring technical, bioinformatical, and interpretational validity, worthwhile for investing in CAP PT costs and own laboratory capacities.

ST18. *PIK3CA*-Mutant Breast Cancer Metastatic Patient-Derived Organoid Approach to Evaluate Alpelisib Treatment for Multiple Secondary Lesions

M. Cioce[1], S. Donzelli[2], A. Sacconi[3], F. Zanconato[4], T. Daralioti[5], G. Orlandi[8], S. Di Martino[7], V.M. Fazio[1,14], G. Alessandrini[9], S. Telera[10], M. Carosi[5], G. Ciliberto[11], F. Goeman[6], C. Botti[12], S. Strano[6], S. Piccolo[4,13], G. Blandino[2]
[1]Campus Biomedico University, Laboratory of Molecular Medicine and Biotechnology General and Clinical Pathology, Rome, Italy; [2]IRCCS Regina Elena National Cancer Institute, Translational Oncology Research Unit, Rome, Italy; [3]IRCCS Regina Elena National Cancer Institute, Clinical Trial Center, Biostatistics and Bioinformatics Unit, Rome, Italy; [4]University of Padua, Department of Molecular Medicine, Padua, Italy; [5]IRCCS Regina Elena National Cancer Institute, Department of Pathology, Rome, Italy; [6]IRCCS Regina Elena National Cancer Institute, SAFU Unit, Rome, Italy; [7]IRCCS Regina Elena National Cancer Institute, Department of Pathology, Biobank, Rome, Italy; [8]IRCCS San Gallicano Dermatological Institute, Scientific Direction, Rome, Italy; [9]IRCCS Regina Elena National Cancer Institute, Thoracic Surgery, Rome, Italy; [10]IRCCS Regina Elena National Cancer Institute, Neurosurgery, Rome, Italy; [11]IRCCS Regina Elena National Cancer Institute, Scientific Direction, Rome, Italy; [12]IRCCS Regina Elena National Cancer Institute, Breast Surgery, Rome, Italy; [13]IFOM, the FIRC Institute of Molecular Oncology, Milan, Italy; [14]National Research Council of Italy (CNR), Institute of Translational Pharmacology, Rome, Italy.

Introduction: Breast cancer (BC) is a powerful example of the intra- and inter-patient heterogeneity of tumours; thus, there remain several grey areas in BC treatment approaches. This is especially true for advanced/metastatic disease (mBC). Organoid cultures are suitable models for studying the histological complexity and genetic heterogeneity of parental tumours and can be used to assess treatment strategies for challenging diseases such as mBC. **Methods:** BC-patient-derived tumor-organoid setup; RNAseq, and drug treatment have been performed. **Results:** Based on the relevant impact of *PIK3CA* gene mutations on breast cancer progression and resistance to therapy, we assessed the efficacy of alpelisib, a specific PI3K-a inhibitor, on organoid cultures derived from multisite mBC samples carrying specific *PIK3CA* gene mutations. In this test case, metastasis-derived patient-derived tumor organoids (PDTOs) were challenged with alpelisib to assess differential response in PIK3CAwt versus PIK3CAmut PDTOs. **Conclusions:** Here, we report a proof-of-concept test case using organoid cultures from metastatic BC specimens to rapidly test drug sensitivity and molecular lesion-driven treatments. Furthermore, establishing specific conditions for the propagation of metastatic material is unprecedented.

ST19. Withdrawn

ST20. Development and Application of Absolute Digital PCR to Detect *TERT* Promoter Mutations in 180 Solid Tumor Samples

S.Y. Kang, K.-M. Kim
Samsung Medical Center, Department of Pathology and Translational Genomics, Seoul, South Korea.

Introduction: Telomerase reverse transcriptase (*TERT*) promoter is mutated at high frequencies in multiple cancer types, most commonly at positions -124 and -146 (designated C228T and C250T, respectively). Detection of these mutations has been challenging because of the high GC content of this region (approximately 80%). High GC contents can result in formation of stable secondary structures, non-specific binding of primers, and reduced amplification efficiency. We developed novel probe-based Absolute Q Digital PCR assays that specifically detect and quantify these 2 hotspot mutations, and applied this technology in formalin-fixed, paraffin-embedded (FFPE) tumor samples from advanced solid cancer patients. The QuantStudio Absolute Q Digital PCR platform partitions a sample into thousands of tiny droplets, each containing a single PCR reaction. This allows individual quantification of target DNA molecules and reduces the effects of PCR inhibition and bias in traditional PCR. **Methods:** Assay designs and running conditions were optimized with genomic DNAs obtained from cancer cell lines harboring C228T or C250T mutations. To develop a highly sensitive and specific assay, each hotspot mutation was independently optimized with many primer/probe designs, various amplification cycles, and diverse PCR modifiers. To validate the novel Absolute Digital PCR technique, 180 FFPE tumor samples with known mutation status by next-generation sequencing (NGS) were used. **Results:** Absolute Digital PCR and NGS-based deep sequencing showed a 100% concordance in detecting TERT mutations in 180 FFPE tumor samples. There were no false positives in FFPE samples. Absolute Digital PCR provided a highly sensitive and specific method for the detection and quantification of *TERT* promoter

mutations in FFPE tissues. Specifically, a melanoma sample with low tumor volume (<30%) and low (11.4%) variant allele frequency was effectively amplified and confirmed to harbor C250T mutation. **Conclusions:** Absolute Digital PCR is considered a gold standard method for the detection and absolute quantification of rare mutated alleles because of its high sensitivity, specificity, and robust quantitative performance characteristics. Because Absolute Digital PCR assays typically require only 1.5 hours of running time and little manipulation of the sample, development of a novel Absolute Digital PCR assay can be easily applied in the clinic. Despite the high GC content, this novel Absolute Digital PCR assay demonstrated a high specificity and sensitivity using DNA extracted from cancer cell lines and FFPE tissue samples from various solid tumor samples, even from advanced cancer patients with metastatic settings. In conclusion, we describe a novel Absolute Digital PCR assay that specifically detected C228T and C250T promoter mutations in the *TERT* gene. Our results raise the potential to become valuable assets in diagnosing and monitoring patients with advanced cancer possessing *TERT* promoter mutations.

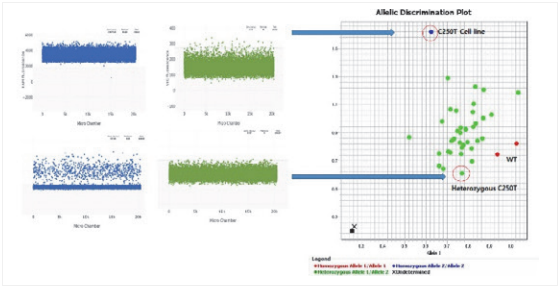

Detection of C250T TERT promoter mutation.
Left panel: 2-dimensional Absolute Digital PCR plots showing the C250T TERT promoter assay. Right panel: Demonstration of specificity using cell line with TERT promoter mutations (C250T) and formalin-fixed, paraffin-embedded (FFPE) samples. Cell line (C250T) and tumor FFPE samples were analyzed with real-time PCR to identify their TERT promoter region. Blue arrows indicate the homozygous cell line C250T mutation and melanoma sample with low tumor volume (<30%) and low (11.4%) variant allele frequency.

ST21. Recurring FGF/FGFR and PAM Pathway Alterations as Potential Therapeutic Targets in Primary Neuroendocrine Carcinoma of the Breast

N.E. Albayrak, B.L. Liu
Icahn School of Medicine at Mount Sinai, Department of Pathology, Molecular and Cell-Based Medicine, New York, NY.

Introduction: Primary neuroendocrine breast carcinoma (NEBC) is an under-diagnosed subtype of breast cancer, which includes small-cell neuroendocrine carcinomas (SCNECs) and large-cell neuroendocrine carcinomas. Given their low prevalence, NEBCs remain a challenge to accurately diagnose. Specifically, they may be misclassified as poorly differentiated invasive breast carcinoma of no special type (IBC-NST), poorly differentiated invasive ductal carcinoma (IDC), or a metastatic neuroendocrine carcinoma (NEC), which most commonly arises in the bronchopulmonary or gastroenteropancreatic tracts. However, in contrast to lung and enteropancreatic NECs, the genomics of breast NECs has not been well characterized. **Methods:** Search of a pathology database from 2010 to 2022 revealed 10 patients with histologically confirmed diagnosis of NEBCs. This represented 0.11% of all registered breast cancer cases (n = 9,068) during 2010 to 2022. Four of them were initially misdiagnosed with either IDC or IBC-NST. FoundationOne (F1) testing was performed on consecutive histological samples and/or on blood samples collected from 10 patients diagnosed with NEBCs. **Results:** The most frequent somatic mutations were in *TP53* (60%) and *RB1* (30%), which were co-altered in 75% (3/4) of SCNECs. Targetable mutations involving the phosphoinositide 3 kinase (PI3K)/Akt/mammalian target of rapamycin (mTOR) (PAM) pathway (i.e., activating *PIK3CA* and *AKT1* mutations) were identified in 40% (4/10) NEBCs. *FGFR1,* which is commonly amplified in estrogen receptor-positive carcinomas, was amplified in 20% (2/10) NEBCs. **Conclusions:** The findings provide insight into the pathogenesis of primary breast NECs, underscore their classification as a distinct tumor type, and highlight genetic similarities to extramammary NECs, including highly prevalent p53/RB pathway aberrations in SCNEC.

ST22. Closing the Gap: Successes and Obstacles in Achieving Rapid and Comprehensive Profiling of Lung Cancer

D. Jones
The Ohio State University, The James Cancer Hospital and Solove Research Institute, Columbus, OH.

Introduction: A worthy goal of cancer molecular diagnostics is to provide the fastest turnaround time (TAT) and most comprehensively actionable genomic profiling of tumor for quick therapy initiation. This is especially critical for non-small-cell lung cancer (NSCLC) where many patients (pts) present with high stage and early mortality is high. **Methods:** To achieve best TAT and completion rate for often limited NSCLC samples, we utilized amplicon-based 50-gene hotspot next-generation sequencing (NGS) supplemented with *ALK, RET, ROS1,* and *MET* fluorescence *in situ* hybridization (PULMOL). For pts with <20-pack year smoking history and driver variant identified, this was followed by 542-gene probe/bait comprehensive genomic panel (CTP) with GOAL-designed/xGEN IDT probes that covered NSCLC actionable gene fusions, copy number variant, microsatellite instability, and mutation burden. RNAseq panels were utilized to confirm novel exon skip variants. PULMOL NGS was initially performed on LifeTech S5 or Genexus with CTP on Illumina NextSeq. Target reporting from tissue receipt was 10 days with PULMOL within 3 to 5 days and CTP within 7 days (inclusive of weekends). **Results:** In all 1,378 pts with newly diagnosed NSCLC were profiled from January 1, 2020, to January 20, 2023, including 171 (12%) biopsied at outside hospitals/referred to our center and 202 (15%) being treated at community hospitals/clinics. Lab TAT target was met in 97% for initial work-up and 79% for reflexed CTP (259 cases, 20%). Failure rate was 1% (15 cases) due to insufficient or poor quality material. However, 34 other cases had no pathogenic/likely pathogenic (P/LP) variant identified after PULMOL/CTP likely due to low tumor for an overall clinical sensitivity rate of 96.4%. The collection-to-answer time was significantly different based on setting, 14 days (median) for material collected at our center, 23 days for community cases, and 40 days for referred patients (P <0.0001), with many more outliers in the last 2 categories. The differences were mostly due to delays in patient referral and material receipt. Additional driver variants seen with CTP included most commonly novel *MET* exon 14 skip variants (12 cases) and *NF1* (14) and *STK11* (12) P/LP variants not covered by the rapid panel. P/LP variants in SMARC/SWI-SNF (16), KEAP1/NFE2L2 (16) and RAS/MAPK (30, less common variants) pathways were potentially targetable. **Conclusions:** A reflex strategy for NSCLC profiling, incorporating smoking history, is cost-effective and easy to implement. The few detection failures can likely be improved by rapid panel design changes underway (adding UMIs and revised gene content). The high cumulative incidence of less common P/LP variants in potentially targetable pathways in reflexed cases highlights a workable model for targeted trial design that could encompass many more patients. For referred or community-treated patients, significant improvements in completion will require resampling at referral or lab assistance with processes outside the lab to improve ordering/insurance approvals and minimizing time for tissue retrieval to have further impact on decreasing delays in treatment initiation in NSCLC.

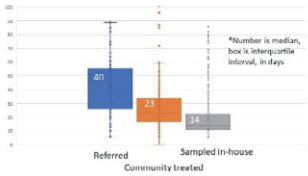

NSCLC: Days from collection to final signout.
Figure 1

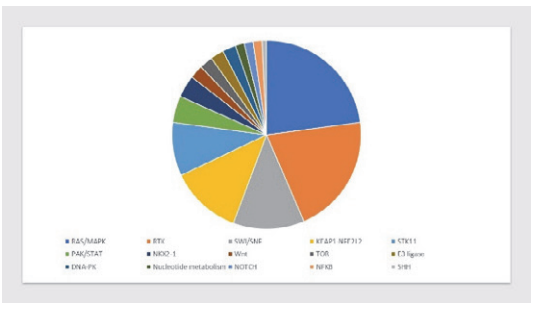

Additional likely driver variants on CTP reflex, by pathway.
Figure 2

ST23. Targeted SLIMamp NGS Technology as a Solution for Localized NGS Testing with Challenging Clinical Samples

S. Zou[1], L. Fink[2,3], N. Stone[2], L. Anderson[3,5], P. Leo[3,5], M. Marshall[3,5], K. O'Byrne[3,4], B. Jaradi[2]
[1]Pillar Biosciences, Natick, USA; [2]XING Genomic Services, Sinnamon Park, Australia; [3]ATCG Queensland University of Technology, Woolloongabba, Australia; [4]The University of Queensland, Diamantina Institute, Faculty of Medicine, Woolloongabba, Australia; [5]Princess Alexandra Hospital, Wooloongabba, Australia.

Introduction: Next-generation sequencing (NGS) is a powerful tool that can be used clinically to identify actionable cancer biomarkers for targeted therapy. However, high failure rates and long turnaround time (TAT) restrict it from being widely adopted. Studies show ~23% to 31% of tumor samples fail comprehensive genomic profiling (CGP), mostly due to insufficient quantity and/or poor sample quality. Additionally, the complex and costly workflow of hybrid capture based NGS testing can only be performed in large reference labs, taking >2 to 3 weeks, whereas most therapy decisions are made within 7 days. SLIMamp is a technology developed by Pillar Biosciences that enables efficient, single-tube, ultra-multiplex PCR reactions by reducing the generation of unwanted, short overlapping regions between amplicons. NGS libraries prepared with SLIMamp result in higher NGS uniformity and reduced background noise, with a preferential amplification of genomic regions of interest. In this study, 48 clinical samples that failed pre-analytic QC of genomic profiling NGS testing were collected and sequenced by Pillar's oncoReveal Solid Tumor Panel (STP). Our results show SLIMamp reduces the requirements for sample quantity and quality, simplifies the NGS workflow, and shortens TAT, making it an ideal NGS solution for any local clinical lab with a sequencing platform. **Methods:** Forty-eight clinical samples from various solid tumors that failed pre-analytical QC criteria (quantity, DNA integrity, and avg. DNA fragment size) of CGP from an ISO15189-accredited lab were collected and tested with oncoReveal STP from Pillar. Data were analysed using Pillar's PiVAT secondary analysis pipeline, and bioinformatics analysis and clinical interpretation were performed in an ISO15189-accredited lab. Post-sequencing QC metric used to predict sample reportability was generated from statistical analysis of variant allele frequency (VAF) of the sequencing results. **Results:** All 48 samples were successfully sequenced with the oncoReveal STP with ≥3,000X coverage, including 40 samples that failed >1 pre-analytical QC metric. Clinical reports were successfully generated for >80% of the testing cohort. Among the 39 samples with a clinical report, 36 (>92%) contained actionable or significant variants to help direct therapy selection. Further analysis of the 9 unreportable samples showed that NGS data of these samples were dominated by artefacts that are not correlated with the pre-analytical QC criteria. On the other hand, we found that these unreportable data can be reliably predicted by applying a novel, post-sequencing QC metric based on the VAF kernel density. **Conclusions:** This study demonstrates the advantages of NGS Library Preparation kit using Pillar's SLIMamp technology on clinical samples of low quality/quantity. In combination with the post-sequencing QC metric, which we developed during this study, SLIMamp kits can be used for clinical testing on a large proportion of the most challenging clinical samples, which otherwise would go untested.

ST24. Evaluating Gene Fusions in Solid Tumors by Next-Generation Sequencing: A Tertiary Centre Experience

P. Gogte[1], S. Epari[1], M. Gurav[1], T. Pai[1], N. Karnik[1], G. Deshpande[1], J. Saha[1], P. Shah[1], R. Iyer[1], P. Joshi[1], K. Vyas[1], S. Dhanavade[1], S. Chavan[1], V. Noronha[2], V. Ostwal[2], O. Shetty[1], S. Desai[1]
[1]Tata Memorial Centre, Department of Pathology, Division of Molecular Pathology, Mumbai, India; [2]Tata Memorial Centre, Department of Medical Oncology, Mumbai, India.

Introduction: Gene fusions have been identified as oncogenic drivers in and across a wide spectrum of solid tumor types. Traditional methods for detecting oncogenic fusion transcripts include fluorescence *in situ* hybridization (FISH) and immunohistochemistry (IHC). However, these methods are limited in scalability and pose significant technical and interpretational challenges. Next-generation sequencing (NGS) is a high-throughput method for detection of gene fusions and provides diagnostic, prognostic, and theranostic information for cancer patients. In this study, we reviewed the frequency of fusion positive cases observed among the solid tumor cases subjected to NGS testing. **Methods:** The current study is a retrospective audit of RNA fusions in 1,570 solid tumor samples subjected to multigene testing during 2021 to 2022 as part of routine diagnostic work-up. Targeted NGS was performed using SOPHiA Solid Tumor Plus Solution (SOPHiA GENETICS, Lausanne, Switzerland), an NGS panel targeting 42 genes using DNA panel, RNA panel comprising 137 fusion genes, microsatellite instability and 24 copy number variations. Sequencing was performed on the MiSeq System (Illumina, San Diego, CA, USA) and results were analyzed using the SOPHiA DDM platform version 5.10.30. The clinical and histological details of all the cases were retrieved from the hospital electronic medical records system. **Results:** On analyzing sequencing data of 1,570 cases among different solid tumor types, 26 cases were

excluded from the cohort due to low read counts (<10,000 reads). Of the remaining 1,544 cases, RNA fusions were detected in 98 cases (6.3%). Recurrent gene fusions were primarily identified in lung adenocarcinomas (n = 86) involving *ALK* (n = 51), *ROS1* (n = 21), *RET* (n = 7), and *MET* (exon 14 skipping) genes (n = 7). Additionally, NGS identified EGFRvIII mutation (deletion of exons 2 to 7) in glioblastoma (n = 2), *NTRK* fusions in secretory breast cancer (n = 2, *ETV6-NTRK3*; n = 1, *DCTN1-NTRK1*) and colorectal cancer (n = 1, *LMNA-NTRK1*). Six other rare fusions including *SDC4-FGFR1* (n = 2), *AGK-BRAF*, *SND1-BRAF*, *GOLGB1-TACC3*, and *FGFR3-TACC3* were detected in thyroid and colorectal cancers. RNA fusion testing by NGS provided a more definitive diagnosis in 12 cases where IHC result for *ALK* was equivocal and *ROS1* was positive. These cases were also orthogonally confirmed by FISH. Moreover, NGS testing led to a change in the therapeutic management of 31/98 patients (31.6%) providing them clinical benefit. **Conclusions:** Gene fusions represent crucial targets in the context of precision medicine. NGS testing for fusion detection not only allows analysis of multiple targets but also saves time and material. The identification of novel fusions in this study also highlights the potential for future therapeutic targets.

ST25. Application of Next-Generation Sequencing Tests for Cancer Treatment to Guide Oncologists in Pakistan

A. Yunus, S. Ghani, N. Islam, A. Nasir, T. Moatter, Z. Ansar Ahmed
Aga Khan University, Pathology and Lab Medicine Molecular Pathology section, Karachi, Pakistan.

Introduction: Genomic tests designed to facilitate decisions about treatment management include those that identify alterations in single genes and multimarker tumor panels. Multimarker panels include targeted gene expression profiling tests that are used to estimate prognosis and/or the likelihood of recurrence. Multimarker panels also include DNA and RNA analysis through next-generation sequencing (NGS) technologies, including custom panels that profile multiple actionable driver genes and tumor characteristics that may guide the selection of targeted therapies. Currently, there are no nationally representative data describing oncologists' awareness, knowledge, and use of NGS testing to inform patient care, especially in community practice settings. **Methods:** This study was performed retrospectively on 73 biopsy specimens received for histopathological work-up at the Aga Khan University Hospital. The specimens were obtained between January 2021 and December 2022. Briefly, DNA from formalin-fixed, paraffin-embedded tissues was extracted and tested through TruSight Tumor 15 (TST15) targeted cancer gene panel Illumina, MiSeq Instrument. **Results:** The histopathological diagnosis was inclusive of 7 cancer origins (lung, melanoma, breast, colon, ovarian, gastric, and prostate). The distribution of cancer types observed was metastatic carcinoma and adenocarcinoma (infiltrating, mucinous, moderately differentiated) in 26 cases of colorectal sigmoid region; invasive ductal grade II and III in 6 cases of breast cancer; infiltrating adenocarcinoma in 3 cases of lung cancer; squamous cell and papillary carcinoma in 2 cases of prostate cancer; gastrointestinal stromal tumor in 2 cases of gastric cancer. One case of melanoma was observed. Out of 73 patients tested, 28 (38.3%) were females and 45 (61.6%) were males with a median age of 52 years, and patients' ages ranged from 20 years to 84 years. Out of the all the samples tested there was no mutation in 14 (19.17%) patients, whereas 59 (80.8%) tested positive with mutations in 7 of the 15 targeted genes. Out of the 15 genes tested, the highest frequency of mutation was observed in *TP53* gene (54.7%), *KRAS* (27%), *EGFR* (12%), *PIK3CA* (10.9%), *ERBB2* or *HER2* (5.5%), *NRAS* (4%), and lowest frequency was observed in *MET* (1%) and *BRAF* (1%). To further analyze colorectal sigmoid cancer, data involving microsatellite instability (MSI) were also gathered. Eighteen patients also got tested for MSI alongside NGS, out of which 16 patients (88.8%) were stable for all 5 markers of MSI, and 2 of the patients (11.1%) were instable (MSI-high). **Conclusions:** Our current study consists of small data with limited targeting of prognostic and actionable markers in solid tumors to predict the targeted therapy and characterize tumors. NGS testing is changing the paradigm for molecular testing in these patients; with time, it should be possible to apply NGS to routine diagnostics. More research is needed to establish the clinical usefulness of these tests and develop evidence-based clinical guidelines for their use in practice.

Cancer origin	Targeted Genes variants							
	TP53	KRAS	PIK3CA	ERBB2	BRAF	MET	NRAS	EGFR
CRC	26	10	3	0	1	1	1	3
BREAST	3	1	3	2	0	0	0	0
LUNG	1	1	0	0	0	0	1	4
GASTRIC	1	0	0	0	0	0	0	0
OTHERS	9	8	2	2	0	0	1	2

Targeted gene variants

ST26. EQA for Classifying Somatic Solid Tumour Sequence Variants: Helping to Harmonise and Improve Patient Results

J.A. Fairley, Z.C. Deans
GenQA, Edinburgh, UK.

Introduction: The introduction of large next-generation sequencing panels for the analysis of solid tumours has led to more variants being identified that have potential clinical impact. Classification systems are required to attempt to

stratify these variants into those with clinical potential and those without. A number of different systems have been proposed that address pathogenicity/oncogenicity and actionability to assist with choice of targeted therapies, prognosis, and diagnosis. **Methods:** GenQA have provided 3 pilot external quality assessments (EQAs) since 2020 to assess classification of somatic sequence variants by clinical laboratories. Participating laboratories enrolled in the EQA via the GenQA website. They were provided with 3 variants for each round of EQA along with a clinical case scenario and were asked to classify the variant according to their usual processes with the results being submitted to the GenQA website via *a proforma*. The results were assessed by at least 2 independent experts and benchmarked against the classification provided by the cohort of laboratories. **Results:** Nine individual cases have been offered since 2020. The criteria used for each case varied depending on the type of variant and the gene. The majority of laboratories used AMP/ASCO/CAP guidelines to classify the actionability of the variants, and ACMG guidelines to classify the pathogenicity of the variant. Benign single nucleotide variants were reported consistently by all laboratories; however, other variants showed considerable differences in the classification provided by laboratories demonstrating variation in application of guidelines. The differences in classification were such that they could potentially impact patient management. **Conclusions:** It is important to provide accurate variant classification is to ensure the patient receives the correct result and clinical management, particularly with respect to targeted therapies in solid tumours. This EQA has demonstrated variability in the use and application of the guidelines and has highlighted the continued need for EQAs to educate and promote standardisation.

ST27. Identification of a Rare Case of Intracranial Adult DICER1 Mutant Sarcoma by Using Epigenomic Profiling

M. Cuomo[1,2], D. Costabile[2], R. Della Monica[2], M. Buonaiuto[1], F. Trio[2], T. Di Risi[2], R. Vinciguerra[2], S. Ferraro[2], R. Visconti[3], L. Chiariotti[1,2]

[1]University of Naples Federico II, Molecular Medicine and Medical Biotechnology, Naples, Italy; [2]CEINGE Biotecnologie Avanzate, Naples, Italy; [3]CNR, Naples, Italy.

Introduction: Brain tumors are still characterized by a very poor prognosis, with often misleading diagnoses. Brain tumor molecular classification, based on genetic and epigenetic modifications, has substantially surpassed pathological classification, as highlighted in the new WHO 2021 edition. Indeed, epigenetic signatures based on DNA methylation and chromatin organization allow characterizing with extreme precision different types of tumors. To date, the epigenetic profile of brain tumors represents an identity card and, notably, the tumor will retain some specific "signatures" of the cell of origin and acquire the typical "signatures" that define the tumor specificity. In this context, primary malignant mesenchymal brain tumors are most of all a diagnostic challenge for pathologists, because they are rare and heterogeneous. We presented the fifth case so far described of an adult, intracranial, primary SCS-RMSlike-DICER1 tumor, genetically and epigenetically characterizing the tumor. **Methods:** DNA methylome was performed by using Epic array 850. Raw data were analysed by a sophisticated algorithm published previously by DKFZ (www.molecularneuropathology.com) and the prediction score associated to the tumor was calculated. The presence of DICER1 mutation, predicted by Methylome analysis, was identified by DNA sequencing of all the 25 exons of *DICER* gene. Bioinformatic analyses were performed by using R-based RnBeads scripts to obtain beta value at single CpG level for both tumors. Only the CpG sites with a difference of at least 25% in DNA methylation between high-grade glioma and DICER1 mutant sarcoma were retained. **Results:** We identified 20,022 CpGs with a lower degree of DNA methylation in DICER1 mutant sarcoma, whereas 8,254 CpG sites were found more methylated in DICER1 mutant sarcoma compared with high-grade glioma. We then associated the differentially methylated CpG sites with the respective genes by using R-based library "GenomicRanges." Only genes with at least 5 differentially methylated CpG sites were considered for the other analyses. By this way, we identified 2,262 hypomethylated genes and 1,190 hypermethylated genes, comparing DICER1 mutant sarcoma and high-grade glioma. We then performed KEGG analysis to identify the enriched pathways for the differentially methylated genes. Particularly, we found that 48 demethylated genes were significantly assigned to MAPK signalling pathway, generally activated in DICER1 mutant tumors and associated with high tumor aggressiveness and high proliferative cellular rate. **Conclusions:** The methylome profiling of DICER1 mutant tumor allows the clear identification of this tumor entity with respect to other brain tumors, unambiguously discriminating it from morphologically similar primary brain tumors. However, the rarity of DICER1 mutant sarcoma renders still challenging the identification of significant and targeted epigenetic markers that may help to better characterize the molecular mechanisms harbouring this so aggressive class of sarcoma.

ST28. Withdrawn

ST29. Targeted Inhibition of the Lysine Methyltransferase SETD8 Restrains Glioblastoma Multiforme Growth *in Vitro* in Association with Wee1 Kinase Inhibitor

R. Della Monica, M. Buonaiuto, D. Costabile, S.F. Cicala, T. Federica, T. Di Risi, R. Vinciguerra, S. Ferraro, R. Visconti, L. Chiariotti, M. Cuomo
CEINGE Biotecnologie Avanzate, Naples, Italy.

Introduction: Glioblastoma multiforme (GBM) is the most aggressive form of brain tumor. GBM standard therapy is based on temozolomide + radiotherapy, and it is largely adopted, but the prognosis remains poor and many patients still present relapses and/or resistance to treatments in a short time. Several preclinical and clinical studies have been developed but the results are not very encouraging due to the high heterogeneity of the tumor. For this reason, the identification of new biomarkers is required to develop target therapies. **Methods:** To perform our experiments we used different glioblastoma cell lines (LN-18, T98, U251, and SW1088). To inhibit SETD8 activity we used a specific chemical inhibitor (UNC0379). We validated the data using an siRNA targeting SETD8. To demonstrate cell cycle arrest and DNA damage we performed MTT assay, FACs analyses, Western blots, and immunofluorescence. To validate mitotic catastrophe we used Caspase assay and time lapse experiments. *In vivo* experiments were performed on xenograft model inoculated with Luc+U251 tumor cells. After tumor implantations we monitored tumor growth in presence or absence of specific treatments. **Results:** In our laboratory, we demonstrated that SETD8, a methyltransferase, is overexpressed in GBM, with an oncogenic role. SETD8 is able to catalyze the mono-methylation of various proteins including the onco-suppressor p53 (leading to its degradation). In this regard, we evaluated the consequences of SETD8 inhibition in GBM using a chemical inhibitor (UNC0379) and genetic silencing. We found that the inhibition of SETD8 activity led to a huge number of γ-H2AX foci by immunofluorescence, demonstrating the induction of DNA damage, which causes cell-cycle arrest in glioblastoma cell lines and primary cells. Based on these considerations, we forced arrested cells to entry into mitosis by inhibiting the kinase Wee1, causing a mitotic-catastrophe death. By combining UNC0379 with adavosertib (Wee1 chemical inhibitor), we found a very low viability in double-treated cells, compared to the single treatment, and a strong caspase activation, with consequent apoptosis induction. We obtained a strong delay in tumor growth also in xenograft models using the combination of the 2 drugs. **Conclusions:** Thus, our preliminary data indicate the association UNC0379+AZD1775 as a successful strategy for glioblastoma treatment, especially for those overexpressing SETD8.

ST30. LTBP1/TGFbeta Axis Reduces Cell Proliferation and Invasion in Melanoma Cells upon ERK5 Inhibition

A. Tubita[1], I. Tusa[1], A. Menconi[1], Z. Lombardi[1], D. Papini[1], A.E. Ogando[2], A.P. Alonso[2], B. Stecca[3], E. Rovida[1]
[1]University of Florence, Department of Experimental and Clinical Biomedical Sciences "Mario Serio", Florence, Italy; [2]Universidad de Salamanca, Centro de Investigación del Cáncer, Salamanca, Spain; [3]Institute for Cancer Research and Prevention (ISPRO), CORE RESEARCH LABORATORY, Florence, Italy.

Introduction: Malignant melanoma is the deadliest skin cancer, with a poor prognosis in advanced stages. Available treatments have improved the survival for this disease, although their long-term benefits are still unsatisfactory. We recently showed that the mitogen-activated protein kinase ERK5 plays a relevant role in melanoma growth, and that ERK5-knockdown (KD) determines cellular senescence and the production of soluble mediators typically involved in the senescence-associated secretory phenotype (SASP). **Methods:** A375 and SK-Mel-5 BRAF V600E-mutated melanoma cells have been used. Conditioned media (CM) from ERK5-KD cells were harvested 14 days post-transduction with lentiviral vectors expressing control or ERK5-targeting shRNA. Invasion assay was performed using a Boyden chamber. Control isotype IgG or neutralizing antibodies were added to CM prior to administration to cells. **Results:** We recently identified CXCL1, CXCL8, and CCL20 as the prominent SASP-related proteins secreted by ERK5-KD melanoma cells. Because TGF-β is secreted as one of the SASP factors and can regulate proliferation and invasion in cancer, we analysed the upstream components of TGF-β signalling pathway by transcriptomic analysis and found that *LTBP1* mRNA was upregulated in both A375 and SK-Mel-5 ERK5-KD cells. LTBP1 is a key regulator of TGF-β, and by using publicly available datasets we found a positive association between high levels of LTBP1 or TGF-β mRNA and a better overall survival as well as disease-free survival in melanoma patients treated with anti-PD1 therapy. Furthermore, we found an increased protein level of TGF-β in whole-cell lysates and in CM of ERK5-KD cells. Moreover, CM recovered from ERK5-KD melanoma cells reduced melanoma cell proliferation. Interestingly, treatment with a neutralizing antibody for TGF-β resulted in the partial restoration of cancer cell proliferation in a concentration-dependent manner. Importantly, performing TGF-β staining on archival xenografts of A375, after systemic administration of ERK5-i, we observed a marked increase of LTBP1 or TGF-β expression. Finally, treatment with the CM recovered from ERK5-KD cells was able to significantly reduce A375 and SK-Mel-5 invasiveness, and neutralizing antibodies for TGF-β were able to restore

their invasion ability, whereas control IgG were not. **Conclusions:** Our results extended the knowledge of the mechanisms by which ERK5 regulates melanoma growth and invasiveness, improving the comprehension necessary to develop new treatments for melanoma.

ST31. Modulation of Invadopodia-Dependent Invasion of Clear Cell Renal Cell Carcinoma by ABL2/TGFβ1/LOX Cross-Talk: Role of Tumor Grade and Matrix Stiffness

S. De Marco[1], I. Morabito[1], B. Torsello[1], N. Zucchini[2], G. Strada[3], C. Bianchi[1]
[1]University of Milano-Bicocca, School of Medicine and Surgery, Monza, Italy; [2]ASST Monza, San Gerardo Hospital, Anatomo-Pathology Unit, Monza, Italy; [3]ASST North Milan, Bassini Hospital, Urology Unit, Cinisello Balsamo, Italy.

Introduction: Clear cell renal cell carcinoma (ccRCC) is the most common and metastatic variant of renal carcinomas. In fact, up to 30% of newly diagnosed and 40% of previously treated ccRCC patients show metastatic disease. The dissemination and metastasizing of solid tumor cells exploit F-actin-rich cell protrusions with matrix-degradative activity known as invadopodia. Invadopodia maturation in different cancer cells is induced by Abl2 kinase through phosphorylation of specific invadopodia components and cytoskeleton rearrangements. Invadopodia maturation in cancer cells is induced also by TGFβ signaling, which specifically enhances ccRCC invasion. Even the extracellular matrix modifying enzyme Lysyl oxidase (LOX), which is overexpressed in ccRCC, has a role in cytoskeleton rearrangement and in modulation of matrix stiffness, inducing cellular migration and invasion. Notably, TGFβ1 treatment of renal tubular cells significantly upregulated Lox production. Here, we studied the role of Abl2 in the modulation of the TGFβ-induced and invadopodia-dependent matrix degradation in an *in vitro* model of primary cell cultures of ccRCC with different Furhman grade. The effect of matrix stiffness and the role of Lox in the stiffness modulation has been also evaluated. **Methods:** We performed immunofluorescence analysis of invadopodia F-actin spots and degradation assay of matrixes with different stiffness using primary cell cultures from human ccRCC tissues of different Fuhrman grade, treated or not with TGFβ1, TGFβ-receptor (SB431542), and Abl2 (imatinib and GNF5) inhibitors. Real-Time PCR and ELISA evaluated Lox expression. We quantified the stiffness of matrixes treated with ccRCC conditioned media by atomic force microscopy. **Results:** Invadopodia F-actin spots and matrix degradation activity of ccRCC cells were increased by TGFβ1 treatment. This effect was reduced when imatinib or GNF5 inhibited Abl2. High-grade (G3-G4) ccRCC cultures showed more invadopodia than low-grade (G1-G2) cultures in all experimental conditions analysed. Moreover, ccRCC cells showed more invadopodia when cultured on stiffer matrix, regardless of grade. Lox transcript and active protein secreted in culture media were more abundant in low-grade ccRCC samples than in high-grade cultures. Furthermore, TGFβ1 treatment of ccRCC cells increased Lox secretion and SB431542 prevented this increment. The evaluation of the effect of different grade ccRCC culture conditioned media, in presence or absence of TGFβ1 treatment, on matrix stiffness is ongoing. **Conclusions:** Our studies show that: 1) Abl2 is necessary for TGFβ1-induced invadopodia maturation of ccRCC cells, regardless of grade; 2) TGFβ1-induced Lox secretion by ccRCC cells could modulate their invasion through the putative induction of matrix stiffness. The cross-talk among Abl2, TGFβ1, and Lox could suggest new therapeutic targets in ccRCC metastatic disease.

ST32. Molecular Landscape of Small-Cell and Large-Cell Neuroendocrine Carcinomas of the Gastroenteropancreatic System (Selected for Oral Presentation, O-01-02)

N.E. Albayrak, B.L. Liu, S.C. Ward
Icahn School of Medicine at Mount Sinai, Department of Pathology, Molecular and Cell-Based Medicine, New York, NY.

Introduction: The World Health Organization subdivides high-grade (G3) gastroenteropancreatic (GEP) neuroendocrine neoplasms into well-differentiated neuroendocrine tumors (NETs) and poorly differentiated neuroendocrine carcinomas (NECs). NECs are highly aggressive neoplasms with a median overall survival (OS) of 11.9 months (vs. OS = 55.6 months in G3 NETs). Yet molecular data for GEP-NECs are limited, and treatment strategies are extrapolated from small-cell lung cancer (SCLC). **Methods:** A search of a pathology database (2010 to 2022) revealed 48 cases of GEP-NECs, including esophageal (5), gastric (4), small intestinal (3), pancreatic (9), biliary (6), and colorectal (21) primary tumors. FoundationOne testing was performed on consecutive histological samples and/or on blood samples collected from 48 patients diagnosed with GEP-NECs. Based on the sequencing of 324 cancer-related genes, we assessed mutations and copy number alterations (CNAs). **Results:** Molecular alterations in *TP53* (85%) proved to be the most commonly observed, regardless of the primary site. Other consistently found molecular alterations included *BRAF* (21%) and *RB1* (19%), which were mutually exclusive, followed by *KRAS* (17%) and *APC* (17%). Nineteen percent of GEP-NECs harbored cell cycle progression pathway-related gene mutations other than *RB1,* including aberrations in

CCNE1, *CDKN2A*, *CCND1,* and *CDK4*. Frequent amplifications/gains were found in *MYC* (19%) and *ERBB2* (10%). Targetable mutations involving the phosphoinositide 3 kinase (PI3K)/Akt/mammalian target of rapamycin (mTOR) (PAM) pathway (i.e., activating *PIK3CA* and *AKT1* mutations or *PTEN* loss) were identified in 15% of GEP-NECs. Mutations and CNAs varied according to primary tumor site, with *BRAF* mutations mainly seen in colon (50%), and *APC* mutations mainly seen in rectal cancers (43%). **Conclusions:** The findings provide insight into the pathogenesis of GEP-NECs and highlight limited similarities to SCLC. Despite the paucity of data about the molecular drivers associated with GEP-NECs, a high fraction of targetable alterations (46% in our cohort) indicates a high potential for better-personalized treatments.

ST33. Utility of ctDNA for Molecular Profiling in NSCLC Patients in Resource-Limited Clinical Setting

P. Joshi[1], A. Nair[1], N. Pawar[2], D. Dhanawade[1], P. Gogte[1], M. Gurav[1], T. Pai[2], R. Kumar[2], N. Karnik[2], G. Wagh[2], J. Saha[1], P. Shah[1], O. Shetty[1], S. Desai[2]

[1]Tata Memorial Hospital, Homi Bhabha National institute,Molecular Pathology Laboratory, Mumbai, India; [2]Tata Memorial Hospital, Homi Bhabha National institute, Department of Pathology, Mumbai, India.

Introduction: In the era of precision medicine, liquid biopsy has become a promising approach for disease monitoring and molecular diagnosis of patients who do not have access to a tissue specimen or an adequate biopsy. Circulating tumor DNA (ctDNA) is a fragmented cell-free DNA (cfDNA) making up as low as 0.01% of the entire cfDNA released from tumor cells. The International Association for the Study of Lung Cancer (IASLC) statement provides the guidelines for the incorporation of ctDNA testing in a clinical setting. The current study summarizes the utility of ctDNA-based molecular diagnosis of lung cancer patients using real-time PCR and next-generation sequencing (NGS) platforms. **Methods:** ctDNA molecular profiling data of the non-small-cell lung cancer (NSCLC) patients (n = 299) diagnosed with variable histology previously and having an inadequate biopsy or are undergoing targeted inhibitor therapy at Tata Memorial Hospital were compiled (2020 to 2022)**.** ctDNA was extracted from the plasma samples of NSCLC patients using the COBAS cfDNA extraction kit (Roche Diagnostics). *EGFR* mutation detection using conventional ARMS-RTPCR (cobas EGFR mutation test V2) was performed for 268 samples. NGS using SOPHiA SOLID TUMOR PLUS SOLUTION targeted panel was used to assess the remaining 31 samples. **Results:** Of the 268 cases tested by real-time PCR 170 (63.4%), cases were reported as wild-type for *EGFR* mutation. Targetable mutations were reported in 96 (35.8%) cases having histology of advanced metastatic adenocarcinoma (n = 78) and squamous cell carcinoma (n = 4). Actionable *EGFR* mutations were reported on the basis of ctDNA from 14 cases in which histological findings were unavailable due to various clinical reasons. Tyrosine kinase inhibitor therapy-resistant mutations (exon 18 and exon 20) were reported in 10 advanced metastatic adenocarcinomas. Due to suboptimal DNA quality, 5 cases were reported as uninterpretable. Of the cases subjected to NGS testing 5 out of 31 cases had targetable alterations with variant allelic frequency ranging from 0.2 to 5.8. In 3 cases that were *EGFR* exon 19 deletion positive on biopsy, ctDNA of the same patient during the longitudinal monitoring did not show any alterations. **Conclusions:** ctDNA analysis is a critical challenge that often leads to false negative results due to biological variables such as stage of the disease, tumor volume, low DNA-shedding, and preanalytical variables. The current study demonstrates the utility of ctDNA as a non-invasive promising tool to detect targetable alterations in situations where tissue biopsy is inaccessible or tumor tissue is depleted. Real-time PCR-based platform is the most preferred option for molecular analysis of ctDNA in clinical settings over NGS, considering factors like cost, turnaround time, and availability of resources.

ST34. Identification of a Functional Relationship between MEK5-ERK5 Pathway and Hypoxia Inducible Factor 1α

A. Menconi[1], I. Tusa[1], A. Gentilini[2], F. Marra[2], E. Rovida[1]

[1]University of Florence, Department of Experimental and Clinical Biomedical Sciences "Mario Serio," Florence, Italy; [2]University of Florence, Department of Experimental and Clinical Medicine, Florence, Italy.

Introduction: Cholangiocarcinoma (CCA) is the second most common liver cancer after hepatocellular carcinoma, and constitutes a heterogeneous group of malignancies that arise from the epithelium of the biliary tree. Each subtype of CCA has a distinct genetic profile that is reflected in a different pathogenesis and prognosis in patients. Genetic heterogeneity opens many opportunities for new personalized and targeted therapies. Currently, in fact, many selective inhibitors are under study. Recently, our group reported the importance of the mitogen-activated protein kinase extracellular-signal regulated kinase 5 (ERK5) in supporting the survival and proliferation of CCA both *in vitro* and *in vivo*. In the attempt to identify additional Achilles' heels to be targeted in CCA, we investigated on the existence of a functional relationship between ERK5 and hypoxia inducible factor 1α (HIF-1α), the main regulator of the response to hypoxia, a condition that is typical of the tumour microenvironment. **Methods:** Two intrahepatic CCA cell lines

(CCLP-1 and HUCCT-1) were grown at different timepoints under normoxia and hypoxia (0.1 % O_2) conditions. Protein expression analysis was performed by Western blot. Effects on cell viability of KC7F2 (HIFi) and XMD8-92 or JWG-071 (ERK5i) were evaluated using MTT assay. **Results:** We found that ERK5 phosphorylation and HIF-1α expression are increased in hypoxia. The increased activity of the latter in hypoxia was confirmed by the consistent increase of its target genes, *Carbonic Anhydrase 9* (*CAIX*) and *Glucose transporter 1* (*GLUT1*). We then performed a combined treatment of ERK5 and HIF inhibitors and found a greater effect of the combination than the single treatments in hypoxic conditions. **Conclusions:** These findings led to the identification of a relationship between ERK5 and HIF-1α in the regulation of CCA homeostasis, and put light on the combined ERK5/HIF-targeting among the new possible therapeutic options for CCA.

ST35. Integrated Molecular Analysis of Diffuse Adult-Type Gliomas: Proposal of Next-Generation Sequencing and FISH Approaches for a Clinically Applicable Molecular Classification

S. Coluccelli[1], T. Maloberti[1], A. De Leo[1], V. Sanza[2], S. Asioli[3], E. Franceschi[4], A. Altimari[2], E. Gruppioni[2], D. de Biase[5], G. Tallini[2]

[1]University of Bologna, Department of Medicine (Dipartimento di Medicina Specialistica, Diagnostica e Sperimentale), Bologna, Italy; [2]IRCCS Azienda Ospedaliero-Universitaria di Bologna, Molecular Pathology Laboratory, Bologna, Italy; [3]Istituto delle Scienze Neurologiche, Bologna IRCCS-ISNB, Department of Biomedical and Neuromotor Sciences (DIBINEM)-Surgical Pathology Section-Alma Mater Studiorum-University of Bologna, Bologna, Italy; [4]IRCCS Istituto delle Scienze Neurologiche di Bologna, Nervous System Medical Oncology Department, Bologna, Italy; [5]University of Bologna, Department of Pharmacy and Biotechnology (FaBiT), Bologna, Italy.

Introduction: The fifth edition of the WHO Classification of tumors of the central nervous system (CNS), updated in May 2021, renewed the incorporation of both histological features and molecular alterations into the diagnostic framework, classifying, and grading of brain tumors. The guidelines emphasized the importance of an integrated histomolecular diagnosis for treatment and follow-up of CNS tumor. According to these recommendations and the diagnostic algorithm proposed for the adult-type diffuse gliomas integrated classification, this study aimed at applying a set of molecular techniques to assess the incidence of adult-type diffuse gliomas in a cohort of consecutive patients, and to evaluate the impact of the update on the adult-type diffuse gliomas diagnosis. **Methods:** A total of 117 patients diagnosed with an adult-type diffuse glioma from January 2022 to January 2023 were characterized by next-generation sequencing (NGS) to determine their isocitrate dehydrogenase (*IDH1/IDH2*) status, as well as other adult-type diffuse gliomas molecular signature markers, among *TP53*, *TERT* mutations, and *MGMT* promoter methylation. Fluorescence *in situ* hybridization (FISH) was performed on all the cohort. A 1p/19q-single-nucleotide polymorphism (SNP) panel was used to support puzzling FISH diagnoses of 1p/19q co-deletion. **Results:** A total of 41 (35%) diffuse gliomas with *IDH*-wild-type were found, out of which 12 (29.7%) had *EGFR* gene amplification and 8 (19.5%) had +7/-10 chromosome copy number changes. Among the 76 (65%) astrocytomas *IDH*-mutant screened for the *CDKN2A/B* homozygous deletion, 11 (14.5%) were positive and designated as astrocytomas *IDH*-mutant CNS WHO grade IV. Ten (13.2%) out of 30 are oligodendrogliomas *IDH*-mutant and co-deleted 1p/19q on FISH. Twenty (66.7%) out of all the *IDH*-mutant diffuse gliomas were further investigated using the 1p/19q-SNP panel, out of which 5 (25%) were designated 1p/19q co-deleted, according to both molecular approaches. Two cases (10%) of this group showed discrepant results after 1p/19q FISH and SNP analysis: In detail, 1 case showed chromosome imbalance according to the SNP panel, inconsistent with 1p/19q co-deletion. In this case, the diagnosis was consistent with astrocytoma *IDH*-mutant, CNS WHO grade III. Another case, CNS WHO grade IV, diagnosed as Chr19q13 deleted by FISH, showed only a partial loss of heterozygosity of the Chr19q13.2-19qter by NGS. **Conclusions:** This molecular algorithm seems to be useful in the classification of adult type- diffuse gliomas analyzed, allowing sufficient integrated histopathologic and molecular diagnosis. The combination of NGS and FISH analysis was consistent to molecular characterization of adult-type diffuse glioma by ancillary markers. NGS analysis was revealed to be essential to support FISH results for equivocal cases, especially in high-grade adult-type diffuse gliomas for 1p/19q co-deletion.

ST36. Impairment of ERK5 Nuclear Localization Restores Sensitivity to ERK5 Kinase Inhibitors

Z. Lombardi[1], L. Gardini[2], A. Menconi[1], I. Tusa[1], M. Lulli[1], E. Rovida[1]

[1]University of Florence, Department of Experimental and Clinical Biomedical Sciences, Filorence, Italy; [2]University of Florence, LENS - European Laboratory for Non-Linear Spectroscopy, Sesto Fiorentino, Italy.

Introduction: The extracellular signal-regulated kinase 5 (ERK5) is emerging as a possible target for melanoma treatment. ERK5 pro-proliferative activities are linked to its presence in the nucleus, but the mechanisms involved in

ERK5 nuclear translocation are poorly characterized. We focused on the elucidation of this process using single molecule tracking and searching for compounds able to prevent ERK5 nuclear shuttling, to design new strategies for cancer treatment. **Methods:** To achieve single ERK5 tracking in living cells, we used super-resolution microscopy. HeLa cells were transfected with an expression vector for ERK5, linked to HaloTag, alone or with a vector for a constitutively active form of the ERK5 activator MEK5 (MEK5DD). The cell-permeable photoactivatable chromophore JaneliaFluor646 was used as a detection technique for super-resolution imaging. As a complementary approach, HEK293 T-cells, transfected with ERK5 and MEK5DD, and A375 melanoma cells were treated with the alpha/beta1 importin-mediated transport inhibitor ivermectin (IVM) or transfected with 2 siRNA targeting importin-β1. MTT, 2D-colony forming assays, and apoptosis evaluation were performed in A375 or HeLa cells treated with IVM in combination with the ERK5-i AX-15836. A375 and HeLa spheroids were used to evaluate the effect of IVM and AX-15836 on a 3D model of *in vitro* tumor growth. **Results:** The HaloTag technology provided the selective binding of JaneliaFluor646 to ERK5, and Highly Inclined and Laminated Optical sheet microscopy allowed us to collect the signal of single molecule ERK5 instances. Data showed that in ERK5-transfected cells, as expected, the protein is mainly localized in the cytoplasm, whereas it moves in the nucleus with the activator MEK5DD, and this effect is partially reversed in cells treated with IVM. Moreover, ERK5 amount in the nuclear fraction of lysates from IVM-treated cells and from KPNB1 KD cells is lower compared to control, suggesting a role of importin α/β1 in ERK5 nuclear transport. Finally, we found that ERK5i AX-15836, which was reported to induce ERK5 nuclear translocation in a paradoxical way, reduced melanoma cell proliferation only in combination with IVM in 2D and 3D growth models. **Conclusions:** The current study demonstrated the involvement of importin α/β1 in ERK5 nuclear translocation. The described super-resolution technique will also help future studies to investigate the mechanism of action of ERK5 in the nucleus. Furthermore, our data showed that impairment of ERK5 nuclear localization restores sensitivity to AX-15836, suggesting that the actors involved in ERK5 nuclear shuttling could be identified as novel targets for ERK5 inhibition, and therefore for a possible anticancer therapy.

ST37. Detecting Gene Fusions with 3D Genomics from FFPE Solid Tumors: Clinical Concordance, Validation, and Actionable Insights from Tumors with Unknown Drivers (Selected for Oral Presentation, O-04-03)

A. Schmitt[1], K. Galbraith[2], K. Sikkink[1], Y. Yang[2], H. Mohamed[2], L. Van Meter[1], M. Movahed-Ezazi[2], I. Tran[2], B. Zeck[2], L. Chiriboga[2], A. Tsirigos[2], S. Chiang[3], G. Jour[2], M. Snuderl[2]

[1]Arima Genomics, Carlsbad, CA; [2]NYU Langone Health, Department of Pathology, New York, NY; [3]Memorial Sloan Kettering Cancer Center, Department of Pathology and Laboratory Medicine, New York, NY.

Introduction: Identifying gene fusions in tumor biopsies is critical for understanding disease etiology; however, clinical next-generation sequencing panels often fail to yield clear genetic drivers. A key challenge is that RNAseq does not perform well in formalin-fixed, paraffin-embedded (FFPE) tissue blocks due to RNA degradation and/or RNA panel design, and cannot detect breakpoints outside of the gene body, which are established clinical biomarkers with mechanistic significance and clinical utility in solid hematological cancers. **Methods:** We developed a novel DNA-based partner-agnostic approach for identifying fusions from FFPE tumors using 3D genomics. We profiled 184 FFPE tumors across various tumor types. This cohort includes 33 tumors with known gene fusions detected by RNA panels for clinical concordance analyses. It also includes 151 FFPE tumors, including 62 central nervous system tumors, 59 gynecological sarcomas, and 22 solid heme tumors, with no detectable genetic drivers from prior DNA and RNA panel CLIA assays (“unknown driver cohort”). Samples were processed using the Arima-HiC+ FFPE kit, and in some cases a capture panel was applied to enrich for specific genes of interest. Libraries were sequenced using Illumina platforms. Data were analyzed using the Arima-SV pipeline, or the Arima Oncology Pipeline, depending on whether the data were genome-wide or targeted, respectively. Overexpression of putative driver genes associated with fusions was confirmed by immunohistochemistry (IHC). **Results:** For clinical concordance, Arima-HiC technology detected 33/33 fusions previously detected by RNA panels. For clinical validation and utility studies in our unknown driver cohort, Arima-HiC detected 1 or more fusions in 72% (109/151) of tumors. To attribute clinical significance according to NCCN guidelines, WHO classification criteria, and OncoKB, 33.8% (51/151) of tumors had fusions implicating FDA-approved therapeutic level biomarkers, 4.0% (6/151) had fusions implicating biomarkers that are the target of ongoing clinical trial therapies, and 14.6% (22/151) had fusions implicating diagnostic or prognostic biomarkers, indicating an overall yield

of clinically actionable biomarkers of 52.3% in unknown driver cases. Several cases with clinically actionable fusions underwent confirmatory IHC testing for oncoprotein expression, and 91.6% (11/12) showed diffuse or focally positive staining. To highlight examples from prospectively analyzed cases from this cohort, we identified a novel *PD-L1* rearrangement in a pediatric glioma tumor that was not detected by DNA or RNA panels, which we confirmed by *PD-L1* IHC, and the patient was administered pembrolizumab after tumor recurrence and has since exhibited stable disease. We also identified a *MYBL1* fusion in a glioma that spared the patient unnecessary chemotherapy post-resection.
Conclusions: Our findings provide evidence of clinical concordance, validation, and utility, and underscores the need for 3D genome profiling to increase diagnostic yield by finding clinically actionable fusions in FFPE solid tumors.

ST38. Utilization of Liquid Biopsies of Different Origin for NGS Studies in the Mexican Population

C. Peñaloza Coronas[1,2], V. Izúcar Ramales[1], L.A. Mendoza Torres[1], M. Wences Carretero[3], S.M. Montilla Fonseca[1]
[1]Labopat Diagnostics, NGS laboratory, Puebla, Mexico; [2]Universidad Nacional de Quilmes, Science and Technology Department, Buenos Aires, Argentina; [3]Instituto Tecnológico y de Estudios Superiores de Monterrey, Science School, Puebla, Mexico.

Introduction: For the past decade, liquid biopsies have become increasingly relevant in the management of cancer patients due to their minimally invasive sample collection process. Liquid biopsy refers to a laboratory test performed on bodily fluids, such as whole blood, cerebrospinal fluid, pleural fluid, ascites fluid, and others to detect circulating tumor nucleic acids (ctNAs). However, there are numerous challenges in the analysis of ctNA, including its short half-life (less than 1.5 hours) and low amounts of nucleic acids in the sample, which are directly linked to the quality of the collection tube. Liquid biopsy is mainly used to analyze tumor heterogeneity, especially when solid biopsy samples are unavailable, as well as for prognostication and evaluation of treatment strategies, therapy resistance, new therapeutic targets, residual disease, and early cancer stage diagnosis.
Methods: In 2022, our laboratory received 8 liquid biopsies of different sources, including 4 peripheral blood, 1 ascites fluid, and 3 cerebrospinal fluids. The samples were collected in ethylenediaminetetraacetic (EDTA) tubes, with a volume of 5 to 10 mL. The samples were processed within 1 hour of collection or were frozen (-20°C) until processing. Cell-free nucleic acids were isolated using MagMAX Cell-free Total Nucleic Acids, evaluating final yield of extraction. After that, an amplicon-based next-generation sequencing was performed by the Oncomine precision assay using the Genexus Integrated Sequencer. The data were analyzed using the Genexus software **(Fig. 1)**. **Results:** All samples had an adequate yield of extraction for the subsequent technique (minimum of 0.33 ng/uL; median yield: 6.501 ng/uL). Single nucleotide variants were detected in *TP53* (25% of the cases) (FA: 87.9% to 76.6%), *KRAS* (FA: 50.1%), *GNAS* (FA: 14.1%), *MAP2K1* (FA: 46.3%), *MTOR* (FA: 6.3%), *PIK3CA* (FA: 38.4%) *y EGFR* (FA: 39.4%), each one in 12.5% of the cases. Additionally, copy number variations in *CDKN2A* were detected in 25% of the cases and *EGFR* (amplification) in 12.5%. Two samples (25%) did not show any alterations.
Conclusions: These results indicate that the isolation methods for circulating tumor nucleic acids were successful in all samples considered in this study, with few variations to the extraction protocols based on sample origin. The use of EDTA tubes did not affect the viability of the sample when processed on the same day of collection. This represents a significant milestone, as access to specialized consumables is limited in México.

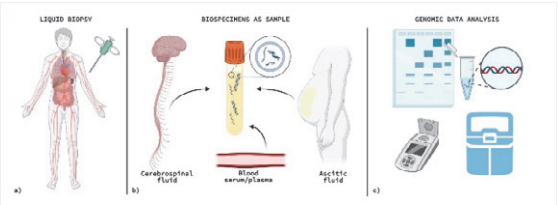

Figure 1.
NGS workflow for liquid biopsies. 1) Sample collection. 2) Different sample sources for ctNA detection. 3) NGS processing and data analysis.

ST39. Clinical Application of Liquid Biopsy across Pan-Cancer: 4baseCare's Experience Using TarGT Indiegene-Liquid Biopsy NGS Panel

A. Ravi, N.A. Tanwar, A. Prakash, K. Verma, S. Jayaraman, L. Varghese, S.R. Peddagangannagari, K.D. Rishi, H. Goswami, R. Malhotra, V.H. Veldore
4baseCare Onco Solutions Pvt. Ltd., Bangalore, India.

Introduction: Precision oncology is a branch of medicine that focuses on using personalized and targeted approaches to treat cancer, based on the specific genetic mutations present in a patient's tumor. The use of liquid biopsy, which analyzes cell-free DNA in the blood, has become a popular tool in precision oncology to monitor cancer progression and response to treatment without invasive tissue biopsy. The TarGT Indiegene Liquid Next-Generation Sequencing (NGS) panel, developed and validated by 4baseCare, is a comprehensive gene panel that covers 1,212 genes, and derived from in-house research on 1,500 pan-cancer patients

tumor tissue profiling on whole exome and transcriptome. **Methods:** A total of 100 patients with 20 different advanced stage cancers were analyzed using the TarGT Indiegene Liquid Biopsy Panel (Fig. 1). Beyond analytical validation, we have analyzed liquid biopsy patients samples from diverse cancer types using the standard Illumina library preparation protocol. Data analysis was performed using DRAGEN BioIT platform. **Results:** Performance matrix of TarGT Indigene Liquid (1,212 genes) biopsy NGS panel along with the diagnostic yield from clinical samples is summarised in Figure 2. Seventy-six patients were observed to harbour oncogenic *alterations, out of which 43% variants were implicated in therapy and 40% more were correlated with prognostic and therapeutic implications. Further, ERBB2 and CCND1 amplification, FGF3/4 co-amplifications and FGFR2::BICC1 gene fusions were identified in the patient cohort, and minimal residual disease (MRD) estimation was evident in a patient as well. Almost 70% of patients had* TP53 *alterations. In a patient with carcinoma of unknown primary, we found actionable mutation in* PIK3CA *(p.Glu545Asp) and* IDH2 *(p.Arg172Trp)* that provided a scope for targeted therapy with repurposing option. The MRD estimation was evident in a breast cancer patient with *ERBB2* amplification detected while the patient was on maintenance trastuzumab. **Conclusions:** This pan-cancer pilot study using the TarGT Indiegene Liquid Biopsy Panel supports the hypothesis that molecular information obtained from liquid biopsy can play a significant role in clinical decision-making, in addition to tissue mutation profiling. The results of this study demonstrate the potential clinical utility of this liquid biopsy panel in identifying actionable genomic alterations in patients with advanced stage cancer. These findings suggest that liquid biopsy has the potential to complement tissue biopsy and provide important molecular information to inform personalized treatment decisions for patients with cancer.

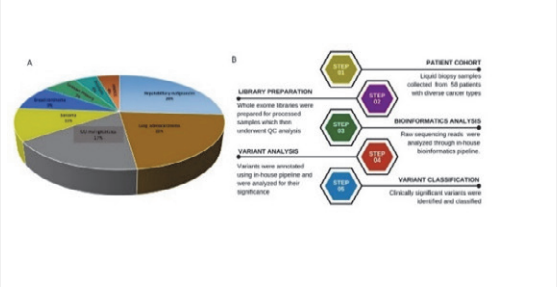

Patient cohort and sample processing end-to-end workflow of TarGT Indiegene Liquid Biopsy NGS panel.

Assay performance metrics and clinical diagnostic yield of TarGT Indiegene Liquid Biopsy NGS panel

ST40. The Senolytic Activity of Quercetin on Doxorubicin-Induced Senescent Fibroblasts Reduced Osteosarcoma Cell Growth and Invasiveness

E. Bientinesi, S. Ristori, M. Lulli, D. Monti
University of Florence, Department of Experimental and Clinical Biomedical Sciences, Florence, Italy.

Introduction: Cellular senescence is a tumour-suppressive mechanism that prevents the proliferation of premalignant cells. However, several studies show that senescent cells (SCs), particularly senescent cancer-associated fibroblasts, can promote tumour progression via the senescence-associated secretory phenotype (SASP). Therefore, potential strategies for mitigating the effects of SCs include senolytic drugs that selectively kill them and interfere with the SASP. In this study, we used quercetin as a senolytic agent on Doxorubicin-induced senescent fibroblasts (SFs), investigating the mechanisms through which it killed senescent cells. Moreover, we studied if the partial elimination of SFs was sufficient to reduce the pro-tumour effects on osteosarcoma cells. **Methods:** WI-38 fibroblasts were induced to senescence with Doxo and then treated with quercetin 40 μM for 3 days. To assess the reduction of senescent cells, we evaluated cell proliferation by Trypan blue exclusion assay, cell cycle arrest by cytofluorimetric analysis, senescence-associated β-galactosidase activity (SA-β-gal), senescence-associated heterochromatin foci (SAHF) by immunofluorescence, and cell death by Annexin/7AAD flow cytometry assay. In addition, the expression of autophagy markers was analysed by Western blot and immunofluorescence. Moreover, we have investigated colony formation capacity and invasiveness of U2OS treated with fibroblast conditioned media (CM). **Results:** Our results showed that quercetin kills 30% of SFs without affecting the proliferating ones. These data were obtained by assessing the decrease of SA-β-gal activity, cell cycle arrest, and increased SAHF presence in quercetin-treated SCs compared to untreated ones. Interestingly, our data suggested that

quercetin could kill SCs by reducing autophagy, a safeguard process frequently enhanced in SCs to counteract endoplasmatic reticulum stress due to the production of SASP. Moreover, our results showed that CM from SFs enhanced proliferation and invasiveness of U2OS cells. On the contrary, CM from quercetin-treated SFs did not induce these aggressive behaviours. **Conclusions:** Our study shows that quercetin exerted a senolytic activity on Doxo-induced senescent fibroblasts, reducing autophagy without affecting the viability of young cells. Reducing autophagy, quercetin probably exposes SFs to proteotoxic stress induced by the high protein synthesis rate involved in the SASP, leading to senolysis.Moreover, our data demonstrated that even if quercetin killed a relatively small amount of SCs (30%), this is sufficient to cancel pro-tumour activity of SFs on osteosarcoma cells. In conclusion, using flavonol quercetin to eliminate chemotherapy-induced SFs could be an excellent strategy to reduce chemotoxicity and metastatic progression, the biggest cause of poor prognosis of osteosarcoma.

ST41. The Profiles of E-cadherin Expression in Different Types of Prostate Adenocarcinoma

R.M. Plesea[1,4], M.S. Serbanescu[3,6], E.I. Plesea[2,5]
[1]Craiova University of Medicine and Pharmacy, Cell and Molecular Biology, Craiova, Romania; [2]"Carol Davila" University of Medicine and Pharmacy, Pathology, Craiova, Romania; [3]Craiova University of Medicine and Pharmacy, Medical Informatics and Biostatistics, Craiova, Romania; [4]Craiova Emergency Clinical County Hospital, Medical Genetics, Craiova, Romania; [5]"Bagdasar-Arseni" Emergency Clinical Hospital, Pathology, Bucharest, Romania; [6]Filantropia Municipal Clinical Hospital, Pathology, Craiova, Romania.

Introduction: E-cadherin (ECHAD) is one of the main cell adhesion molecules related to the formation and growth of epithelial malignancies. The aim of this study is to compare the expression of ECHAD in 2 morphological variants of prostate adenocarcinoma: the classic form (PADK) and the ductal form (DADK) according to the degree of differentiation assessed with the Gleason system. **Methods:** A series of 525 prostatic tissue areas with different individual patterns of the Gleason system of were immunohistochemically (IHC) stained with ECHAD and images were evaluated through a proprietary computational algorithm. The group consisted of 435 areas of PADK, and 90 were areas of DADK. The algorithm marked the pixels where the red channel was more intense than the other channels. Then the overall colour intensity of the previously selected mask was inverted and considered as the value for the intensity of the IHC staining. Larger values have meant more intense staining. ECHAD expression location was stratified as follows: E1 = Membrane only, E2 = Membrane + Cytoplasm, E3 = Cytoplasm only. **Results:** ECHAD expression site evolved differently in the 2 variants of prostate adenocarcinoma. In PADK, ECHAD had a dominant E1 expression in well-differentiated (WD) areas and evolved towards a predominant E3 expression in poorly differentiated (PD) areas, with a chi-square test p value <0.0001. In DADK, in turn, ECHAD had different types of expression in the 4 main types of Gleason patterns (chi-square test p value = 0.022) but with an oscillating trend of expression, with obviously dominant E1 expression in the most PD areas (Gleason pattern 5), followed by moderately (Gleason pattern 3) and WD areas (Gleason pattern 2), and predominant E3 expression only in Gleason pattern 4 areas. **Conclusions:** The degree of intercellular adhesion, expressed by the ECHAD presence on cell membrane dominantly, does not always correlate with a lower degree of differentiation in prostate adenocarcinomas.

ST42. Efficient Lung Cancer Molecular Diagnostics by Combining Next-Generation Sequencing with Reflex Idylla GeneFusion Assay Testing

D. Nkosi, H. Liu, M. Buldo, M. Velez, Z.N. Oltvai
University of Rochester, Pathology and Laboratory Medicine, Rochester, MN.

Introduction: Molecular testing for lung cancer is well established, but how to provide rapid, precise, and cost-effective testing modalities for optimal patient care remains unresolved. Here, we show that DNA-only <50 gene next-generation sequencing (NGS) panels combined with ultra-rapid reflex testing for fusion transcripts (*ALK*, *ROS1*, *RET*, *NTRK1-3*) and *MET* exon 14 splice mutations using the Biocartis Idylla GeneFusion assay provides a rapid and cost-effective testing pathway for most lung cancer cases. We also demonstrate the need for additional reflex testing capability on larger DNA and fusion panels for a small subset of cases. **Methods:** We performed retrospective analyses of all lung tumor samples submitted for NGS and fluorescence *in situ* hybridization (FISH) for *ALK* and *ROS1* rearrangements in a 1-year time period (July 2021 to June 2022) at our institution. NGS data were obtained on the DNA portion of the Oncomine Focus Assay (OFA) (Thermo Fisher), which tested 35 genes for single nucleotide variants (SNVs) and small indels and 18 genes for gene amplification. We also sent out 4 in-house NGS/FISH negative specimens for comprehensive mutation and fusion profiling to a large commercial laboratory and performed Idylla GeneFusion assay testing on them. **Results:** In-house OFA NGS testing identified a pathogenic or likely pathogenic variant in more than 75% of lung tumor specimens. In contrast, FISH for *ALK* and *ROS1* rearrangements proved positive in only 3% of cases. We did

not detect a pathogenic or likely pathogenic variant by NGS in any specimens that were positive for *ALK* or *ROS1* rearrangement. Follow-on comprehensive mutation and fusion profiling of 4 NGS negative-, *ALK/ROS1* FISH negative cases identified SNVs and fusions in genes not tested on the OFA NGS panel. This included a case with detected *FGFR3-TACC3* fusion transcript and a specimen with a Met exon 14 splice junction mutation that was not detectable by the OFA panel but could be detected by the Idylla GeneFusion assay which we validated recently. **Conclusions:** DNA-only <50 gene NGS panels can identify oncogenic mutations in the majority of lung tumor cases. In contrast, FISH testing for *ALK* and *ROS1* rearrangement is overwhelmingly negative and does not justify their use for initial testing. Instead, NGS negative lung tumor specimens can be reflexed to the Idylla GeneFusion assay, which provides results within 4 hours. Rare specimens that are both NGS and Idylla GeneFusion negative need to be promptly assessed by comprehensive mutation and fusion profiling for rare driver mutations and fusion transcripts. Similar testing blueprints could be established for all solid tumor types for which extensive gene/fusion variant results are available both in the treatment-naïve and post-therapy settings.

ST43. Molecular Characteristics of a *C11orf95-RELA* Fusion Gliosarcoma: A Case Report

T. Feldman[1], E. Vlodavsky[1], S. Sarji[1], A. Yousef Abu El Hija[1], M. Benifla[2], L. Oren[3], M. Ben-Arush[3], Y. Zohar[1]
[1]Rambam Health Care Campus, Department of Pathology, Haifa, Israel; [2]Rambam Health Care Campus, Children's Neurosurgery Department, Haifa, Israel; [3]Rambam Health Care Campus, Division of Pediatric Hematology/Oncology, Ruth Rappaport Children's Hospital, Haifa, Israel.

Introduction: Gliosarcoma (GSM) is a rare variant of *IDH*-wild-type glioblastoma (GBM), an aggressive astrocytic tumor with a poor prognosis. Ependymomas are rare glial tumors arising from ependymal cells which are classified according to molecular and anatomical features. The combination of ependymoma and gliosarcoma elements in the same tumor is extremely rare, and the molecular characteristics of these entities are not clear. Here we present a rare case of an aggressive gliosarcoma harboring *C11orf95-RELA* fusion and its mutational landscape suggesting an aberrant activation of the RAS/MAPK signaling pathway. **Methods:** A 12-year-old male was admitted to our institute and was diagnosed with a left frontoparietal brain tumor which was operated and resected. Following a period of 10 months, the tumor recurred, and the patient was re-operated. Formalin-fixed, paraffin-embedded tissue samples from both operations were sectioned, stained with hematoxylin-eosin and subjected to a histopathological examination. In addition, DNA and RNA were extracted from the tissue of the second operation and a library using the Oncomine Comprehensive Assay Plus kit was prepared, covering more than 500 unique genes. Library products were sequenced using the Ion GeneStudio S5 Prime semiconductor sequencer, and analysis was performed using the Ion Torrent Suite and Ion Reporter Software. **Results:** The sections from the original operation demonstrated a highly cellular, biphasic tumor composed of spindle cells with marked atypia and 30 mitoses in 10 HPF, alongside another population of large atypical epithelioid cells, focally positive for GFAP and EMA. A final diagnosis of undifferentiated sarcoma was made. Molecular studies revealed the presence of *C11orf95-RELA* fusion transcript in RNA, whereas DNA sequencing revealed somatic mutations in *HRAS*, *NF1, TP53*, *BCOR,* and *STAG2* genes. **Conclusions:** In this report we present an extremely rare case of *C11orf95-RELA* fusion supratentorial ependymoma that underwent a complete sarcomatous transformation. The presence of *C11orf95-RELA* fusion in this case highlights the importance of considering the diagnosis of ependymoma in sarcomatous brain tumors and of performing unbiased molecular studies in these cases. Importantly, this report sheds light on key biological and evolutionary aspects of this rare tumor, such as an aberrant overactivation of the RAS/RAF/MAPK signaling pathway. Consequently, the sensitivity of these tumors to MEK inhibition should be assessed in future studies.

ST44. Gold Nanoparticles Obtained by Pulsed Laser Ablation as Inducer of Tumor Vessel Normalization

A. Chillà[1], C. Anceschi[1], E. Frediani[1], T. Del Rosso[2], G. Fibbi[1], M. Del Rosso[1], F. Margheri[1], A. Laurenzana[1]
[1]University of Florence, Department of Experimental and Clinical Biomedical Sciences "Mario Serio", Florence, Italy; [2]Pontifical Catholic University of Rio de Janeiro, Department of Physics, Rio de Janeiro, Brazil.

Introduction: Tumor neovascularization is essential for the progression of solid tumors, supporting their demand for nutrients and oxygen. However, the structure and function of new vessels are immature and deformed because of influence by excessive proangiogenic factors. Abnormal tumor vessels have low blood perfusion and thereby decrease oxygen infusion into tumors, thus creating a hypoxic tumor microenvironment, impeding the infiltration of immune cells and facilitating the intravasation of tumor cells into the circulation and consequently metastasis. Most of the therapies currently used for cancer treatment have focused primarily on inhibiting angiogenesis in tumors by cutting off their blood supply. However, these antiangiogenic drugs have limited efficacy and drug resistance. Moreover, some antiangiogenic

drugs increase the production of proangiogenic factors promoting pathological angiogenesis due to the reduction of the oxygen supply, thus leading to the increased tumor metastasis and relapse in some cancers. New antiangiogenic therapies focus on tumor vascular normalization with the aim of remodeling and stabilizing the immature vascular structures through the integration of vascular mural cells. Restoring aberrant tumor blood vessels has been shown not only to be capable of reducing tumor invasion and metastasis, but also of improving the efficiency of chemotherapy, radiation therapy, and immunotherapy. **Methods:** To test the effect of gold nanoparticles (Au-NPs) obtained by pulsed laser ablation (PLA) on the endothelial colony forming cells' (ECFCs') ability to form vessel structures, we performed experiments of capillary morphogenesis on Matrigel. To reproduce tumor microenvironment, the 3D model of tumor was composed of M6 melanoma spheroids which were placed in the presence of LA-Au-NPs-loaded ECFCs. A 3D invasion assay with Boyden chamber and scratch assay were used to test invasion and migration capacity of tumor cells, instead of WST-8 colorimetric assay, to assess their proliferation. **Results:** In this work we have shown that Au-NPs obtained by PLA release CO formed in the ablation process, triggering a cascade of events that stimulates neo-angiogenesis by a particular class of EPCs known as ECFCs, which play a fundamental role in tumor angiogenesis. Moreover, the migration and the enhanced angiogenic properties of PLA-Au-NPs-enriched ECFCs were also confirmed in 3D melanoma culture. In parallel, the same Au-NPs induced the inhibition of melanoma and breast cancer cell invasion and proliferation. **Conclusions:** These preliminary experiments showed that PLA-Au-NPs are a promising nanomaterial due not only to their inherent anti-neoplastic activity typical of Au-NPs, but for inducing a strong proangiogenic activity in endothelial progenitor cells. Based on these properties, promising experiments are now being conducted to test these NPs as tumor vessel normalization inducers.

ST45. DNA Methylation Changes in HPV-Positive and HPV-Negative Cervical Adenocarcinoma

S.A. Farkas[1], M. Kaliff[1], B. Sorbe[3], L. Bohr Mordhorst[3], G. Lillsunde-Larsson[4,1]

[1]Örebro University, Örebro University Hospital, School of Medical Sciences, Faculty of Medicine and Health, Örebro, Sweden; [2]Örebro University, School of Medical Sciences, Faculty of Medicine and Health, Örebro, Sweden; [3]Örebro University, Örebro University Hospital, Oncology, Faculty of Medicine and Health, Örebro, Sweden; [4]Örebro University, School of Health Sciences, Örebro, Sweden.

Introduction: Persistent human papilloma virus (HPV) infection is considered the main cause of cervical cancer. There are more than 200 different subtypes of HPV, classified into high risk or low risk. The cytological screenings and vaccines against HPV are powerful tools to combat cervical cancer; however, the incidence has increased in developing countries in the past decades. There are 2 main histological types of cervical cancer, squamous cell carcinoma, and adenocarcinoma (AC). Changes in DNA methylation patterns are one of the hallmarks of cancer, where certain changes may lead to progression and aggressiveness. The aim of the current work was to study DNA methylation changes in HPV-positive and HPV-negative cervical adenocarcinoma to aid in the knowledge about the epigenetic changes that occur due to HPV infection. **Methods:** We have analysed DNA methylation profile in 15 HPV-positive AC, and 8 HPV-negative AC samples using the Illumina EPIC array. Samples were collected at the Department of Oncology, Örebro, University Hospital. The DNA was extracted from formalin-fixed, paraffin-embedded material. The differential methylation analysis was performed using R package CHAMP. **Results:** The differential methylation analysis resulted in a limited number of differentially methylated CpG sites (see Fig. 1). A total number of 377 differentially methylated CpG sites were identified with an adjusted p-value <0,05. The vast majority of the CpG sites were hypermethylated in the HPV-positive adenocarcinoma. Top 10 hypermethylated CpG sites were located in the *KCNK12* (cg13913015), *PPP1R1C* (cg21566370), *FAM155A* (cg14119999), *C1orf114* (cg14119999), *PDE4D* (cg11258089), *VSTM2B* (cg18802754), *SOX2OT* (cg02650401), *SYT9* (cg24678137), *SST* (cg24678137), and *ONECUT1* (cg17500265) genes. The difference in methylation (Δ-β value) between the 2 groups ranged between 0.37 and 0.49. **Conclusions:** HPV infection affects the DNA-methylation pattern in cervical adenocarcinoma, specifically, more hypermethylation was observed.

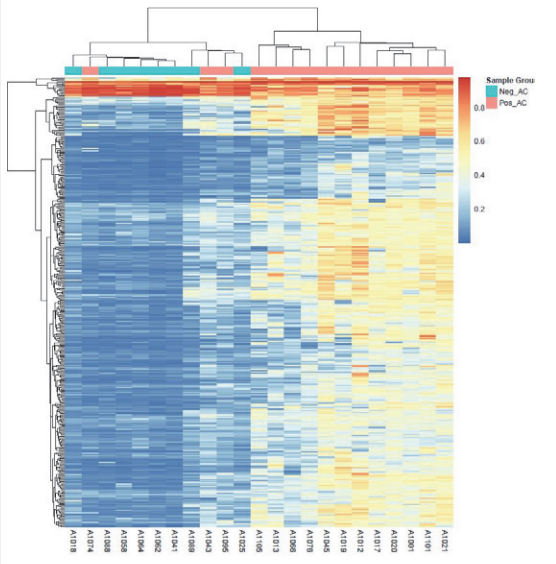

Figure 1.
Differentially methylated CpG sites in HPV-positive and HPV-negative adenocarcinoma.

Selected Other Abstracts

OTH01. PD-L1 Testing of Pulmonary and Non-pulmonary Malignancies: A Cytology/Histology Correlation Study
K. Ijaz, L. Layfield, M. Esebua
University of Missouri Hospital and Clinics, Department of Pathology and Anatomical Sciences, Columbia, MO.

Introduction: Immunotherapy and related PD-L1 testing are standard of care for many patients with advanced malignancies at a variety of body sites. Many studies have correlated PD-L1 testing results of cytology and histology specimens from pulmonary carcinomas, but fewer have been reported for malignancies arising at other body sites. We report our findings for PD-L1 testing in a series of pulmonary and non-pulmonary malignancies. **Methods:** An electronic search for all PD-L1 testing of cytologic specimens performed over a 48-month period (January 1, 2019, to June 30, 2022) was undertaken. Each case identified by the search was reviewed for corresponding biopsy or resection specimens. Representative histologic slides from the surgical specimens underwent immunohistochemical testing for PD-L1. Two observers independently scored the cytologic and histologic PD-L1 stained slides with correlation analyzed by Cohen's kappa. **Results:** Thirty-four cytology specimens with PD-L1 results were identified, which had subsequent surgical biopsies or resection specimens. Twenty-two cases were pulmonary carcinomas and 12 were non-pulmonary malignancies (8 pancreatic adenocarcinomas, 3 head and neck squamous carcinomas, and 1 mesothelioma). Overall, the observed agreement between cytologists for PD-L1 results was 97.1% with expected agreement of 40.0% and a kappa of 0.95. Observed correlation of cytologic and histologic PD-L1 staining was 82.4%, with expected agreement of 36.8% with a Cohen's kappa of 0.72. Observed agreement of pulmonary cases for cytologic-histology correlation was 86.4% with a kappa of 0.78, and for non-pulmonary cases observed agreement was 75% with a Cohen's kappa of 0.62 (Table 1). **Conclusions:** Correlation between observers for PD-L1 scoring was strong, as was agreement between cytologic and histologic specimens for PD-L1 results. Correlation between cytologic and histologic specimens was higher for pulmonary specimens (86.4%) than for non-pulmonary malignancies (0.78%), but the difference was not statistically significant ($p = 0.5$).

Table 1: Correlation results for PD-L1 testing

Comparison	Cases	Observed Agreement	Expected Agreement	Kappa (95% CI)
Cytologist 1 vs Cytologist 2	34	97.1%	40.0%	0.95 (0.83-1.00)
Cytology vs Histologic Diagnosis	34	82.4%	36.8%	0.72 (0.51-0.91)
Cytology vs Histology (Pulmonary cases)	22	86.4%	39.3%	0.78 (0.54-1.00)
Cytology vs Histology (Other cases)	12	75%	33.6%	0.62 (0.30-1.00)

Correlation results for PD-L1 testing

OTH02. Next-Generation Sequencing of Cytology Specimens: A Practical Review
K. Ijaz, M. Esebua, L. Layfield
University of Missouri Hospital and Clinics, Department of Pathology and Anatomical Sciences, Columbia, MO.

Introduction: Cytologic samples often constitute the only available material for diagnosis and ancillary testing, especially in advanced stage cancers. Cellblock preparations represent a valid method for next-generation sequencing (NGS), especially for predicting response to targeted therapies. FoundationOne CDx Solid Tumor Panel is a qualitative NGS-based diagnostic test which includes 315 genes, as well as introns of 28 genes with known rearrangements, and cancer biomarkers including tumor mutational burden (TMB) and microsatellite instability (MSI). We examined NGS results of cytologic material to determine the frequency of therapeutically useful results. **Methods:** Following Institutional Review Board approval, the NGS reports of 54 cytology specimens (48 fine needle aspirations and 6 fluids) were reviewed. Reports were analyzed for tumor type, tumor location, presence of actionable mutations, mutations without specific drug assignment, MSI, and TMB. Tumor sites include lymph node, lung, pancreas, liver, pleural fluid, peritoneal fluid, and bronchial washings (Table 1). Thirty-seven cases were tumors of pulmonary origin (30

adenocarcinomas, 4 squamous cell carcinomas, 1 each small cell carcinoma, carcinosarcoma, and neuroendocrine neoplasms). Six cases were pancreatic adenocarcinomas, while 4 were squamous cell carcinomas of the head and neck. Three adenocarcinomas of the breast, 1 adenocarcinoma of the gallbladder, 1 esophageal adenocarcinoma, along with a single squamous cell carcinoma of unknown origin, and a single urothelial carcinoma of the bladder. Thirty-eight of 54 cases had adequate tissue for analysis. **Results:** Five specimens from adenocarcinomas of the lung contained targetable mutations (4 *EGFR* and 1 *ROS1*) (Table 1). No other specifically targetable mutations were found in this series. Mutations of potential utility for protocol selection were found in 21 specimens of lung neoplasms and a single breast adenocarcinoma. Nine mutations of prognostic significance were found in lung adenocarcinomas, and 1 each in adenocarcinoma of the pancreas, breast, and gallbladder. TMB data were obtained in 27 of 54 cases, but none showed high mutational burdens. MSI was documented in none of the 29 cases successfully tested. **Conclusions:** Adequate material for NGS was obtainable in 68.5% of cases. NGS panel provided useful information in most cases. Targetable mutations were found in 9% of cases, but mutations potentially impacting protocol selection were found in 39% of cases, indicating the value and applicability of NGS to cytology specimens.

Tumor Type	Origin	Case number	Driver mutations detected	Cancer biomarkers (MSI/TMB) detected	Cases with variants associated with treatment in patient's tumor type	Cases with variants associated with treatment in different tumor types	Cases with variants associated with no treatment	Clinical trial	Insufficient tumor quantity (QNS)
Adenocarcinoma	total	29	17/29(58.6%)	13/29(44.8%)	8/29(27.5%)	0/29(51.0%)	17/29(58.6%)	16/29(55.1%)	13/29(44.8%)
	lung	19/29(65.5%)	10/17(58.8%)	6/13(46.15%)	5/8(62.5%)	5/9(55.5%)	12/17(70.5%)	9/16(56.2%)	8/13(61.5%)
	Pancreas	5/29(17.2%)	3/17(17.6%)	2/13(15.3%)	0/8(0.0%)	1/9(11.11%)	2/17(11.7%)	2/16(12.5%)	4/13(30.7%)
	Breast	3/29(10.3%)	3/17(17.6%)	3/13(23.0%)	2/8(25%)	3/9(33.3%)	3/17(17.6%)	3/16(18.7%)	0/13(0.0%)
	Esophagus	1/29(3.4%)	1/17(5.8%)	1/13(7.6%)	1/8(12.5%)	1/9(11.1%)	1/17(5.8%)	1/16(6.2%)	0/13(0.0%)
	Gallbladder	1/29(3.4%)	1/17(5.8%)	1/13(7.6%)	0/8(0.0%)	0/9(0.0%)	1/17(5.8%)	1/16(6.2%)	0/13(0.0%)
squamous cell carcinoma	total	9	6/9(66.6%)	6/9(66.6%)	3/9(33.3%)	3/9(33.3%)	6/9(66.6%)	5/9(55.5%	3/9(33.3%)
	lung	1/9(11.1%)	1/6(16.6%)	1/6(16.6%)	1/3(33.3%)	1/3(33.3%)	1/6(16.6%)	1/5(20.0%)	0/3(0.0%)
	Head and Neck	1/9(11.1%)	1/6(16.6%)	1/6(16.6%)	1/3(33.3%)	1/3(33.3%)	1/6(16.6%)	1/5(20.0%)	0/3(0.0%)
	Lymph node	7/9(77.7%)	4/6(66.6%)	4/6(66.6%)	1/3(33.3%)	1/3(33.3%)	4/6(66.6%)	3/5(60.0%)	3/3(100%)
Neuroendocrine tumor	Total	3	3/3 (100%)	3(100%)	2(66.6%)	1(100%)	3(100%)	3(100%)	2(0%)
	lung	2/3(66.6%)	2/3(66.6%)	2/3(66.6%)	1/2(50.0%)	2/3(66.6%)	2/3(66.6%)	2/3(66.6%)	0/2(0.0%)
	Lymph node	1/3(33.3%)	1/3(33.3%)	1/3(33.3%)	1(50.0%)	1/3(33.3%)	1/3(33.3%)	1/3(33.3%)	0/2(0.0%)
Unknown primary and non small cell lung carcinomas (NOS)	Lung	10	9/10(90.0%)	6/10(60.0%)	5/10(50.0%)	6/10(60.0%)	9/10(90.0%)	7/10(70.0%)	0/10(0%)
Carcinosarcoma	Lung	1	1/1(100%)	1/1(100%)	0/1 (0%)	0/1 (0%)	1/1(100%)	1/1(100%)	0/1 (0%)
Urothelial carcinoma	Bladder	1	1/1(100%)	1/1(100%)	0/1 (0%)	0/1 (0%)	1/1(100%)	1/1(100%)	0 /1(0%)

NGS Results Summarized in Cytology Cases of Pulmonary and Non-pulmonary Malignancies

OTH03. Development and Validation of an AI-Based Tumour Cell Estimation Algorithm for Use in a Lung Adenocarcinoma Molecular Pathology Workflow (Selected for Oral Presentation, O-02-03)

R.C. Wyatt[1], D. Dorward[2], D. Mulkern[1], P. Caie[1], C. Corless[3]
[1]Indica Labs, Albuquerque, NM; [2]NHS Lothian, Department of Pathology, Edinburgh, United Kingdom; [3]Oregon Health & Science University, Department of Pathology and Laboratory Medicine, Portland, OR.

Introduction: The development of targeted therapies has led to an increasing volume of molecular testing on formalin-fixed, paraffin-embedded tissue samples. This has increased the workload for pathologists, who review haematoxylin and eosin (H&E) stained slides, mark a tumour-dense region suitable for macrodissection, and estimate the percentage of tumour cells within the area. These estimates also suffer from subjectivity and inter-observer variability; pathologists typically overestimate the proportion of tumour. Accurate knowledge of the tumour fraction is critical for interpreting molecular results and avoiding false negatives. Computational assessment of cell counts can standardise tumour fraction measurements, bringing efficiency and quality gains to the molecular pathology workflow. More accurate results and faster turnaround times will reduce workloads and benefit patients. Here, we present an AI-based algorithm for the clinical scoring of pulmonary oncology samples to support pathologists and increase consistency. **Methods:** HALO Lung Macrodissect AI was developed and validated on routine, H&E-stained lung adenocarcinoma (ADC) diagnostic cases, including cytology, core biopsy, and resection specimens from primary and metastatic lesions. Across 91 images from 2 institutes (institute 1: n = 47 [52%]; institute 2 n = 44 [48%]), 173,374 annotations were split into training (n = 146,852 [84.7%]) and validation (n = 26,522 [15.3%]) pools. These were used to train a ResNet 18-based network to classify all cells within a whole slide image (20x magnification) as either "tumour" or "other." The resultant algorithm was validated at the cell level using 28,733 annotations (tumour: n = 15,523 [54%]; other: n = 13,210 [46%]) from 30 unseen images (institute 1: n = 17, 57%; institute 2: n = 13, 43%). All annotations were verified by expert pathologists. The algorithm was then run on 25 unseen images within regions marked for macrodissection by pathologists during their routine clinical workflow. The percentage of cells identified as tumour by the classifier was compared with a pathologist's estimate. **Results:** The median image F1-score for combined cell level validation was 0.88 (IQR, 0.84 to 0.93). The median F1-score for tumour and other cells was 0.90 (IQR, 0.85 to 0.94) and 0.87 (IQR 0.82 to 0.92), respectively. In regions marked for macrodissection, the median tumour cell percentage score from the pathologist was 55% (IQR, 35% to 65%) compared with 48% (IQR, 36% to

57%) (p = 0.007) from the algorithm. The median difference between estimates was 7.9% (IQR 3.8% to 14.5%). The AI scores were within 10% of the pathologist's estimate in 15 (60%) cases. **Conclusions:** Tumour cell percentage scores from HALO Lung Macrodissect AI agree with pathologist estimates in routine lung ADC cases annotated for macrodissection. Cell level validation shows that the algorithm detects tumour cells with a high level of accuracy. Use of this classifier in a diagnostic setting can support pathologists by saving time, standardising results, and improving the quality of molecular readouts.

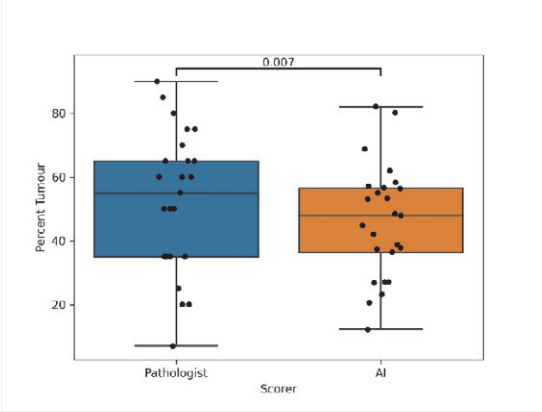

Tumour cell percentage scores
Plot to show tumour cell percentage scores measured in regions marked for macrodissection on 25 unseen images. The median score from the pathologist was 55% (IQR, 35% to 65%) compared with 48% (IQR, 36% to 57%) (p = 0.007) from HALO Lung Macrodissect AI.

OTH04. Technical Validation of the Idylla Microsatellite Instability Assay on FFPE Tissue in Colorectal Cancers
S. Kalachian, R. Abdul Khalik, F. Abbas, R. Mahfouz
American University of Beirut Medical Center (AUBMC), Pathology and Lab Medicine, Beirut, Lebanon.

Introduction: Microsatellite instability (MSI) is a molecular hallmark for some colorectal cancers (CRCs) in which short tandem repeats are prone to mutations along with DNA sequences. Microsatellites are strands of DNA with a repetitive sequence of 1 to 10 nucleotides duplicated from 5 to 50 times that are wildly distributed throughout the human genome. These tandem repeats are particularly unstable and susceptible to mutations with rates of 103 to 105 per cell generation. The mutations that escape from the DNA mismatch repair (MMR) system form new alleles at the microsatellite loci and are inherited by the next cell generation. MMR proteins (MLH1, PMS2, MSH2, MSH6) are a major system of DNA repair that specifically repairs DNA base-base mismatch pairs introduced into microsatellites during DNA synthesis to maintain genomic stability. MMR system deficiency (MMR-D) particularly affects microsatellites and results in alterations in their repeat length, named MSI, and in loss of expression of MMR proteins in tumor tissue. Therefore, MSI status detected by MSI testing actually reflects MMR proficiency. MSI testing is used to classify CRC tumors as MSI-high (MSI-H), MSI-low, and microsatellite stable tumors. This classification also aids in making treatment management decisions. In fact, MSI-H or MMR deficient tumors have shown the best prognosis among all CRCs, so MSI testing is considered as a good prognostic marker. **Methods:** MSI status was determined on 12 archived formalin-fixed, paraffin-embedded tissue sections with Idylla technology. The Idylla MSI Test performs a qualitative detection of 7 monomorphic homopolymer biomarkers (ACVR2A, BTBD7, DIDO1, MRE11, RYR3, SEC31A, SULF2) for identification of colorectal cancer with MSI. The Idylla MSI results were compared with previously obtained findings by routine testing methods. Immunohistochemistry (IHC) looks at MLH1, MSH2, MSH6, and PMS2 staining on tumor samples to identify the loss of protein expression that characterizes MMR-D as a surrogate for MSI. **Results:** Ten out of 12 samples showed concordance between the results obtained with the Idylla MSI Test and the IHC staining profile. The 2 discordant samples were non-colorectal tumors. Indeed, recent studies have shown a higher rate of discordance between microsatellite status and MMR immunophenotype in non-CRC. Moreover, different types of MMR-D immunostaining from the classical MLH1/PMS2 or MSH2/MSH6 loss have also been described. Consequently, the rising amount of MMR testing, particularly in non-CRC, has led to an increase in the number of unusual MMR-D cases. The origin and functional consequences of these unusual MMR-D profiles are not documented; nor was their clinical impact evaluated. **Conclusions:** The Idylla MSI Test was successfully technically validated as an adequate tool for the evaluation of the MSI status in CRC.

OTH05. Yin/Yang Effectiveness of Gold Nanoparticles: Tumor Progression Control or Promotion of Vascularization of Defective Angiogenesis Diseases

C. Anceschi[1], E. Frediani[1], A. Chillà[1], F. Scavone[1], F. Margheri[1], P. Armanetti[3], L. Menichetti[3], F. Ratto[2], T. Del Rosso[4], G. Fibbi[1], M. Del Rosso[1], A. Laurenzana[1]
[1]University of Florence, Experimental and Clinical Biomedical Sciences, Florence, Italy; [2]National Research Council, Institute of Applied Physics "N. Carrara" Sesto Fiorentino, Italy; [3]National Research Council, Institute of Clinical Physiology (IFC), Pisa, Italy; [4]Pontifical Catholic University of Rio de Janeiro, Department of Physics, Rio de Janeiro-RJ, Brazil.

Introduction: The application of nanomaterials in the fields of medicine and biotechnology is of enormous interest, particularly in the areas where traditional solutions have failed. Nanoparticles can offer clear advantages compared to traditional therapies: 1) fewer side effects of delivered drugs; 2) increased versatility in formulation; and 3) display of optical or magnetic properties that can be tuned to detect early disease (diagnosis) or to cause damage to cancer cells (therapy). Certainly, the biological activity of nanoparticles (NPs) depends on chemical and physical factors such as size and shape, surface area, agglomeration state, chemical composition, surface chemistry (charge and hydrophilicity), surface activity, solubility, dose, and so on. In particular, gold NPs, due to the chemically inert nature of gold and the relative ease of surface chemistry manipulation for downstream applications, have received much attention. **Methods:** The current work describes the effects and biological interaction of two different types of gold NPs on progenitor endothelial cells (EPCs). Capillary morphogenesis, matrigel plug assay, real-time PCR, and Western blot analysis were used to evaluate the angiogenic properties and phenotype of EPCs. Inductively coupled plasma mass spectrometry and transmission electron microscopy were employed to assess cellular gold uptake and retention. Confocal microscopy and photoacoustic imaging (PAI) were used to evaluate the distribution of AuNPs inside 3D tumor models and to detect the optical imaging of NIR AuNP-doped EPCs. **Results:** We surprisingly identified pro-angiogenic properties of gold nanoparticles (Au-carbenoids), having a peak of absorbance at 510nm, that are heavily taken by EPCs. We demonstrated that EPCs, loaded with these particular gold nanoparticles, show an improved angiogenic phenotype *in vitro* and *in vivo.* We also demonstrated that the same cell line can be heavily loaded with near infrared (NIR) AuNPs and be used as theranostic vector. Indeed, NIR AuNP-loaded EPCs enhanced AuNP optical properties and exhibited excellent thermotransductive property when exposed to NIR light. Moreover, EPC loaded with NIR AuNPs are able to reach hypoxic areas of a 3D tumor model and could possibly re-sensitize tumors to radiotherapy. **Conclusions:** Au-carbenoids might represent a differential therapeutic option for patients with diseases associated with progressive loss of microvasculature. Nonetheless, NIR AuNP-doped EPCs represent a powerful theranostic tool for tailored early disease detection and innovative medical treatment.

OTH06. Measurable Residual Disease Detection in Mantle Cell Lymphoma (MCL) Subjects Using NGS B-Cell MRD Assay

P. Shah[1], Y. Huang[1], O. Diaz II[1], A. Jacobson[1], N. Hill[1], A. M. Herrera[2], A. Zlotnicki[1]
[1]Invivoscribe, Product Development, San Diego, CA; [2]Universitario de Salamanca, Hospital Clínico, San Vicente, Spain.

Introduction: Mantle cell lymphoma (MCL) is an aggressive, rare form of non-Hodgkin B-cell lymphoma. Measurable residual disease (MRD) assessment can provide useful information when assessing and tracking response to therapy, refining treatment, and predicting clinical outcome for subjects with B-cell lymphoproliferative diseases. One method of MRD detection is to identify and track specific clonal immunoglobulin heavy chain (IGH) gene rearrangement sequences on a next-generation sequencing platform. Here, we present the NGS-based B-cell MRD Assay with 10^{-6} sensitivity for detecting MRD in malignancies in MCL. **Methods:** Residual DNA samples from different specimen types (44 bone marrow [BM] and 77 peripheral blood [PB]) at different post-treatment time points were obtained from anonymized 47 MCL subjects that had been enrolled in a study approved by the Spanish Group of Lymphoma and Autologous Stem Cell Transplantation (clinical trial: NCT02682641, publication reference: 10.1200/JCO.21.02321). A total of 121 of these follow-up samples were tested by the B-cell MRD Assay by tracking the clonal sequences detected in corresponding baseline samples. Among them, 90 follow-up samples were paired PB and BM samples. The B-cell MRD Assay workflow consists of DNA extraction and PCR-based library preparation with proprietary multiplex master mixes targeting either IGH Framework 1 (FR1) or 3 (FR3) regions, which both track the patient- and tumor-specific CDR3 sequence. Purified libraries are then equimolar pooled and sequenced on Illumina's NextSeq Dx platform. The FASTQ output files from sequencing are analyzed using Invivoscribe's B-Cell MRD Software-NextSeqDx. Results from Invivoscribe were compared to the results from the Salamanca lab that were generated by qPCR. **Results:** Based on the results from the B-cell MRD Assay, 115/121 (95%) samples were valid, 42/115 (37%) valid samples had, "MRD Detected," and 73/115 (63%)

samples had, “MRD Not Detected," with a “MRD Detection” rate of 28% in PB and 50% in BM specimen types. When comparing MRD detectable status between paired PB and BM samples from 36 MCL subjects, 30/44 (68%) paired samples had the same MRD call and were concordant, whereas 14/44 (32%) calls were discordant. More specifically, 12/14 (86%) discordant samples had PB specimen type with a “MRD Not detected” call, whereas the paired BM specimen showed a “MRD Detected” call. Overall, in comparison with the MRD results (n = 84) provided by the Salamanca lab using the qPCR method, the B-cell MRD Assay demonstrated concordance of 80%, positive percent agreement of 79%, and negative percent agreement of 80% for MRD detection in MCL samples. **Conclusions:** Good concordance was observed between Salamanca and the B-cell MRD Assay. It is important to note that the BM specimen type was determined to be more sensitive in detecting MRD when compared to BM in assessment of paired PB and BM samples. These results demonstrate that the B-cell MRD Assay can be utilized for MRD detection in follow-up sample types for MCL subjects.

OTH07. Evaluation of *EGFR* and GeneFusion Assay Using Biocartis Idylla Technology in Lung Adenocarcinoma

R. N. Abdel Khalek, S. Kalachian, F. Abbas, R. Mahfouz
American University of Beirut Medical Center, Pathology and Laboratory Medicine, Beirut, Lebanon.

Introduction: Lung cancer is the second most common cause of cancer death in the world. Thus, the tyrosine kinase inhibitor (TKI) therapy is established for cancer driven by an oncogenic kinase. The detection of actionable mutations such as epidermal growth factor receptor (*EGFR*), anaplastic lymphoma kinase (*ALK*), c-ros oncogene 1 (*ROS1*), ret proto-oncogene (*RET*) or neurotropic tyrosine receptor kinase (*NTRK*) is very crucial in patients with lung adenocarcinoma. Patients carrying *EGFR* mutations or gene fusion variants may be candidates for a targeted therapy, whereas those developing resistance to first-generation TKI expressed the T790M *EGFR* mutation. This study aims to evaluate the clinical performance of the Idylla *EGFR* and Idylla GeneFusion on the Idylla Biocartis System. **Methods:** In this evaluation, 10 formalin-fixed, paraffin-embedded (FFPE) tumor tissue sections previously tested with Cobas *EGFR* gene mutation assay were retested by real-time PCR amplification using Idylla *EGFR* Mutation assay. The Idylla *EGFR* detects a total of 51 mutations on exon 18 (G719A/S/C), 36 deletions in exon 19, exon 20 (T790M, S768I), and 5 insertions in exon 20 and exon 21 (L858R, L861Q). Eight FFPE samples from patients with adenocarcinoma were retested using the Idylla GeneFusion assay, which detects gene fusion for *ALK, ROS1, RET* as well as *MET* exon 14 skipping and expression imbalance for *ALK, ROS1, RET,* and *NTRK1/2/3* by reverse transcription of mRNA followed by real-time PCR amplification. **Results:** A concordance frequency of 100% (10/10) was observed between the Idylla *EGFR* and Cobas *EGFR* Mutations Test V2. Eight of the 10 tumors were lung biopsy, one pleural fluid, and one iliac bone biopsy. Six out of 8 samples tested by Idylla GeneFusion showed concordant results for *ALK, ROS1,* and *RET* fusion in comparison with immunohistochemistry (IHC) staining. One of the discrepant samples was a pleural fluid and the second a vertebral biopsy. This failure may be due to loss and/or degradation of RNA, which might be countered by increasing the amount of sample input. **Conclusions:** The Idylla *EGFR* testing is an accurate and simple tool useful for the early screening of *EGFR* mutations. The Idylla GeneFusion is a potential screening panel with short turnaround time using a minimal amount of tissue and might be considered as a relevant complementary testing to IHC in diagnostic molecular laboratories.

OTH08. Irish Healthcare Providers' Knowledge, Confidence, and Practice Regarding Molecular Pathology: Measurement and Attitudes, Including towards Clinical Informatics to Support Implementation of Molecular Pathology, amongst Diverse Health Care Providers in Various Specialities in a Large Irish University Teaching Hospital

S. Kearney
University College Dublin, School of Medicine, Dublin, Ireland; Beacon Hospital, Oncology Department, Dublin, Ireland.

Introduction: The purpose of this study was to measure Irish healthcare providers’ (HCPs) subjective self-appraisal of their knowledge of molecular pathology (MP) tests and techniques, combined with obtaining an objective assessment of such knowledge. We measured HCPs' self-confidence regarding MP tasks, including ordering, interpreting, and explaining MP tests. Aside from measuring knowledge and confidence, we ascertained HCPs' attitudes and opinions regarding how clinical informatics tools and ancillary supports (such as genetic counsellors, molecular tumour boards, and accessing second opinions) might assist MP workflows. We also investigated general attitudes and opinions on MP clinical informatics issues including interoperability, artificial intelligence, mobile access, and preference for paper versus digital workflows. Finally, we enquired whether HCPs viewed MP as a mainly research-oriented activity or as being clinically essential. **Methods:** The survey was conducted via electronic means, utilising Google Forms, which was distributed to a wide variety of HCPs. Thirty HCPs associated with a single hospital replied, including nurses of various grades, doctors in

training in various specialities (both medical and surgical), general practitioners, and qualified consultants. **Results:** More than half of respondents (65.6%) thought they knew less than enough regarding MP to do their jobs (Fig. 1). Amongst all types, grades, and specialities of HCPs, there was a distinct subset of doctors who thought they knew enough or more than enough to do their jobs. However, only a minority of this cohort actually had relatively high levels of objective MP knowledge, as measured via a battery of tests (Fig. 2). Regarding confidence in all the steps of ordering, interpreting, and explaining MP tests, only a minority were fully or somewhat confident. The majority of HCPs were positively predisposed to utilising clinical informatics to assist with MP workflows and tasks, were in favour of genetic counsellors (GCs) assisting their practice, were comfortable with accessing second opinions, and thought that molecular tumour boards (MTBs) were essential to successful implementation. Only one HCP had a strong preference for paper over digital workflows, whereas the majority were comfortable with AI. The majority had poor access to healthcare data interoperability and mobile access. Finally, the majority (83.9%) were supportive or strongly supportive that MP was important to their clinical practice, rather than research, within their speciality. **Conclusions:** Despite a small subset of respondents having high self-appraisals of their MP knowledge, when objectively measured most Irish HCPs lack knowledge and confidence in MP, like their international peers. However, clinical informatics tools and professional supports, such as MTBs, GCs, and second opinions, may help to overcome such limitations in knowledge and confidence. This is important, given the growing prominence of MP in mainstream clinical practice, as reported by respondents.

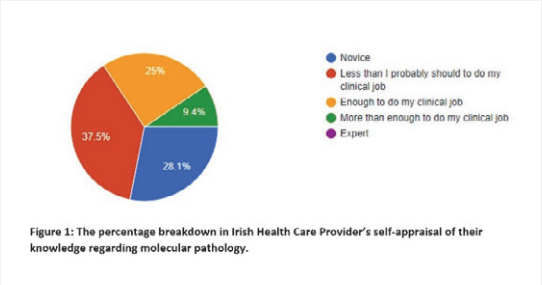

Figure 1: Irish HCPs' Subjective Knowledge of Molecular Pathology
The percentage breakdown in Irish Health Care Providers' self-appraisal of their knowledge regarding molecular pathology.

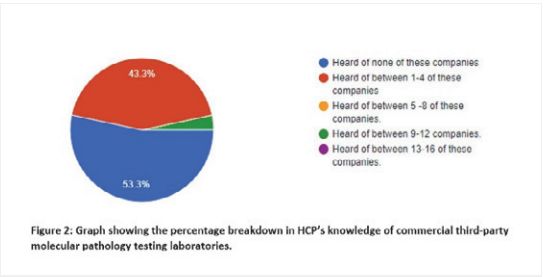

Figure 2: Irish HCP's Objective Knowledge of Molecular Pathology
Graph showing the percentage breakdown in HCP's knowledge of commercial third-party molecular pathology testing laboratories.

OTH09. Exosomal PD-L1 Expression Reduction by uPAR/PAI-1 Blockade: A New Strategy for Cancer Immunotherapy?

E. Frediani, C. Anceschi, F. Scavone, A. Chillà, G. Fibbi, M. Del Rosso, A. Mocali, A. Laurenzana, F. Margheri
Università degli studi di Firenze, Dipartimento di Scienze Biomediche Sperimentali e Cliniche, Firenze, Italy.

Introduction: Over the last few years, immunotherapy has revolutionized cancer therapy. Immune checkpoint inhibitors, such as antibodies against PD-L1 and PD-1, have shown effectiveness against a large number of cancer types, including melanoma and non-small-cell lung cancer. Emerging evidence suggests that improved prognosis and clinical outcomes in melanoma patients subjected to anti- PD-L1 therapy are associated with high PD-L1 positivity. Recently, Tseng *et al*. showed that targeting plasminogen activator inhibitor 1 (PAI-1) by its inhibitor tiplaxtinin (TPX) synergizes with anti-PD-L1 checkpoint blockade in a model of murine melanoma, thus paving the way for a more effective melanoma treatment. The membrane-associated plasminogen activation system (urokinase-type plasminogen activator, uPA; uPA receptor, uPAR; uPA inhibitor type-1, PAI-1) is considered one of the main systems involved in tumor invasion and metastasis. Moreover, previous data have reported that PD-L1 on exosomes surface can inhibit antitumor immune responses: cancer cells package PD-L1 into exosomes by shedding PD-L1 on their surface. Thus, PD-L1-positive exosomes promote immunosuppression. On this basis, we propose to inhibit PD-L1 endocytosis targeting LRP-1/uPAR and or/PAI-1 complex in order to reduce the expression of exosomal PD-L1 and maintain the receptor at membrane level. **Methods:** A375M6 (metastatic melanoma cells) and A549 (non-small cell lung cancer cells) were treated with TPX 28mM to evaluate the modulation of TPX treatment on exosomal PD-L1. Conditioned media collected from untreated and TPX-treated tumor cells were used for exosome isolation, through two sequential steps of

ultracentrifugation. PAI-1 and uPAR silencing by siRNA and uPAR/LRP-1 complex inhibition by specific antibodies were performed to block PD-L1 endocytosis and increase PD-L1 membrane levels on A375M6 and A549 surface. In particular, PD-L1 membrane levels were analyzed by flow cytometry and confocal immunofluorescence. **Results:** We demonstrated that in A375M6 and in A549, PAI-1 and uPAR silencing by siRNA, or uPAR/LRP-1 complex inhibition by specific antibodies, is able to block the PD-L1 internalization and, consequently, to increase PD-L1 membrane levels on cancer cells. Moreover, our result evidenced that exosomes from TPX-treated A375M6 and A549 show a decrease of exosomal PD-L1 levels, compared to untreated cancer cells. **Conclusions:** Our data demonstrated that uPAR silencing or uPAR/LRP-1 inhibition results in a significant increase in surface PD-L1 levels. In parallel, our results evidenced that PAI-1 inhibition and, consequently, the blockade of PAI-1-dependent PD-L1 endocytosis showed a decrease of exosomal PD-L1 levels. These findings open the way for new combined therapeutic strategies with anti-uPAR/PAI-1 and anti-PD-1/PD-L1, and could have significant implications for immunotherapeutic approaches to cancer treatment.

OTH10. MPQAP EQAS Scheme for FISH *HER2/neu* Gene Amplification Assay: Excerpts from Five Rounds of Proficiency Testing Cycle

R. Iyer, O. Shetty, T. Shet, P. Joshi, P. Gogte, M. Gurav, N. Karnik, T. Pai, G. Deshpande, S. Epari, C. Hingnekar, S. Desai

Tata Memorial Hospital, Homi Bhabha National Institute, Molecular Pathology Laboratory, Department of Pathology, Mumbai, India.

Introduction: Analysing amplification status of *HER2/neu* gene is a prerequisite for providing targeted therapy to breast cancer patients, thereby necessitating the need for accurate test results. Monitoring the quality of technical procedures and analytical interpretation for diagnosis is the primary role of EQAS providers. Molecular Pathology Quality Assurance Program (MPQAP) is a first EQAS initiative in India for solid tumor diagnostics started in the year 2019 which is actively conducting quality assurance schemes for fluorescence *in situ* hybridization (FISH) and PCR-based tests. The current study presents the findings and excerpts from the summation of five rounds of an EQAS scheme for a FISH *HER2/neu* test. **Methods:** Previously tested and reported cases of breast cancer tissues (formalin-fixed, paraffin-embedded) were selected as survey material. Tissue microarrays containing 5 to 6 cores each having varied *HER2* gene amplification status was prepared. These were circulated to registered participants of the test scheme (2019 to 2022). Participants were required to test the samples using their routine diagnostic protocols and report their findings. During the pandemic, apart from routine EQAS, an image interpretation module was also released to assess the post-analytical aspect of testing. The participants were assessed and scored based on accurate interpretation, data entry, and timely completion of the survey. The score system was as follows: >90 = "Very Good Performance," 70 to 80 = "Good Performance," and <70 = "Needs Improvement." Based on these scores, participant summaries were prepared. The test results were anonymised for the evaluator's assessment and a report was issued to all participants. **Results:** A total of 21 centres participated in the scheme, with 4 centres in the first round followed by 13 to 15 centres, each in subsequent cycles. From the obtained 61 datasets of test results, overall 81% (17/21) centres showed "Very Good Performance," 7% (1/21) showed "Good Performance," and 12% (2/21) were graded as "Needs Improvement." Three centres participated in all 5 rounds and showed consistent "Very Good Performance." During the third circulation, inconsistency in performance of centres was observed where 57% (12/21) of centers scored 70 to 90 and 14% (3/21) centers scored <70. Based on this trend, an online session was conducted as an educational exercise to address the concerns of result discrepancies. The session focused on 1) ASCO/CAP 2018 recommendations for FISH reporting; 2) analysing samples with low tumor content; 3) genomic heterogeneity; and 4) known control samples for internal quality assurance. Post-session, the performance of participants rose to an average of 96% in the fourth and fifth rounds, depicting the importance of monitoring the role of EQAS providers. **Conclusions:** MPQAP augmented the monitoring criteria of the quality testing by providing educational EQAS programs. The program provides continual support to participating laboratories by imparting recommendations for enhancing quality practices in solid tumor diagnostics to improve performance, thereby ensuring reliability of testing.

OTH11. Rapid qPCR Based *IDH1/IDH2* Mutation Screening in Solid Tumors and Hematologic Malignancies without Extraction (Selected for Oral Presentation, O-03-03)

E. Dikoglu, D. Kim, R. Chan, B. S. Gray, A. Yun, P.A. Salazar, H.A. Patel, I. Rijo, T. Bale, M.D. Ewalt, L. Borsu, M. Hameed, K. Nafa, M.E. Arcila

Memorial Sloan Kettering Cancer Center, Pathology/Molecular Genetic Pathology, New York, NY.

Introduction: Recurrent mutations in isocitrate dehydrogenase 1 and 2 (*IDH1* and *IDH2*) are important actionable biomarkers in hematologic malignancies and solid tumors. Rapid, accurate, and robust screening is important for

diagnosis, prognosis, and/or therapeutic management, depending on the disease setting. In this study, we describe the use of a fully automated system to enable ultra-rapid assessment of *IDH1/2* hotspot mutation status on various sample types without the need for prior DNA extraction. **Methods:** Tumor samples submitted for routine clinical mutation assessment were selected. Rapid screening was performed using a newly developed, cartridge-based assay with flexible design for the Idylla platform. The Idylla *IDH1-2* mutation assay kit consists of an automated agnostic cartridge and a vial containing the specific primers and probes for testing. By design, the assay detects mutations involving specific codons in *IDH1* (R132) and *IDH2* (R140 and R172) but does not discriminate the specific amino acid substitution. Results were compared to concurrently performed clinical testing by next-generation sequencing (MSK-IMPACT, MSK-ACCESS) and/or digital PCR as reference methods. Performance characteristics were assessed including accuracy, sensitivity, specificity, and reproducibility. **Results:** In all, 42 samples were assessed (32 positive, 10 negative) including both extracted and unextracted material: 13 formalin-fixed, paraffin-embedded (FFPE) tissue sections (5µm thick), 24 extracted DNA, and 5 unextracted blood/bone marrow (BL/BM) samples in EDTA. Overall, we achieved 100% accuracy in mutation detection (34 mutations) compared to the reference method (14 *IDH1* R132, 6 *IDH2* R140, 2 double mutant *IDH1* R132 and *IDH2* R140, 10 *IDH2* R172 and 10 *IDH1/2* negative). Mutations were detected over a broad variant allele frequency (VAF) range of 2.2% to 44.2%. Sensitivity studies showed a limit of detection between 2% and 3%, and provided sufficient input with excellent reproducibility. Minimal input studies, performed on extracted DNA, showed ≥10ng were required to consistently detect a mutation known to be present at 5% VAF. Unextracted material input requirements varied according to sample type, quality, and quantity (>9 mm^2 for tissue, 10µl BL/BM). A cycle of quantification of ≤36 (internal control) is needed to maintain detection of variants at 5% VAF. The technical hands-on time averaged 5 minutes, and time from set-up to instrument report generation was 95 minutes. **Conclusions:** The *IDH1/IDH2* cartridge-based assay for the Idylla system allows ultra-rapid, sensitive, and robust screening for recurrent mutations at residues R132 in *IDH1* and R140 or R172 in *IDH2*. The system provides reliable analysis of both extracted and pre-extraction tumor tissue from numerous sources beyond FFPE, including direct blood and bone marrow samples. It markedly simplifies the workflows in the lab and enables rapid treatment decisions.

OTH12. Development and Validation of TarGT Indiegene: World's First Indian Population-Specific Cancer Gene Panel

V. Javle, R. Malhotra, N.A. Tanwar, N. Jaiswal, B. Shreenath, S.P. Kuntia, A.P. Satheesh, S.R. Peddagangannagari, L. Varghese, K.D. Rishi, H.M. Goswami, V.H. Veldore
4basecare Onco solutions Pvt Ltd, Bengaluru, India.

Introduction: Next-generation sequencing (NGS) testing has emerged as a backbone in precision oncology practice in the last decade to improve understanding of the disease and provide accurate treatment decisions. Geographic diversity and ethnic variation among individuals contribute significantly to the disease onset and aggressiveness. Therefore, it is important to research the diversity of cancer in local populations to overcome challenges in treatment. We share here our efforts for the development and validation of India's first cancer gene panel, TarGT Indiegene, specifically tailored to the Indian population. **Methods:** As part of Illumina accelerator support, tumors from 1,500 cancer patients across 28 different cancer types were subjected to whole-exome and whole-transcriptome profiling using Illumina NGS Panels using standard procedure. The data were analyzed using the proprietary DRAGENIT Platform from Illumina. Systematic filtration of variants was carried out for the entire exome/transcriptome data to eliminate non-pathogenic variants. The true somatic pathogenic variants were derived using a variant effect predictor and multiple cancer-specific databases such as ClinVar, CBioPortal, MyCancerGenome, and OncoKB, as depicted in Figure 1. **Results:** The TarGT Indiegene panel was created by collating genes with pathogenic alterations found in multiple cancers and through a literature survey. The panel consists of 1,212 genes including 1,064 single nucleotide variations/insertions and deletions (SNVs/indels), 570 copy number alterations, and 299 gene fusions. The panel has undergone analytical and clinical validation, showing 100% specificity, 98% sensitivity, and 100% reproducibility with a detection limit of 5% for SNVs and 10% for indels. **Conclusions:** TarGT Indiegene is the first of its kind to narrate the tumor mutation spectrum in the Indian population, making it unique compared to other panels that rely solely on data from Western populations or worldwide cancer databases. The *ab initio* approach used in its development not only revealed insights into the existing mutation cohort, but also identified novel biomarkers that were specific to the Indian population, and rare driver mutations. This study could provide opportunities for new targeted therapies and chemotherapy options.

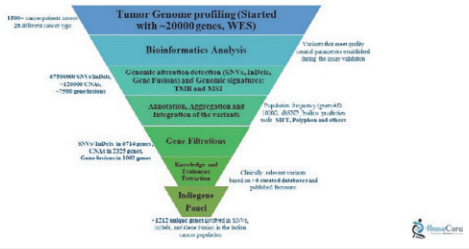

Development of TarGT Indiegene Panel

Parameter	Analytical
Specificity	100%
Sensitivity	>98%
Accuracy	>98%
Precision	100%
Reproducibility	100%
Limit of Detection	5% for SNV and 10% for Indels (<10 bp)
PPV	100%
NPV	100%

Performance Metrics of TarGT Indiegene Pan-Cancer Solid Tumor Panel

OTH13. Targeting Microglial A20/TNFAIP3 as a Novel *Leishmania infantum* Strategy to Curtail the NF-κB/NLRP3-Mediated Neuroinflammatory Response in Alzheimer Disease

E. Calvo Alvarez[1], M. Saresella[2], G. Pepe[3], F. La Rosa[2], E. Vegeto[3], D. Taramelli[1], M. Clerici[4,2], N. Basilico[5]
[1]University of Milan, Department of Pharmacological and Biomolecular Sciences, Milan, Italy; [2]IRCCS Fondazione Don Carlo Gnocchi, Laboratory of Molecular Medicine and Biotechnology, Milan, Italy; [3]University of Milan, Department of Pharmaceutical Sciences, Milan, Italy; [4]University of Milan, Department of Physiopathology and Transplants, Milan, Italy; [5]University of Milan, Department of Biomedical, Surgical and Dental Sciences, Milan, Italy.

Introduction: The detrimental effect of extensive neuroinflammation on the pathological trajectory of Alzheimer disease (AD) is widely recognized. Overactivated microglia (MG) are the main players of the neuroinflammatory cascade, and rewiring their immune activation state holds promise for novel therapeutic interventions. While the nuclear factor kappa B (NF-κB) is a key mediator of brain inflammation in AD, the negative regulator A20/TNFAIP3 terminates NF-κB signaling, leading to the inhibition of the NLRP3 inflammasome-dependent neuroinflammation, and MG inactivation. *Leishmania infantum* (*Li*) are eukaryotic parasites and professional immune evaders in macrophages. We have previously demonstrated the parasite-dependent NLRP3 inhibition in both macrophages and AD-like MG. Yet, the mechanistic insights are unknown. Here, we investigated the molecular tools used by these parasites to counteract the NF-κB/NLRP3-mediated MG hyperactivation, as a potential bio-inspired immunosuppressive approach to attenuate neuroinflammation in AD. **Methods:** *Ex vivo* primary MG isolated from postnatal mice and an MG cell line were infected with WT or dual bioluminescent/fluorescent *Li* (Ppy-tdT+Li) parasites (ratio 1:10 MG:parasites), and treated with canonical NLRP3 activators including amyloid-β peptide (Aβ), and NF-κB pharmacological inhibitors. Phagocytosis was studied by live-cell fluorescent imaging and Giemsa staining. The expression of A20 and NLRP3-related factors was investigated by qPCR, Western blot, and ELISA, and reactive oxygen species (ROS) levels were assessed by ROS-Glo (Promega). NF-κB signaling, A20 subcellular localization, and lysosomal integrity were analyzed by immunofluorescence. **Results:** In AD, the transcriptional regulation of NLRP3 components is mediated by NF-κB nuclear trafficking in response to Aβ. Our results demonstrate that *Li* parasites interfere with the NF-κB signaling in AD-like MG by preventing the nuclear translocation of the transcription factor concomitantly with a downregulation of *Nlrp3* and *pro-il-1β* transcripts, thus impairing the NLRP3 priming step upstream of NLRP3 activation. This inhibitory effect is accompanied by the upregulation of A20 in infected cells, and an increased A20 accumulation in parasite-containing phagolysosomes, as evidenced by co-localization studies with lysosomal markers. Since the A20-lysosome association is crucial for proper inhibitory activity, these observations indicate an active parasite-mediated process to trigger an effective termination of the NF-κB signaling. Additionally, it is known that Aβ enhances the NF-κB/NLRP3 axis through lysosomal rupture and ROS generation. Interestingly, we also found that *Li* preserves microglial lysosomal integrity and reduces ROS production in the presence of Aβ. **Conclusions:** Overall, these results uncover an unexpected mechanism by *Li* to impair the NF-kB/NLRP3 axis in AD-like MG. Imposing a parasite-driven brake on overactivated MG might open novel therapeutic avenues against neuroinflammation in AD.

OTH14. Unifying NGS Workflows: A Modularized Automated Approach for Streamlining Clinical Molecular Diagnostics Laboratories

F.A. San Lucas[1], H. Pelicano[1], J. Gascoyne[1], J. Mercado[1], S. Ninan[1], J. Ozenci[1], D. Duose[4], R. Yang[3], M. Routbort[1,3], K. Patel[1,2], S. Roy[1,2], I. Wistuba[4], R. Luthra[1], J. Medeiros[2], H. Alvarez[1,2]

[1]The University of Texas MD Anderson Cancer Center, Molecular Diagnostics Laboratory, Houston, TX; [2]The University of Texas MD Anderson Cancer Center, Department of Hematopathology, Houston, TX; [3]The University of Texas MD Anderson Cancer Center, Department of Pathology, Houston, TX; [4]The University of Texas MD Anderson Cancer Center, Department of Translational Molecular Pathology, Houston, TX.

Introduction: The Molecular Diagnostics Laboratory at The University of Texas MD Anderson Cancer Center underwent a transformation aimed at streamlining complex next-generation sequencing (NGS) workflows and enhancing their efficiency. The increasing diversity and volume of NGS testing in the past decade resulted in a complex laboratory environment that was becoming increasingly difficult to manage. To address this issue, the laboratory implemented a modularized automated approach, consisting of four liquid handler robots and a custom laboratory information management system to create a single, unified workflow for the entire NGS process. **Methods:** The robots in the workflow were responsible for various tasks, including sample tissue deparaffinization, blood fractionation, simultaneous DNA and RNA extraction, cDNA and library preparation, and NGS hybrid capture. The accompanying software system facilitated connectivity, real-time monitoring of the workflow, and streamlined troubleshooting by tracking sample and control movements and status changes throughout the process. **Results:** The results of this transformation were significant. The modular design of the robots and their flexibility in batch sizes supported a wide range of applications, including NGS applications for solid tumor assays such as MDA MAPP (a 700+ gene panel), exome sequencing, and whole-genome sequencing, as well as liquid biopsy applications. The new workflow resulted in a reduction of hands-on time for technologists by 80% and a decrease in the number of required technologists and supervisors by 67% when implementing three assays. Moreover, the development time for new assays was streamlined, reducing the time required for technology familiarization and training. **Conclusions:** In conclusion, the Molecular Diagnostics Laboratory at MD Anderson Cancer Center successfully transformed their complex NGS workflows into a single, unified, and automated process, resulting in improved efficiency and reliability. This approach has the potential to be applied to any clinical laboratory performing NGS sequencing, simplifying operations and facilitating the rapid implementation of additional NGS assays.

OTH15. Epidermal Growth Factor Receptor: Immunohistochemical, Variant Gene Characterization and *in Silico* Analysis in Canine Mammary Cancer – A Comparative Genomics Approach

S. Monteiro[1], A.B. Gonçalves[1], A. Alves[2,4], M. dos Anjos Clemente Pires[2,4], A. Gama[2,4], E. Bastos[1,3]

[1]University of Trás-os-Montes e Alto Douro (UTAD), Department of Genetics and Biotechnology, School of Life and Environmental Sciences (ECVA), Vila Real, Portugal; [2]University of Trás-os-Montes e Alto Douro (UTAD), Department of Veterinary Sciences, School of Agrarian and Veterinary Sciences (ECAV), Vila Real, Portugal; [3]University of Trás-os-Montes e Alto Douro (UTAD), Center of the Research and Technology of Agro-Environmental and Biological Sciences (CITAB), Vila Real, Portugal; [4]University of Trás-os-Montes e Alto Douro (UTAD), Animal and Veterinary Research Centre (CECAV), Vila Real, Portugal.

Introduction: Finding inhibitors of Epidermal Growth Factor Receptor (EGFR) protein binding is the aim of different studies. Using databases such as STRING and KEGG can be an interesting *in silico* approach. This strategy has been recently described by Ongko *et al.* (2022) and previously by Majhi *et al.* (2018) in humans; however, this same approach can be applied to other species, such as the canine species, based on comparative genomics. *Canis familiaris* is a natural and spontaneous model for different diseases, including neoplastic and inflammatory diseases, as well as periodontal disease. Our group published a review regarding this model and its advantages compared with other animal models (Albuquerque *et al*., 2012). Mammary tumours are the most frequent neoplasm diagnosed in intact female dogs, and EGFR is a transmembrane receptor involved in the regulation of cell proliferation, differentiation, motility, and survival. Although frequently studied in human breast cancer, few studies have been dedicated to analysing EGFR in canine mammary tumours, especially regarding the search for *EGFR* gene variants and using *in silico* strategies. The aim of the current study is to describe EGFR immunoexpression and the presence of *EGFR* gene variants in this animal model, based on the EGFR expression evaluated by immunohistochemistry (IHC) in 111 mammary malignant tumours, 68 lymph node metastases, and 12 lung metastases. Herceptest scoring system was used for EGFR evaluation, with 2+ and 3+ cases considered positive (complete membrane staining in >10% cells). EGFR overexpression was observed in 53.2% of primary tumours, 47.1% of node metastases, and 25% of lung metastases. EGFR expression in primary tumours and node

metastases was significantly associated (P <0.0001), with a concordance in 79.4% samples. The search for *EGFR* exon 19 sequence variants from 30 frozen mammary tissue samples (20 primary carcinomas and 10 adjacent non-neoplastic tissue) followed, using the steps of DNA extraction, PCR, and Sanger sequencing. Four intronic variants were detected in six samples, corresponding to four female dogs (four carcinomas vs. two paired non-neoplastic adjacent tissues). Although three of these carcinomas also overexpressed EGFR (detected by IHC), the remaining positive EGFR samples failed to reveal gene variants. Additional studies using a larger series are already being implemented, and *in silico* search is starting to be used to answer the following question: What is the real role of the *EGFR* gene and its variants in human and dog mammary tumours? The comparative genomics is our starting point for our contribution to this scientific question.
Methods: TBA. **Results:** TBA. **Conclusions:** TBA.

OTH16. Identification of Therapeutically Relevant Mutations in Circulating Tumor DNA at Baseline to Assist in Treatment Decision Making

P. van der Leest[1], A. Sartori[2], P. Rozendal[1], N. Rifaela[1], A.J. van der Wekken[3], L.C. van Kempen[1], T.J.N. Hiltermann[3], E. Schuuring[1]
[1]University of Groningen, University Medical Center Groningen, Department of Pathology, Groningen, Netherlands; [2]Agena Bioscience GmbH, Hamburg, Germany; [3]University of Groningen, University Medical Center Groningen, Department of Pulmonary Medicine, Groningen, Netherlands.

Introduction: According to current guidelines, molecular tumor profiling is performed on tumor cells of lung cancer patients to facilitate treatment decision making. Liquid biopsy approaches, especially the detection of circulating tumor DNA (ctDNA) in the bloodstream, are emerging as sensitive and reliable alternatives for routine diagnostic testing relying on tumor tissue biopsy specimens. Here, we analyze serially collected baseline plasma samples of lung cancer patients to determine the agreement between tumor tissue-based and ctDNA-based molecular tumor profiling and the consequent clinical implications. Additionally, as molecular profiling of the tumor fails in 10% to 20% of the cases, we determine the additional value of liquid biopsy testing when tumor tissue next-generation sequencing (NGS) data are unavailable.
Methods: Between July 2018 and December 2021, 180 serially collected baseline plasma samples were included. Using 2mL of plasma, circulating cell-free DNA (ccfDNA) was extracted and analyzed with the UltraSEEK Lung Panel v2 on the MassARRAY System (Agena Bioscience, San Diego, US), which detects 78 common (actionable) mutations in *BRAF*, *EGFR*, *ERBB2*, *KRAS,* and *PIK3CA*. CcfDNA is retrospectively quantified using the LiquidIQ Panel (Agena Bioscience) to evaluate discrepant results. **Results:** Tumor tissue NGS analysis was available for 132 non-small cell lung cancer patients (73%). An 82% concordance has been observed between mutations detected in tumor tissue and in plasma. More mutations were reported with tumor tissue NGS in 19 patients, whereas in 4 patients additional mutations have been found in plasma. No particular factors affect retrieval of tumor-derived mutations in the ccfDNA. In the absence of tumor tissue NGS data, five therapeutically targetable mutations were detected. Molecular tumor profiling based on tissue allocated showed 60 patients eligible for tyrosine kinase inhibitor (TKI) treatments, of which 15 (8%) were for rearrangements not covered by the UltraSEEK Lung Panel. Forty-one patients (23%) were eligible for TKI against mutations in *BRAF*, *EGFR,* and *KRAS*. **Conclusions:** Molecular tumor profiling using ctDNA with the UltraSEEK Lung Panel identified therapeutically relevant mutations at a rate comparable to tumor tissue NGS, and might therefore serve as a prescreening tool for baseline actionable variant identification in the absence of tumor tissue, or as a complementary test in addition to tumor tissue NGS.